Supporting Information

for

Group VIII Coordination Complexes of Bidentate *P^N* Ligands Bearing π-Extended *N*-Heterocycles

*Rajarshi Mondal[a], Jason D. Braun[a], Issiah B. Lozada[a], Rachel Nickel[b], Johan van Lierop[b,c], David E. Herbert[a,c]**

[a] Department of Chemistry, University of Manitoba, 144 Dysart Rd, Winnipeg, MB, R3T 2N2, Canada; *david.herbert@umanitoba.ca

[b] Department of Physics and Astronomy, University of Manitoba, 31A Sifton Rd, Winnipeg, MB, Canada, R3T 2N2

[c] Manitoba Institute for Materials, University of Manitoba, 20 Sifton Rd, Winnipeg, MB, Canada, R3T 2N2

Table of Contents

General Experimental Information

Unless otherwise stated, all air sensitive manipulations were carried out in an N_2-filled glove box or on a Schlenk line under Ar. Anhydrous $FeBr_2$ and $FeSO_4 \cdot (NH_4)_2SO_4 \cdot 6(H_2O)$ were purchased (Sigma Aldrich) and used as received. (4-bromo-2-methyl)phenanthridine,[1] $^{\mathbf{Phen}}\mathbf{L}^{\mathbf{H,Ph}}$,[2] $^{\mathbf{Phen}}\mathbf{L}^{\mathbf{Me,Ph}}$,[3] $^{\mathbf{Quin}}\mathbf{L}^{\mathbf{H,Ph}}$ [3] and *cis*-$(DMSO)_4RuCl_2$ [4] were synthesized following published procedures. Organic solvents were dried over appropriate reagents and deoxygenated prior to use. NMR spectra were recorded on a Bruker Avance 300 MHz or Bruker Avance-III 500 MHz spectrometer. Absorbance spectra were collected on a Cary 5000 UV-Vis NIR spectrophotometer. Solutions were prepared in 10 × 10 mm^2 quartz cuvettes at room temperature, at concentrations on the order of 1.0 x 10^{-4} mol L^{-1}. Elemental analyses were performed at the University of Manitoba using a Perkin Elmer EA2400 CHN Analyzer. Solid-state magnetic moments were collected using a Johnson Matthey M.S.B. instrument. High-resolution mass spectra were collected on a Bruker microOTOF-QIII mass spectrometer.

For electrochemical analysis, 5-10 mg of each compound investigated was dissolved in 15 mL of 0.1 M [nBu$_4$N][PF_6] in CH_2Cl_2 or CH_3CN as noted and purged with Ar before analysis. All electrochemical experiments were conducted under inert (Ar) atmosphere using a CHI 760c bipotentiostat, a 3 mm diameter glassy carbon working electrode, a Ag/Ag+ quasi-non-aqueous reference electrode separated by a Vycor tip, and a Pt wire counter electrode. Cyclic voltammetric (CV) experiments were conducted using scan rates of 50-800 mV/s. Differential pulse voltammetry (DPV) experiments were also conducted, using a 5 mV increment, 50 mV amplitude, 0.1 s pulse width, 0.0167 s sample width, and 0.5 s pulse period. Upon completion of all CV and DPV analyses, ferrocene (FcH) was added to the solution as an internal standard, with all potentials reported versus the $FcH^{0/+}$ redox couple. Spectroelectrochemical measurements were conducted

using a Jasco-720 spectrophotometer to collect UV–vis data from solutions in a custom-built cell to which a potential was applied using a CH Instruments electrochemical analyzer and a three-electrode scheme with platinum working, platinum auxiliary, and a Ag/AgCl reference electrode.

Ligand and Complex Synthesis

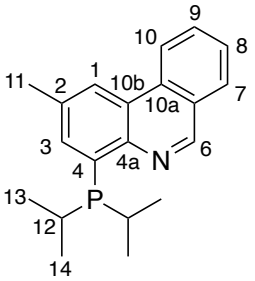

(4-di-*iso*-propyl-phosphino-2-methyl)phenanthridine ($^{Phen}L^{Me,iPr}$): A 50 mL Schlenk flask was charged with 4-bromo-2-methylphenanthridine (0.54 g, 2.0 mmol) and Et_2O (3 mL) and stirred for 15 min at -78 °C. A solution of *sec*-butyllithium (1.6 M; 1.60 mL, 2.0 mmol) in cyclohexane was then added dropwise and the mixture stirred for 5 h at the same temperature. Next, a solution of chlorodiisopropylphosphine (0.40 g, 2.0 mmol) in Et_2O (4 mL) was added dropwise. The reaction mixture was then warmed overnight to room temperature with stirring, at which point the solution color had changed to yellow. The mixture was dried *in vacuo* to leave a gummy residue which was redissolved in hexanes (15 mL) and filtered through a small plug (~ 1 cm) of silica. The filtrate was filtered a second time through another short plug (~ 1 cm) of silica, which was subsequently washed with hexanes (10 mL). The collected filtrate and washings were combined and dried *in vacuo* to give a light yellow semi-solid. Yield = 0.38 g (63%). ^{1}H NMR ($CDCl_3$, 500 MHz, 25 °C): δ 9.29 (s, 1H; C_6H), 8.60 (d, $^3J_{HH}$ = 8.3 Hz, 1H; $C_{10}H$), 8.37 (s, 1H; C_1H), 8.02 (d, $^3J_{HH}$ = 7.6 Hz, 1H; C_7H), 7.81 (ddd, J_{HH} = 8.3, 7.1, 1.3 Hz, 1H; C_8H), 7.69-7.66 (overlapped m, 2H; $C_{9,3}$H), 2.65 (s, 3H, $C_{11}H$), 2.38 (dh, $^3J_{HH}$ = 6.8 Hz, $^2J_{HP}$ = 1.4 Hz, 2H; $C_{12}H$), 1.16 (dd, $^3J_{HP}$ = 14.0 Hz, $^3J_{HH}$ = 7.0 Hz, 6H; $C_{13}H$), 0.98 ppm (dd, $^3J_{HP}$ = 12.1 Hz, $^3J_{HH}$ = 7.0 Hz, 6H; $C_{14}H$). $^{13}C\{^1H\}$ NMR ($CDCl_3$, 126 MHz, 25 °C): δ 151.5 (s; C_6=N), 146.3 (d, $^2J_{CP}$ = 15 Hz; C_{4a}), 137.2 (d, $^1J_{CP}$ = 21 Hz; C_4), 135.8 (d, J_{CP} = 11 Hz, C_1), 135.1 (C_2), 132.7 (C_3), 130.6 (C_9), 128.7 (C_7), 127.4 (C_8), 126.4 (C_{6a}),

123.9 (d, $^3J_{CP}$ = 2 Hz, C_{10b}), 122.6 (C_1), 122.1 (C_{10}), 23.5 (d, $^1J_{CP}$ = 14 Hz; C_{12}), 22.2 (s; C_{11}), 20.4 (d, $^2J_{CP}$ = 18 Hz; C_{13}), 19.9 (d, $^2J_{CP}$ = 12 Hz; C_{14}). $^{31}P\{^1H\}$ NMR ($CDCl_3$, 121 MHz, 25 °C): δ -0.2 ppm (s, *P*(*i*Pr$_2$)).

Synthesis of (($^{Phen}L^{H,Ph}$)FeBr)$_2$(μ-Br)$_2$: A solution of $^{Phen}L^{H,Ph}$ (0.091 g, 0.25 mmol) in CH_2Cl_2 (10 mL) was added dropwise to a suspension of $FeBr_2$ (0.054 g, 0.25 mmol) in THF (15 mL) in a 20 mL scintillation vial with constant stirring under nitrogen atmosphere. The reaction mixture was stirred overnight, leading to a color change from yellow to deep orange. The mixture was then filtered through a plug of Celite and the filtrate dried under reduced pressure to leave an orange solid, which was further washed with Et_2O (5 mL). Yield = 0.093 g (65%). Single crystals suitable for X-ray diffraction were grown via diffusion of hexane vapours into a CH_2Cl_2 solution. ^1H NMR ($CDCl_3$, 300 MHz, 25 ˚C): δ = 23.2, 18.1 (br), 16.6 (br), 13.1, 12.9, 11.5, -3.8, -5.4 (v br), -7.2, -7.9 ppm (br). Anal. Calc. for $C_{25}H_{19}FeNPBr_2$: C, 51.77; H, 3.30. Found: C, 51.63; H, 3.54.

Synthesis of ($^{Phen}L^{Me,Ph}$)FeBr$_2$: ($^{Phen}L^{Me,Ph}$)$FeBr_2$ was prepared analogously to (($^{Phen}L^{H,Ph}$)FeBr)$_2$(μ-Br)$_2$ but using $^{Phen}L^{Me,Ph}$ (0.093 g, 0.25 mmol) and $FeBr_2$ (0.054 g, 0.25 mmol). Yellow crystals. Yield = 0.107 g (72%). ^1H NMR ($CDCl_3$, 300 MHz, 25 ˚C): δ = 22.6, 18.1 (br), 17.3 (v br), 13.2, 13.0, 2.2, -4.0, -5.9 (v br), -7.6, -8.2 ppm. Anal. Calc. for $C_{26}H_{20}FeNPBr_2$: C, 52.65; H, 3.40. Found: C, 52.59; H, 3.64.

Synthesis of ($^{Phen}L^{Me,iPr}$)FeBr$_2$: ($^{Phen}L^{Me,iPr}$)$FeBr_2$ was been synthesized analogously to (($^{Phen}L^{H,Ph}$)FeBr)$_2$(μ-Br)$_2$ but using $^{Phen}L^{Me,iPr}$ (0.074 g, 0.25 mmol) and $FeBr_2$ (0.054 g, 0.25 mmol). Yellow crystals. Yield = 0.830 g (65%). ^1H NMR ($CDCl_3$, 300 MHz, 25 ˚C): δ = 22.6,

20.7 (br), 14.1, 13.7, 9.1 (br), 3.0, -4.9 (br), -9.8 ppm. Anal. Calc. for $C_{20}H_{24}Br_2FeNP$: C, 45.75; H, 4.61. Found: C, 45.76; H, 4.74.

Synthesis of $[(^{Phen}L^{Me,Ph})_3Fe][PF_6]_2$: $^{Phen}L^{Me,Ph}$ (0.071 g, 0.188 mmol) was dissolved in a mixture of CH_2Cl_2 (4 mL) and CH_3CN (2 mL) and added to a solution of $FeSO_4{\cdot}(NH_4)_2SO_4{\cdot}6(H_2O)$ (0.024 g, 0.063 mmol) in a mixture of degassed EtOH (3 mL) and H_2O (1 mL) in a 50 mL Schlenk flask under an atmosphere of Ar. The resulting mixture was stirred for 4 h at ambient temperature, after which it was observed that the color had changed to orange. Next, a solution of $NaPF_6$ (0.021g, 0.126 mmol) in degassed H_2O (5 mL) was added and stirring continued for 30 min, at which point the color had changed to deep red. The reaction mixture was dried *in vacuo*, then redissolved in CH_2Cl_2 (15 mL) and passed through a short plug of Celite and dried again to give a brown solid. The solid was crystallized from a mixture of CH_2Cl_2/Et_2O to give a deep orange-brown crystalline product. Yield = 0.043 g (47%). ^{1}H NMR (CD_2Cl_2, 500 MHz, 25 °C): δ 8.55 (m, 3H; $^{Phen}C_{Ar}H$), 8.51 (s, 3H; $^{Phen}C_{Ar}H$), 8.08 (s, 3H; $^{Phen}C_{Ar}H$), 8.01 (m, 3H; $^{Phen}C_{Ar}H$), 7.59 (m, 3H; $^{Phen}C_{Ar}H$), 7.51 (m, 3H; $^{Phen}C_{Ar}H$), 7.39 (br overlapped, 6H; $^{Ph}C_{Ar}H$), 7.33 (br, 3H; $^{Ph}C_{Ar}H$), 7.18 (d, 3H; $^{Phen}C_{Ar}H$), 7.03 (m overlapped, 6H; $^{Ph}C_{Ar}H$), 6.68 (m, 3H; $^{Ph}C_{Ar}H$), 6.21 (m overlapped, 6H; $^{Ph}C_{Ar}H$), 6.01 (br overlapped, 6H; $^{Ph}C_{Ar}H$), 2.59 ppm (s, 9H, CH_3). $^{13}C\{^1H\}$ NMR (CD_2Cl_2, 126 MHz, 25 °C): δ 162.9 (s, $C_{Ar}H$), 148.2 (br s, C_{Ar}), 141.5 (s, $C_{Ar}H$), 137.3 (s, $C_{Ar}H$), 135.7 (s, $C_{Ar}H$), 135.2 (br m, $C_{Ar}H$), 133.5 (m, C_{Ar}), 132.6 (s, $C_{Ar}H$), 132.4 (s, $C_{Ar}H$), 131.6 (m, C_{Ar}), 131.2 (br m, $C_{Ar}H$), 130.3 (s, $C_{Ar}H$), 129.9 (s, $C_{Ar}H$), 129.8 (s, $C_{Ar}H$), 129.7 (br, $C_{Ar}H$), 128.2 (s, $C_{Ar}H$), 128.0 (br m, $C_{Ar}H$), 127.7 (s, $C_{Ar}H$), 127.3 (br, C_{Ar}), 122.6 (s, $C_{Ar}H$), 21.9 ppm (CH_3). $^{31}P\{^1H\}$ NMR (CD_2Cl_2, 121 MHz, 25 °C): δ 56.8 (s; PPh_2), -144.6 ppm (h, $^1J_{PF}$ = 709 Hz; PF_6). ^{19}F NMR (CD_2Cl_2, 470 MHz,

22 °C): -73.2 ppm (d, J_{PF} = 709 Hz). Anal. Calc. for $C_{78}H_{60}F_{12}FeN_3P_5$: C, 63.38; H, 4.09. Found: C, 63.22; H, 4.19.

Synthesis of [($^{Quin}L^{Me,Ph}$)$_3$Fe][PF$_6$]$_2$: The complex was prepared following the same protocol as for [($^{Phen}L^{Me,Ph}$)$_3$Fe][PF$_6$]$_2$ but using $^{Quin}L^{Me,Ph}$ (0.061 g, 0.188 mmol), $FeSO_4 \cdot (NH_4)_2SO_4 \cdot 6(H_2O)$ (0.024 g, 0.063 mmol) and $NaPF_6$ (0.021g, 0.126 mmol). Yield = 0.041 g (49%). ^{1}H NMR (CD_2Cl_2, 500 MHz, 25 °C): δ 8.02 (m, 3H; $^{Quin}C_{Ar}H$), 7.74 (s, 3H; $^{Quin}C_{Ar}H$), 7.50 (m, 3H; $^{Quin}C_{Ar}H$), 7.40-7.33 (overlapped m, 12H; $^{Quin}C_{Ar}H$ and $^{Ph}C_{Ar}H$), 7.06-7.01 (overlapped m, 12H; $^{Ph}C_{Ar}H$), 6.59-6.56 (overlapped m, 6H; $^{Ph}C_{Ar}H$), 5.99 (overlapped br, 6H; $^{Quin}C_{Ar}H$) and 2.50 ppm (s, 9H; CH_3). ^{13}C{^{1}H} NMR (CD_2Cl_2, 126 MHz, 25 °C): δ 157.9 (s; C_{Ar}H), 153.2 (m; C_{Ar}), 140.6 (s; C_{Ar}), 140.2 (s; C_{Ar}H), 139.9 (s; C_{Ar}H), 135.2 (m; C_{Ar}), 133.4 (s; C_{Ar}H), 132.6 (s; C_{Ar}H), 131.2 (br m; C_{Ar}), 130.5 (s; C_{Ar}H), 129.7 (m; C_{Ar}), 128.5 (m; C_{Ar}), 125.3 (s; C_{Ar}H), 21.5 ppm (s; CH$_3$). ^{31}P{^{1}H} NMR (CD_2Cl_2, 121 MHz, 25 °C): δ 55.5 (s; PPh$_2$), -144.6 ppm (hep, $^1J_{PF}$ = 709 Hz; PF$_6$). ^{19}F NMR (CD_2Cl_2, 470 MHz, 22 °C): -73.1 ppm (d, $^1J_{PF}$ = 709 Hz). Anal. Calc. for $C_{66}H_{54}FeN_3P_5F_{12}$: C, 59.70; H, 4.10. Found: C, 59.63; H, 3.91.

Synthesis of [($^{Quin}L^{Me,Ph}$)$_3$Fe][BPh$_4$]$_2$: The complex has prepared following the procedure for the preparation of the PF$_6^-$ salt but using $^{Quin}L^{Me,Ph}$ (0.061 g, 0.188 mmol), $FeSO_4 \cdot (NH_4)_2SO_4$ (0.024 g, 0.063 mmol) and sodium tetraphenylborate (0.043 g, 0.125 mmol). Yield = 0.054 g (51%). ^{1}H NMR (CD_2Cl_2, 500 MHz, 25 °C): δ 7.74 (s, 2H, $^{Quin}C_{Ar}H$), 7.61 (m, 3H, $^{Quin}C_{Ar}H$), 7.47-7.41 (m, 9H, $^{Quin}C_{Ar}H$), 7.32 (overlapped m, 23H, $^{Ph}C_{Ar}H$, $^{BPh_4}C_{Ar}H$), 7.17 (br, 2H, $^{Quin}C_{Ar}H$), 7.02-6.96 (overlapped m, 26H, $^{Ph}C_{Ar}H$ and $^{BPh_4}C_{Ar}H$), 6.82 (br, 9H, $^{Ph}C_{Ar}H$), 6.56 (br, 7H, $^{Ph}C_{Ar}H$), 5.97 (br, 5H, $^{Ph}C_{Ar}H$), 2.49 ppm (s, 9H, CH_3). ^{13}C{^{1}H} NMR (CD_2Cl_2, 126 MHz, 25 °C): δ 164.5 (quartet,

BPh_4) 157.6 (s, $C_{Ar}H$), 153.2 (br, C_{Ar}), 140.8 (s, C_{Ar}), 140.5 (s, $C_{Ar}H$), 140.3 (s, $C_{Ar}H$), 136.4 (br m, C_{Ar}), 135.0 (s, C_{Ar}), 133.5 (s, $C_{Ar}H$), 132.7 (s, $C_{Ar}H$), 131.1 (br m, C_{Ar}), 130.6 (s, $C_{Ar}H$), 129.7 (br m, C_{Ar}), 128.6 (br m, C_{Ar}), 126.3 (br, $C_{Ar}H$), 125.5 (br, C_{Ar}), 122.2 (s, $C_{Ar}H$), 21.7 ppm (CH_3). $^{31}P\{^1H\}$ NMR (CD_3CN, 121 MHz, 25 °C): δ 55.8 ppm (s, PPh_2).

($^{Phen}L^{Me,Ph}$)Ru(DMSO)$_2$Cl$_2$/($^{Phen}L^{Me,Ph}$)$_2$RuCl$_2$: The protocol used here was adapted from a literature procedure for an analogous complex of 8-(dimethylphosphino)quinoline.[5] A solution of $^{Phen}L^{Me,Ph}$ (0.094 g, 0.25 mmol) in $CHCl_3$ (10 mL) was added to solution of *cis*-$(DMSO)_4RuCl_2$ (0.121 g, 0.25 mmol) in $CHCl_3$ (10 mL) and the mixture was heated to reflux at 85 °C for 2 h. After cooling to ambient temperature, the solution was filtered through a small plug of Celite (~1 cm) and concentrated nearly to dryness. Et_2O (20 mL) was added concentrated reaction mixture producing a deep red precipitate which was collected by filtration and washed with further Et_2O (10 mL). This solid was collected and dried *in vacuo*. The solid was identified by $^{31}P\{^1H\}$ NMR spectroscopy and HR-MS as a mixture of a mixture of ($^{Phen}L^{Me,Ph}$)Ru(DMSO)$_2$Cl$_2$ and ($^{Phen}L^{Me,Ph}$)$_2$RuCl$_2$. Recrystallization of the mixture from CH_2Cl_2/diethylether deposited single crystals of ($^{Phen}L^{Me,Ph}$)$_2$RuCl$_2$ suitable for X-ray analysis. $^{31}P\{^1H\}$ NMR ($CDCl_3$, 202 MHz, 25 °C): 55.8 (s; major product, ($^{Phen}L^{Me,Ph}$)Ru(DMSO)$_2$Cl$_2$), 63.9 (d, $^2J_{PP}$ = 33 Hz; minor product, ($^{Phen}L^{Me,Ph}$)$_2$RuCl$_2$), 55.2 ppm (d, $^2J_{PP}$ = 36 Hz; minor product, ($^{Phen}L^{Me,Ph}$)$_2$RuCl$_2$). HR-MS(ESI+) m/z calcd. for ($^{Phen}L^{Me,Ph}$)Ru(DMSO)$_2$Cl$_2$ [$C_{30}H_{32}Cl_2NO_2PRuS_2$–(DMSO)Cl] 592.0203, found 592.0237. HR-MS(ESI+) m/z calcd. ($^{Phen}L^{Me,Ph}$)$_2$RuCl$_2$ [$C_{52}H_{40}Cl_2N_2P_2Ru$–Cl] 891.1404, found 891.1476.

[(^{Phen}L^{Me,Ph})$_3$Ru][PF$_6$]$_2$: The mixture of (^{Phen}L^{Me,Ph})Ru(DMSO)$_2$Cl$_2$ and (^{Phen}L^{Me,Ph})$_2$RuCl$_2$ obtained prior to recrystallization in the previous step was used for the subsequent preparation of [(^{Phen}L^{Me,Ph})$_3$Ru][PF$_6$]$_2$. This red solid (0.044 g) and an additional two equivalents of ^{Phen}L^{Me,Ph} (0.048 g, 0.125 mmol) were combined in ethylene glycol (8 mL) and refluxed at 200 °C for 2 d. The mixture was then cooled to 50 °C and an excess NH_4PF_6 in water (0.041 g in 5 mL) was added. Stirring was continued for 30 min with the heating bath removed, over which time a light yellow precipitate formed. The precipitate was filtered and washed with water (5 mL). The solid was recrystallized from CH_2Cl_2 solution upon slow diffusion of diethylether vapors. Yield = 0.078 g (82 %). ^{1}H NMR (CD_3CN, 500 MHz, 25 °C): δ 8.63 (m, 3H; ^{Phen}C$_{Ar}$*H*), 8.59 (s, 3H; ^{Phen}C$_{Ar}$*H*), 8.54 (s, 3H; ^{Phen}C$_{Ar}$*H*), 8.01 (m, 3H; ^{Phen}C$_{Ar}$*H*), 7.61 (m, 3H; ^{Phen}C$_{Ar}$*H*), 7.55-7.48 (overlapped m, 9H; ^{Ph}C$_{Ar}$*H*), 7.42 (m, 3H; ^{Phen}C$_{Ar}$*H*), 7.31 (br s, 3H; ^{Phen}C$_{Ar}$*H*), 7.06 (br, 6H; ^{Ph}C$_{Ar}$*H*), 6.56 (m, 3H; ^{Ph}C$_{Ar}$*H*), 6.14 (m, 6H; ^{Ph}C$_{Ar}$*H*), 6.10-6.07 (overlapped br, 6H; ^{Ph}C$_{Ar}$*H*), 2.51 ppm (s, 3H; C*H*$_3$). ^{13}C{^{1}H} NMR (CD_3CN, 126 MHz, 25 °C): δ 160.8 (*C*$_{Ar}$H), 146.6 (*C*$_{Ar}$), 141.4 (*C*$_{Ar}$), 137.8 (*C*$_{Ar}$H), 135.5 (*C*$_{Ar}$), 135.4 (*C*$_{Ar}$H), 133.5 (*C*$_{Ar}$), 132.9 (*C*$_{Ar}$H), 137.7 (*C*$_{Ar}$), 131.4 (*C*$_{Ar}$H), 130.1 (*C*$_{Ar}$H), 129.9 (*C*$_{Ar}$), 129.6 (*C*$_{Ar}$H), 128.2 (*C*$_{Ar}$H), 128.1 (*C*$_{Ar}$), 127.8 (*C*$_{Ar}$), 123.0 (*C*$_{Ar}$H), 21.3 ppm (*C*H$_3$). ^{31}P{^{1}H} NMR (CD_3CN, 121 MHz, 25 °C): δ 58.2 (s; *P*Ph$_2$), -143.62 ppm (hep, $^1J_{PF}$ = 705 Hz; PF$_6$). ^{19}F NMR (CD_3CN, 470 MHz, 22 °C): -73.1 ppm (d, $^1J_{PF}$ = 705 Hz). HR-MS(ESI+) m/z calcd. for [(^{Phen}L^{Me,Ph})$_3$Ru][PF$_6$]$_2$ [$C_{78}H_{60}F_{12}N_3P_5Ru$–PF$_6$] 1378.2701, found 1378.2787.

[(^{Quin}L^{Me,Ph})$_3$Ru][PF$_6$]$_2$: This complex was prepared via the same protocol as [(^{Phen}L^{Me,Ph})$_3$Ru][PF$_6$]$_2$ but using ^{Quin}L^{Me,Ph} (0.081 g, 0.25 mmol) and *cis*-(DMSO)$_4$RuCl$_2$ (0.121 g, 0.25 mmol) in $CHCl_3$ (10 mL). After removing the solvent, the fine red residue was washed with Et_2O (3 × 5 mL) leaving a red solid identified by ^{31}P NMR spectroscopy as containing largely

($^{\mathbf{Quin}}\mathbf{L}^{\mathbf{Me,Ph}}$)$RuCl_2(DMSO)_2$ with a minor product, likely ($^{\mathbf{Quin}}\mathbf{L}^{\mathbf{Me,Ph}}$)$_2RuCl_2$, also present. $^{31}P\{^1H\}$ NMR ($CDCl_3$, 121 MHz, 25 °C): 55.8 (s; major product, ($^{\mathbf{Quin}}\mathbf{L}^{\mathbf{Me,Ph}}$)$Ru(DMSO)_2Cl_2$), 60.3 (s; minor product), 53.7 ppm (d, $^2J_{PP}$ = 33 Hz; minor product). HR-MS(ESI+) m/z calcd. for ($^{\mathbf{Quin}}\mathbf{L}^{\mathbf{Me,Ph}}$)$Ru(DMSO)_2Cl_2$ [$C_{26}H_{30}Cl_2NO_2PRuS_2$-(DMSO)-Cl] 542.0045, found 542.0080. For ($^{\mathbf{Quin}}\mathbf{L}^{\mathbf{Me,Ph}}$)$_2RuCl_2$ [$C_{44}H_{36}Cl_2N_2P_2Ru$-Cl] 791.1089, found 791.1162. [($^{\mathbf{Quin}}\mathbf{L}^{\mathbf{Me,Ph}}$)$_3Ru$][$PF_6$]$_2$ was then prepared in an analogous fashion to [($^{\mathbf{Phen}}\mathbf{L}^{\mathbf{Me,Ph}}$)$_3Ru$][$PF_6$]$_2$ using this mixture of ($^{\mathbf{Quin}}\mathbf{L}^{\mathbf{Me,Ph}}$)$RuCl_2(DMSO)_2$ and ($^{\mathbf{Quin}}\mathbf{L}^{\mathbf{Me,Ph}}$)$_2RuCl_2$ (0.041 g) and ($^{\mathbf{Quin}}\mathbf{L}^{\mathbf{Me,Ph}}$) (0.041 g, 0.126 mmol) in ethylene glycol (8 mL). White solid. Yield = 0.063 g (74 %). ^1H NMR (CD_2Cl_2, 500 MHz, 25 °C): δ 8.08 (m, 3H, $^{Quin}C_{Ar}H$), 7.77-7.74 (m, 6H, $^{Quin}C_{Ar}H$), 7.54 (m, 3H, $^{Quin}C_{Ar}H$), 7.46 (br, 6H, $^{Ph}C_{Ar}H$), 7.35 (br, 3H, $^{Ph}C_{Ar}H$), 7.13 (m, 3H, $^{Ph}C_{Ar}H$), 7.07 (m, 6H, $^{Ph}C_{Ar}H$), 6.96 (m, 3H, $^{Quin}C_{Ar}H$), 6.51 (m, 6H, $^{Ph}C_{Ar}H$), 6.03 (br, 6H, $^{Ph}C_{Ar}H$) and 2.49 ppm (s, 9H, $^{Quin}C_{methyl}$). $^{13}C\{^1H\}$ NMR (CD_2Cl_2, 126 MHz, 25 °C): δ 154.7 ($C_{Ar}H$), 150.3 (C_{Ar}), 140.6 ($C_{Ar}H$), 140.4 (C_{Ar}), 140.2 ($C_{Ar}H$), 135.0 (br m; C_{Ar}), 133.9 (m; C_{Ar}), 132.9 ($C_{Ar}H$), 132.8 ($C_{Ar}H$), 131.9 (m; C_{Ar}), 131.0 (m; C_{Ar}), 130.7 (br m; $C_{\underline{Ar}}$), 130.5 ($C_{Ar}H$), 130.1 (m; C_{Ar}), 129.8 (m; C_{Ar}), 128.3 (m; C_{Ar}), 125.3 ($C_{Ar}H$), 21.5 ppm (CH_3). $^{31}P\{^1H\}$ NMR ($CDCl_3$, 121 MHz, 25 °C): δ 56.2 (s; PPh_2), -143.62 ppm (hep, $^1J_{PF}$ = 705 Hz; PF_6). ^{19}F NMR ($CDCl_3$, 470 MHz, 22 °C): -73.1 ppm (d, $^1J_{PF}$ = 705 Hz). HR-MS(ESI+) m/z calcd. for [($^{\mathbf{Quin}}\mathbf{L}^{\mathbf{Me,Ph}}$)$_3Ru$][$PF_6$]$_2$ [$C_{66}H_{54}F_{12}N_3P_5Ru-2PF_6$] 1084.2787, found 1084.2665.

X-Ray Crystallography Experimental Details

For each sample analyzed, crystal structure data was using collected from multi-faceted crystals of suitable size and quality selected from a representative sample of crystals of the same habit using an optical microscope. Crystals were mounted on MiTiGen loops and data collection carried out in a cold stream of nitrogen (150 K; Bruker D8 QUEST ECO). All diffractometer manipulations were carried out using Bruker APEX3 software.[6] Absorption corrections were applied using SADABS.[7] Structure solution and refinement was carried out using XS, XT and XL programs,[8] either as part of Bruker's SHELXTL interface or embedded within the OLEX2 software suite. For each structure, the absence of additional symmetry was confirmed using ADDSYM incorporated in the PLATON program.[9] CCDC Nos. 2054101-2054108 contain the supplementary crystallographic data for this paper. The data can be obtained free of charge from The Cambridge Crystallographic Data Centre via www.ccdc.cam.ac.uk/structures.

Crystal structure data for $((^{Phen}L^{H,Ph})FeBr)_2(\mu\text{-}Br)_2$ (CCDC 2054101):

Orange plates; $C_{52}H_{40}Br_4Fe_2N_2P$ 1327.94 g/mol, triclinic, space group P-1; a = 10.360(2) Å, b = 10.778(3) Å, c = 13.244(3) Å, α = 107.886(3)°, β = 110.763(3)° γ = 97.176(3)°, V = 1269.7(5) Å^3; Z = 1, ρ_{calcd} = 1.737 g cm^{-3}; crystal dimensions 0.230 x 0.050 x 0.050 mm; $2\theta_{max}$ = 61.23°; 54704 reflections, 7256 independent (R_{int} = 0.0952), intrinsic phasing; absorption coeff (μ = 4.030 mm^{-1}), absorption correction semi-empirical from equivalents (SADABS); refinement (against F_o^2) with SHELXTL V6.1, 298 parameters, 0 restraints, R_1 = 0.0610 ($I > 2\sigma$) and wR_2 = 0.1657 (all data), Goof = 0.899, residual electron density 1.085/−0.690 Å^{-3}.

Crystal structure data for $(^{Phen}L^{Me,Ph})FeBr_2$ (CCDC 2054102):

Yellow blocks; $C_{26}H_{20}Br_2NPFe$ 593.07 g/mol, Triclinic, space group P-1; a = 9.8976(2) Å, b = 10.5112(2) Å, c = 11.5804(3) Å, α = 81.7680(10)°, β = 86.7250(10)° γ = 77.7680(10)°, V =

1164.84(4) Å^3; Z = 2, ρ_{calcd} = 1.691 g cm^{-3}; crystal dimensions 0.250 x 0.160 x 0.060 mm; $2\theta_{max}$ = 61.11°; 44982 reflections, 7128 independent (R_{int} = 0.0487), intrinsic phasing; absorption coeff (μ = 4.160 mm^{-1}), absorption correction semi-empirical from equivalents (SADABS); refinement (against F_o^2) with SHELXTL V6.1, 281 parameters, 0 restraints, R_1 = 0.0338 ($I > 2\sigma$) and wR_2 = 0.0695 (all data), Goof = 1.035, residual electron density 1.081/−0.771 Å^{-3}.

Crystal structure data for ($^{Phen}L^{Me,iPr}$)$FeBr_2$ (CCDC 2054103):

Yellow blocks; $C_{20}H_{24}Br_2NPFe$ 525.04 g/mol, Triclinic, space group P-1; a = 8.8150(2) Å, b = 9.4545(3) Å, c = 13.5012(4) Å, α = 89.4920(10)°, β = 89.6670(10)° γ = 64.9490(10)°, V = 1019.32(5) Å^3; Z = 2, ρ_{calcd} = 1.711 g cm^{-3}; crystal dimensions 0.130 x 0.060 x 0.020 mm; $2\theta_{max}$ = 61.22°; 33233 reflections, 6255 independent (R_{int} = 0.0419), intrinsic phasing; absorption coeff (μ = 4.741 mm^{-1}), absorption correction semi-empirical from equivalents (SADABS); refinement (against F_o^2) with SHELXTL V6.1, 231 parameters, 0 restraints, R_1 = 0.0388 ($I > 2\sigma$) and wR_2 = 0.0962 (all data), Goof = 1.052, residual electron density 0.615/−0.632 Å^{-3}.

Crystal structure data for [($^{Phen}L^{Me,Ph}$)$_3$Fe][PF_6]$_2$ (CCDC 2054104):

Red blocks; $C_{78}H_{60}F_{12}N_3Fe$ 1477.99 g/mol, Triclinic, space group P-1; a = 13.9092(14) Å, b = 14.2075(14) Å, c = 21.287(2) Å, α = 72.199(5)°, β = 78.434(5)° γ = 75.908(5)°, V = 3848.3(7) Å^3; Z = 2, ρ_{calcd} = 1.276 g cm^{-3}; crystal dimensions 0.320 x 0.220 x 0.100 mm; $2\theta_{max}$ = 49.638°; 134036 reflections, 13211 independent (R_{int} = 0.0382), intrinsic phasing; absorption coeff (μ = 0.372 mm^{-1}), absorption correction semi-empirical from equivalents (SADABS); refinement (against F_o^2) with SHELXTL V6.1, 899 parameters, 0 restraints, R_1 = 0.1005 ($I > 2\sigma$) and wR_2 = 0.2293 (all data), Goof = 1.032, residual electron density 6.424/−1.611 Å^{-3}.

Crystal structure data for $[(^{Quin}L^{Me,Ph})_3Fe][BPh_4]_2$ (CCDC 2054105):

Yellow plates; $C_{66}H_{54}F_9N_3P_{4.5}Ru$ 1300.55 g/mol, Trigonal, space group P-3; a = 13.9917(8) Å, b = 13.9917(8) Å, c = 18.8197(12) Å, $\alpha = \beta = 90°$ $\gamma = 120°$, V = 3190.7(4) Å^3; Z = 2, ρ_{calcd} = 1.354 g cm^{-3}; crystal dimensions 0.650 x 0.650 x 0.030 mm; $2\theta_{max}$ = 55.21°; 66182 reflections, 4905 independent (R_{int} = 0.0710), intrinsic phasing; absorption coeff (μ = 0.426 mm^{-1}), absorption correction semi-empirical from equivalents (SADABS); refinement (against F_o^2) with SHELXTL V6.1, 253 parameters, 0 restraints, R_1 = 0.0817 ($I > 2\sigma$) and wR_2 = 0.2008 (all data), Goof = 1.062, residual electron density 1.61/−1.23 Å^{-3}.

Crystal structure data for $[(^{Phen}L^{Me,Ph})_2RuCl_2$ (CCDC 2054106):

Orange blocks; $C_{78}H_{60}F_{12}N_3P_5Ru$ 1523.21 g/mol, triclinic, space group P-1 ; a = 13.8277(6) Å, b = 14.1535(7) Å, c = 21.4310(10) Å, α = 71.268(2)°, β = 78.496(2)°, γ = 76.944(2)°, V = 3832.6(3) Å^3; Z = 2, ρ_{calcd} = 1.320 g cm^{-3}; crystal dimensions 0.370 x 0.210 x 0.170 mm; $2\theta_{max}$ = 55.264°; 105451 reflections, 17778 independent (R_{int} = 0.0759, intrinsic phasing; absorption coeff (μ = 0.381 mm^{-1}), absorption correction semi-empirical from equivalents (SADABS); refinement (against F_o^2) with SHELXTL V6.1, 900 parameters, 27 restraints, R_1 = 0.0770 ($I > 2\sigma$) and wR_2 = 0.2327 (all data), Goof = 1.044, residual electron density 3.84/−1.65 Å^{-3}. PLATON was used to find two solvent voids of 229.5 and 291.7 Å^3 containing 58.5 and 65.6 electrons, respectively, that could not be satisfactorily modelled and so were masked using the embedded SQUEEZE protocol.[9]

Crystal structure data for $[(^{Phen}L^{Me,Ph})_3Ru][PF_6]_2$ (CCDC 2054107):

Yellow blocks; $C_{114}H_{94}B_2FeN_3P_3$ 1676.30 g/mol, monoclinic, space group $P2_1/c$; a = 15.2667(14) Å, b = 15.9297(14) Å, c = 40.090(4) Å, $\alpha = \gamma = 90°$, β = 99.585(3)°; V = 9613.5(15) Å^3; Z = 4, ρ_{calcd} = 1.158 g cm^{-3}; crystal dimensions 0.300 x 0.280 x 0.080 mm; $2\theta_{max}$ = 49.99°; 187695 reflections, 16781 independent (R_{int} = 0.0920), intrinsic phasing; absorption coeff (μ = 0.256

mm^{-1}), absorption correction semi-empirical from equivalents (SADABS); refinement (against F_o^2) with SHELXTL V6.1, 1111 parameters, 0 restraints, R_1 = 0.1365 ($I > 2\sigma$) and wR_2 = 0.2693 (all data), Goof = 1.190, residual electron density 0.924/−1.022 $Å^{-3}$. PLATON was used to located two equal solvent voids of 771.9 $Å^3$, occupied by 167.6 electrons each that could not be satisfactorily modelled and so were masked using the embedded SQUEEZE protocol.[9]

Crystal structure data for $[(^{Quin}L^{Me,Ph})_3Ru][PF_6]_2$ (CCDC 2054108):

Yellow plates; $C_{53.19}H_{42.37}Cl_{4.37}N_2P_2Ru$ 1027.51 g/mol, orthorhombic, space group Pccn; a = 33.4946(15) Å, b = 14.0731(7) Å, c = 23.4674(11) Å, $\alpha = \beta = \gamma = 90°$, V = 11061.9(9) $Å^3$; Z = 8, ρ_{calcd} = 1.234 g cm^{-3}; crystal dimensions 0.330 x 0.110 x 0.070 mm; $2\theta_{max}$ = 55.16°; 295194 reflections, 12779 independent (R_{int} = 0.1153), intrinsic phasing; absorption coeff (μ = 0.586 mm^{-1}), absorption correction semi-empirical from equivalents (SADABS); refinement (against F_o^2) with SHELXTL V6.1, 589 parameters, 0 restraints, R_1 = 0.0485 ($I > 2\sigma$) and wR_2 = 0.1294 (all data), Goof = 1.085, residual electron density 0.98/−0.57 $Å^{-3}$.

Mössbauer Spectroscopy

Mössbauer spectroscopy experiments were performed in zero field in a transmission geometry with a 10 GBq ^{57}Co in Rh source and a WissEl constant acceleration drive. Spectra were collected at 10 K using a Janis SHI-850 closed-cycle refrigerator and were calibrated relative to α-Fe at room temperature.

Table S1. ^{57}Fe Mössbauer spectral parameters (10 K).

Compound	δ (mm s^{-1})	ΔE_Q (mm s^{-1})	Line Width (FWHM; mm s^{-1})	Relative Area (%)
$((^{Phen}\mathbf{L}^{H,Ph})FeBr)_2(\mu\text{-}Br)_2$	0.9587(17)	2.954(13)	0.1646(57)	55.6
	0.9530(19)	3.336(13)	0.1510(66)	44.4
$(^{Phen}\mathbf{L}^{Me,Ph})FeBr_2$	0.8047(13)	2.9591(25)	0.1380(20)	100
$(^{Phen}\mathbf{L}^{Me,iPr})FeBr_2$	0.8095(11)	3.1539(23)	0.1434(18)	100
$[(^{Phen}\mathbf{L}^{Me,Ph})_3Fe][PF_6]_2$	0.4535(12)	0.2792(19)	0.1353(17)	100
$[(^{Quin}\mathbf{L}^{Me,Ph})_3Fe][PF_6]_2$	0.4642(46)	0.289(11)	0.2234(89)	100

Computational Methodology

Calculations were performed using Gaussian 16, Rev. C.01[10], and at the density functional level of theory with the restricted Kohn-Sham formalism. Cartesian coordinates from solid-state structures were used as starting input, and solvent effects were accounted implicitly using the solvation model based on density (SMD[11]; solvent = CH_3CN). Singlet ground-state geometry optimizations for $[(^{\mathbf{Phen}}\mathbf{L}^{\mathbf{Me,Ph}})_3Fe]^{2+}$ and $[(^{\mathbf{Quin}}\mathbf{L}^{\mathbf{Me,Ph}})_3Fe]^{2+}$ were carried out with the dispersion corrected (D3-BJ[12]) B3LYP[13–16] functional and def2-SVP[17] basis sets on all atoms [*i.e.* SMD-rB3LYP-D3(BJ)/def2-SVP]. The absence of imaginary frequencies confirm that all optimized geometries were at minima. Time-dependent DFT (TDDFT) single point calculations at the optimized singlet ground state geometries were subsequently performed to simulate the UV-Vis spectra of the complexes in acetonitrile. A total of 100 excited singlet states were considered to cover the visible and a portion of the UV regions of the electromagnetic spectrum. All single point calculations, including TDDFT, were conducted using the meta-hybrid GGA functional TPSSh[18,19] (HF = 10%) and the def2-SVP[17] basis sets on all atoms. Relevant ground state molecular orbitals (MOs) were generated using Avogadro. Simulated UV-Vis spectra from TDDFT calculated vertical excitation energies were generated with the GaussSum package.[20] Electron-hole density maps of relevant excited states, and population analysis on all presented MOs were generated using Multiwfn.[21]

To further understand the effect of benzannulation to the electronic structure of the complexes, we performed charge decomposition analysis (CDA)[22] on the optimized geometry of $[(^{\mathbf{Phen}}\mathbf{L}^{\mathbf{Me,Ph}})_3Fe]^{2+}$ again using Multiwfn.[21] To simplify the analysis, only a single $^{\mathbf{Phen}}\mathbf{L}^{\mathbf{Me,Ph}}$ ligand was considered using coordinates from the optimized complex geometry. Two fragments were considered (a) $^{\mathbf{Quin}}\mathbf{L}^{\mathbf{Me,Ph}}$ and (b) butadiene in the *cis* configuration. Since these fragments are

bound covalently, the interaction between the fragments was treated as an open-shell case, as described in the Multiwfn manual.[21] Single point calculations were done on these fragments at the SMD-TPSSh/def2-SVP level of theory, both with multiplicity of 3 (S = 1). A single point calculation was also conducted on the $^{\mathbf{Phen}}\mathbf{L}^{\mathbf{Me,Ph}}$ ligand at the same level of theory with multiplicity of 1 (S = 0). CDA was subsequently carried out on $^{\mathbf{Phen}}\mathbf{L}^{\mathbf{Me,Ph}}$ and the two fragments ($^{\mathbf{Quin}}\mathbf{L}^{\mathbf{Me,Ph}}$, *cis*-butadiene) using Multiwfn and an orbital interaction diagram printed out.

Table S2. Selected solid-state and SMD-rB3LYP-D3(BJ)/def2-SVP optimized ground state structural parameters of $[(^{\mathbf{Quin}}\mathbf{L}^{\mathbf{Me,Ph}})_3\mathrm{Fe}]^{2+}$ and $[(^{\mathbf{Phen}}\mathbf{L}^{\mathbf{Me,Ph}})_3\mathrm{Fe}]^{2+}$.

	$[(^{\mathbf{Quin}}\mathbf{L}^{\mathbf{Me,Ph}})_3\mathrm{Fe}]^{2+}$		$[(^{\mathbf{Phen}}\mathbf{L}^{\mathbf{Me,Ph}})_3\mathrm{Fe}]^{2+}$	
Bond / Å	**XRD**	**DFT**	**XRD**	**DFT**
$Fe–N_1$	2.080	2.085	2.076	2.082
$Fe–N_2$	2.080	2.082	2.080	2.083
$Fe–N_3$	2.080	2.065	2.087	2.066
$Fe–P_1$	2.287	2.307	2.298	2.311
$Fe–P_2$	2.287	2.316	2.293	2.309
$Fe–P_3$	2.287	2.324	2.290	2.317
Angle / °	**XRD**	**DFT**	**XRD**	**DFT**
$(N–Fe–N)_{average}$	89.5	90.4	90.4	90.7
$(P–Fe–P)_{average}$	100.5	99.6	100.5	99.9
$(P–Fe–N)_{average}$	171.5	172.7	172.0	172.8

Table S3. Fragment contributions (%) to the ground state MOs of $[(^{\mathbf{Quin}}\mathbf{L}^{\mathbf{Me,Ph}})_3\mathrm{Fe}]^{2+}$ using Hirshfeld atomic population method (SMD-rTPSSh/def2-SVP//SMD-rB3LYP-D3(BJ)/def2-SVP).

MO	Fe	$C=N^{Quin}$	Ar^{Quin}	PPh_2	Me
LUMO+4	42	6	7	45	0
LUMO+3	43	6	6	44	0
LUMO+2	2	23	66	7	1
LUMO+1	2	25	65	6	1
LUMO	2	28	63	6	1
HOMO	78	6	8	8	0
HOMO-1	77	5	8	9	0
HOMO-2	78	5	8	9	0

Table S4. Fragment contributions (%) to the ground state MOs of $[(^{Phen}L^{Me,Ph})_3Fe]^{2+}$ using Hirshfeld atomic population method (SMD-rTPSSh/def2-SVP//SMD-rB3LYP-D3(BJ)/def2-SVP).

MOs	Fe	$C{=}N^{Phen}$	Ar^{Phen}	PPh_2	Me
LUMO+7	36	7	22	35	0
LUMO+6	28	5	35	32	0
LUMO+5	11	4	67	17	1
LUMO+4	11	4	68	17	1
LUMO+3	3	3	82	11	1
LUMO+2	3	32	58	6	1
LUMO+1	3	32	58	6	1
LUMO	2	37	55	4	1
HOMO	77	6	8	8	0
HOMO-1	75	6	9	9	0
HOMO-2	76	6	8	9	0

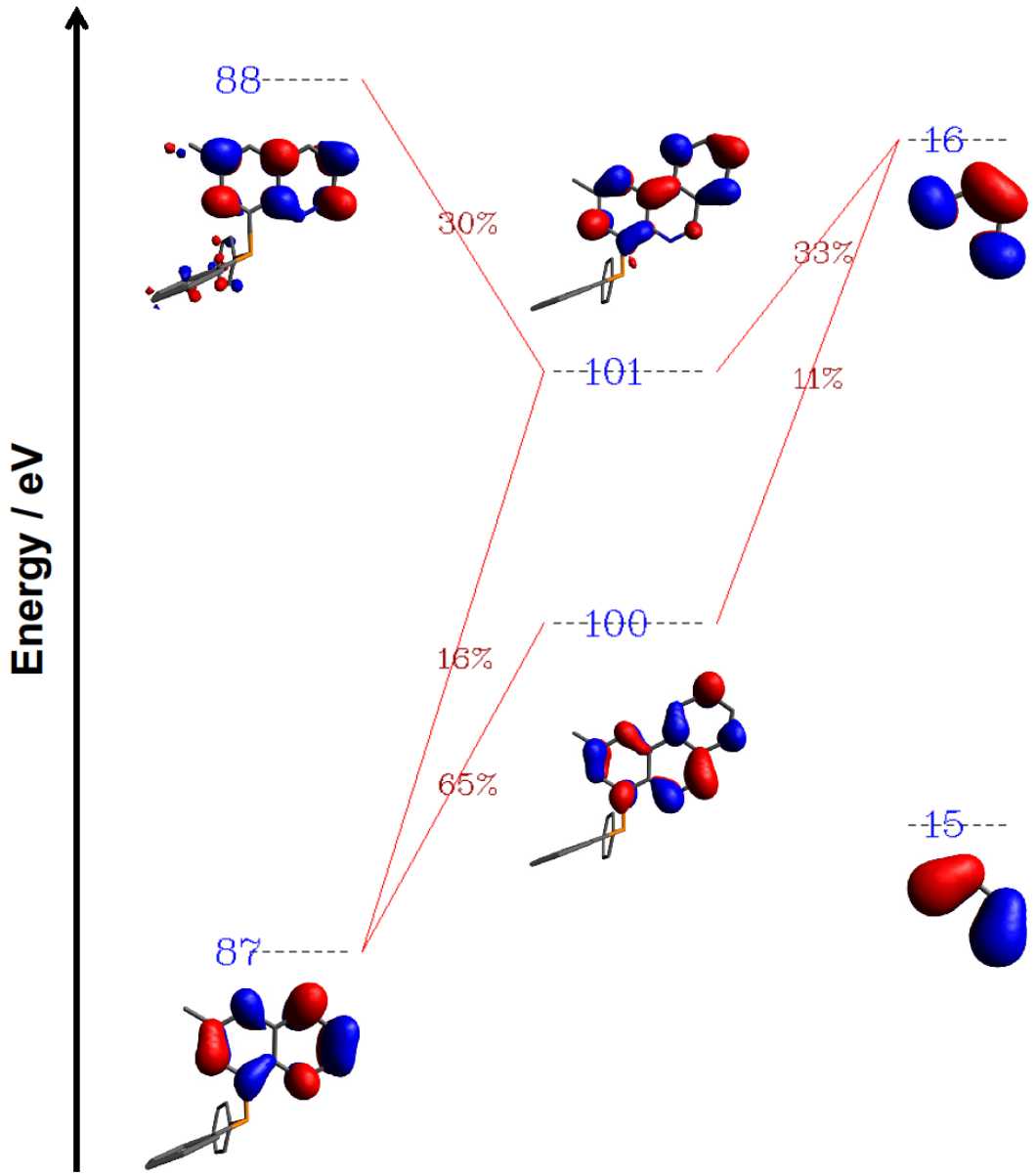

Figure S1. Orbital interaction diagram of relevant $^{Quin}L^{Me,Ph}$ and s-*cis*-butadiene alpha-fragment orbitals, and fragment orbital contributions to the $^{Phen}L^{Me,Ph}$ LUMO (MO 100) and LUMO+1 (MO 101). All isosurface values and fragment orbital contributions are set to 0.04 and >10%, respectively.

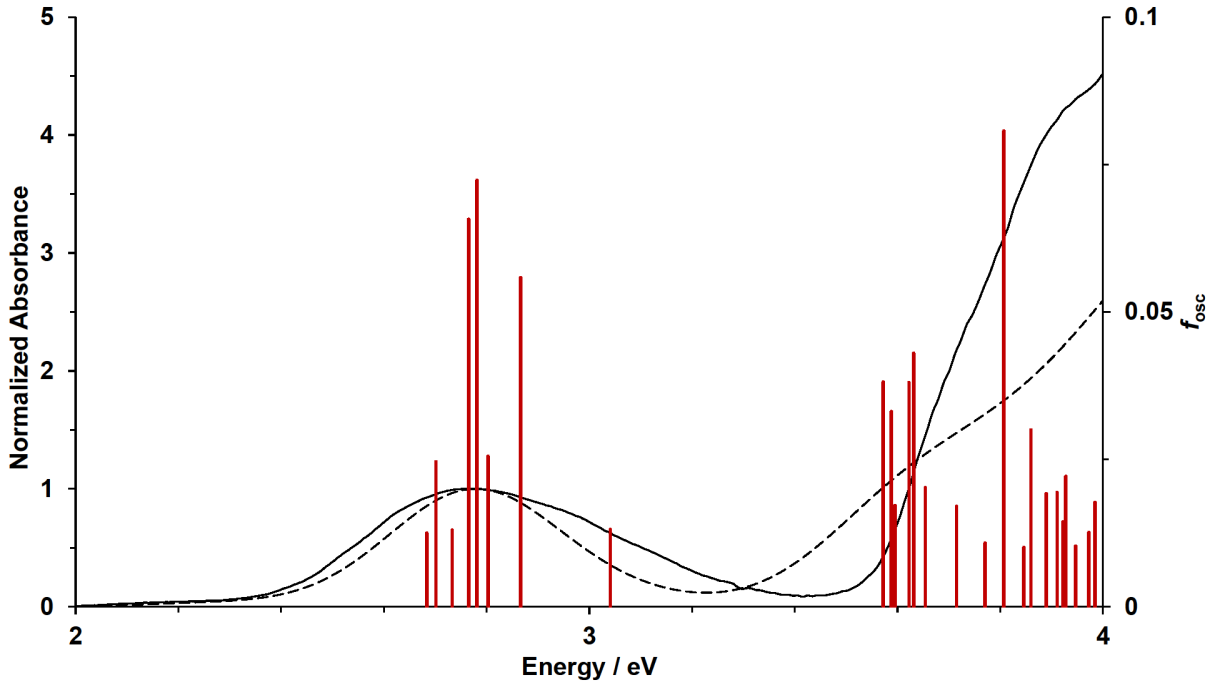

Figure S2. TD-DFT simulated spectrum (---) and calculated vertical excitation energies (red) superimposed on the experimental spectrum (−) of $[(^{Quin}\mathbf{L}^{Me,Ph})_3Fe]^{2+}$ in CH_3CN (SMD-rTPSSh/def2-SVP)//SMD-rB3LYP-D3(BJ)/def2-SVP); FWHM = 3000 cm-1 ; $f_{osc} > 0.01$).

Table S5. TD-DFT predicted vertical excitation energies, oscillator strengths ($f_{osc} > 0.01$) and MO contributions (> 10%) for $[(^{Quin}\mathbf{L}^{Me,Ph})_3Fe]^{2+}$.

No.	E / eV	f_{osc}	Major Contributions
4	2.66	0.004	HOMO→LUMO (75%)
5	2.68	0.013	H-1→LUMO (46%), H-1→L+1 (21%)
6	2.70	0.025	H-2→L+2 (15%), HOMO→L+1 (64%)
7	2.73	0.013	H-2→LUMO (19%), H-2→L+1 (12%), H-2→L+2 (11%), H-1→L+1 (16%), HOMO→L+1 (13%), HOMO→L+2 (10%)
9	2.76	0.066	H-2→LUMO (14%), H-1→LUMO (22%), HOMO→L+2 (42%)
10	2.78	0.072	H-2→LUMO (20%), H-2→L+1 (45%), H-1→LUMO (10%), HOMO→L+2 (10%)
11	2.80	0.026	H-2→L+2 (28%), H-1→L+2 (53%)
12	2.87	0.056	H-2→L+1 (11%), H-2→L+2 (26%), H-1→L+1 (14%), H-1→L+2 (25%)
13	3.04	0.013	H-2→L+3 (50%), HOMO→L+4 (14%)
16	3.57	0.038	H-3→LUMO (92%)
17	3.59	0.033	H-4→LUMO (28%), H-3→L+1 (64%)
18	3.59	0.017	H-4→LUMO (59%), H-3→L+1 (31%)
19	3.62	0.038	H-4→L+1 (88%)
20	3.63	0.043	H-3→L+2 (80%)
21	3.65	0.020	H-4→L+2 (80%)
23	3.71	0.017	H-5→LUMO (89%)
27	3.77	0.011	H-6→LUMO (76%)
29	3.81	0.081	H-5→L+1 (27%), H-5→L+2 (59%)
31	3.85	0.010	H-8→LUMO (25%), H-8→L+1 (12%), H-8→L+2 (14%), H-7→LUMO (22%)
33	3.86	0.030	H-7→L+1 (53%), HOMO→L+6 (13%)
35	3.89	0.019	H-10→LUMO (12%), H-9→LUMO (10%), H-8→L+1 (17%), H-7→LUMO (25%), H-7→L+2 (15%)
38	3.91	0.019	H-9→LUMO (13%), H-7→L+2 (42%), HOMO→L+7 (14%)
40	3.92	0.014	H-1→L+6 (71%)
41	3.93	0.022	H-9→LUMO (10%), H-9→L+1 (35%)
43	3.95	0.010	H-9→L+2 (16%), H-1→L+7 (14%), HOMO→L+8 (31%)
46	3.97	0.013	H-10→LUMO (18%), H-1→L+7 (29%), HOMO→L+8 (12%)
48	3.98	0.018	H-11→LUMO (14%), H-10→L+2 (16%), H-9→L+2 (20%), H-1→L+7 (16%), HOMO→L+8 (10%)

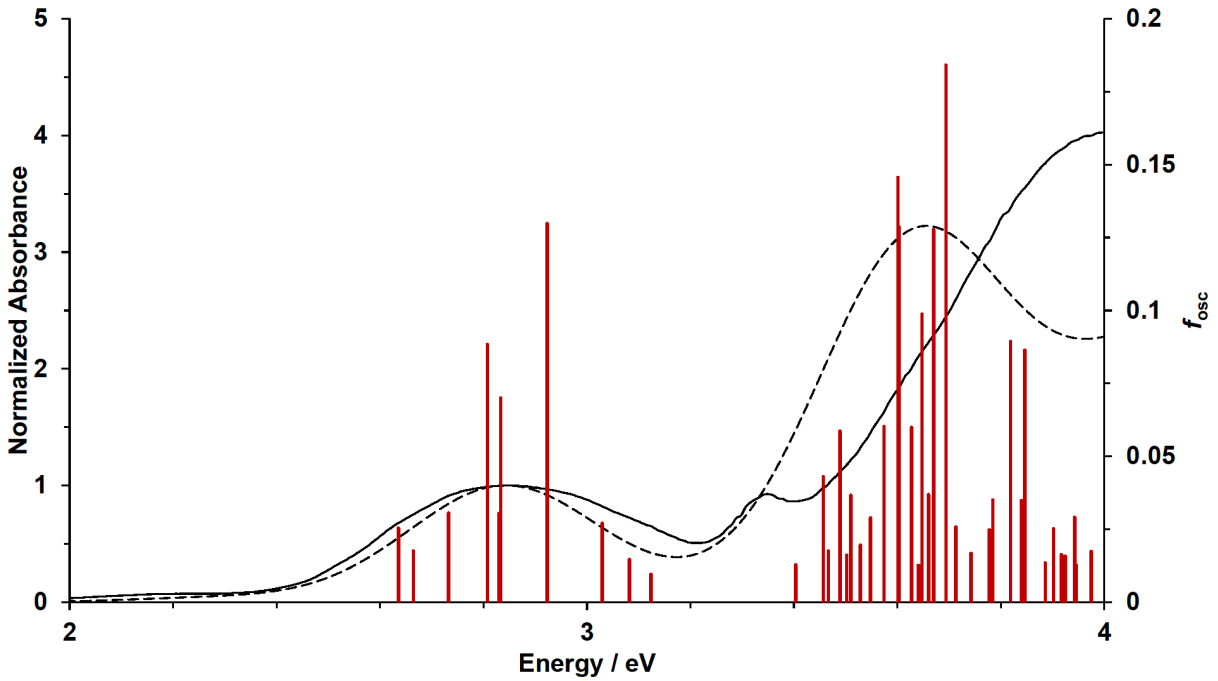

Figure S3. TD-DFT simulated spectrum (---) and calculated vertical excitation energies (red) superimposed on the experimental spectrum (−) of $[(^{Phen}\mathbf{L}^{Me,Ph})_3Fe]^{2+}$ in CH_3CN (SMD-rTPSSh/def2-SVP)//SMD-rB3LYP-D3(BJ)/def2-SVP); FWHM = 3000 cm-1 ; $f_{osc} > 0.01$).

Table S6. TD-DFT predicted vertical excitation energies, oscillator strengths ($f_{osc} > 0.01$) and MO contributions (> 10%) for $[(^{Phen}\mathbf{L}^{Me,Ph})_3Fe]^{2+}$.

No.	E / eV	f_{osc}	Major Contributions
4	2.64	0.025	HOMO→LUMO (81%)
5	2.66	0.018	H-1→LUMO (77%)
7	2.73	0.031	H-2→LUMO (29%), HOMO→L+1 (46%)
9	2.81	0.088	H-2→L+2 (10%), H-1→L+1 (25%), HOMO→L+1 (16%), HOMO→L+2 (27%)
10	2.83	0.030	H-2→L+1 (33%), H-1→L+2 (18%), HOMO→L+2 (28%)
11	2.83	0.070	H-1→L+2 (49%), HOMO→L+2 (27%)
12	2.92	0.130	H-2→L+2 (42%), H-1→L+1 (37%)
13	3.03	0.027	H-2→L+1 (10%), H-2→L+5 (11%), H-2→L+6 (24%)
14	3.08	0.015	H-2→L+2 (18%), H-2→L+7 (22%), HOMO→L+6 (11%)
15	3.12	0.010	H-1→L+4 (19%), H-1→L+7 (41%)
18	3.40	0.013	H-1→L+3 (36%), HOMO→L+4 (29%)
21	3.46	0.043	H-3→LUMO (48%), H-1→L+5 (14%)

22	3.47	0.018	H-3→LUMO (17%), H-1→L+4 (14%)
23	3.49	0.059	H-4→LUMO (24%), H-1→L+5 (27%)
24	3.50	0.016	H-5→LUMO (15%), H-4→LUMO (20%), H-2→L+5 (20%)
25	3.51	0.037	H-4→LUMO (22%), H-2→L+5 (26%), H-2→L+6 (10%), H-1→L+4 (13%)
26	3.53	0.020	H-6→LUMO (25%), H-5→LUMO (36%), H-1→L+4 (11%)
28	3.55	0.029	H-6→LUMO (50%), H-5→LUMO (35%)
29	3.57	0.060	H-3→L+1 (84%)
31	3.60	0.146	H-4→L+1 (33%), H-3→L+2 (38%)
32	3.60	0.129	H-4→L+1 (41%), H-3→L+2 (29%)
33	3.63	0.060	H-4→L+2 (83%)
34	3.64	0.013	H-6→L+1 (15%), H-5→L+1 (65%)
35	3.65	0.099	H-6→L+1 (70%), H-5→L+1 (10%)
36	3.66	0.037	H-8→LUMO (36%), H-5→L+2 (48%)
37	3.67	0.128	H-8→LUMO (12%), H-6→L+2 (68%)
38	3.69	0.184	H-8→LUMO (29%), H-6→L+2 (14%), H-5→L+2 (41%)
39	3.71	0.026	H-7→L+1 (84%)
40	3.74	0.017	H-7→L+2 (87%)
41	3.78	0.025	H-8→L+1 (78%)
42	3.78	0.035	H-9→LUMO (72%)
43	3.82	0.089	H-8→L+2 (86%)
44	3.84	0.035	H-11→LUMO (62%), H-10→LUMO (15%)
45	3.85	0.086	H-11→LUMO (20%), H-10→LUMO (60%)
47	3.89	0.013	H-13→LUMO (14%), H-12→LUMO (38%), H-10→LUMO (10%)
48	3.90	0.025	H-12→LUMO (10%), H-9→L+1 (58%), H-9→L+2 (17%)
49	3.92	0.016	H-13→LUMO (36%), H-12→LUMO (23%)
50	3.92	0.016	H-14→LUMO (44%), H-11→L+2 (17%)
51	3.94	0.029	H-10→L+1 (15%), H-9→L+2 (17%), H-1→L+8 (45%)
52	3.95	0.013	H-11→L+1 (27%), H-10→L+1 (23%), H-1→L+8 (35%)
55	3.97	0.017	H-13→LUMO (12%), HOMO→L+9 (51%)

State	Electron-Hole Density Map	Character Assignment
5	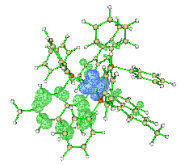	MLCT
6	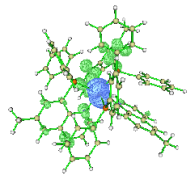	MLCT
7	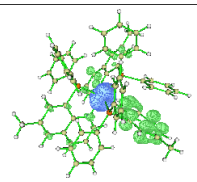	MLCT
9	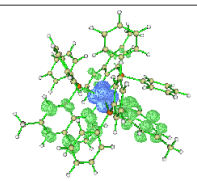	MLCT
10	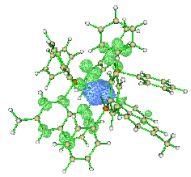	MLCT
11	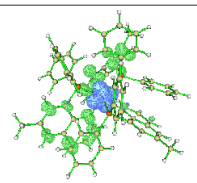	MLCT
12	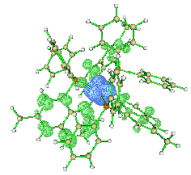	MLCT
13	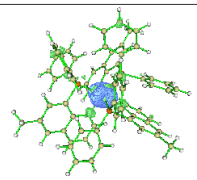	MC

Figure S4. Electron-hole density maps and characters of the relevant electronic excitations (f_{osc} > 0.01; isosurface = 0.002) in the lowest energy absorption band of $[(^{Quin}\mathbf{L}^{Me,Ph})_3Fe]^{2+}$.

State	Electron-Hole Density Map	Character Assignment
4	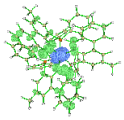	MLCT
5	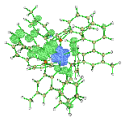	MLCT
7	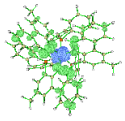	MLCT
9	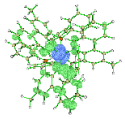	MLCT
10	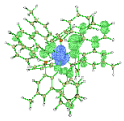	MLCT
11	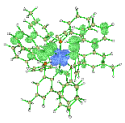	MLCT
12	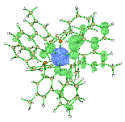	MLCT
13	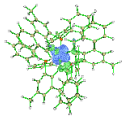	MC
14	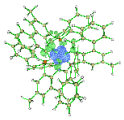	MC
15	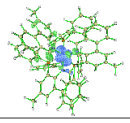	MC

Figure S5. Electron-hole density maps and characters of the relevant electronic excitations (f_{osc} > 0.01; isosurface = 0.002) in the lowest energy absorption band of $[(^{\mathbf{Phen}}\mathbf{L}^{\mathbf{Me,Ph}})_3Fe]^{2+}$.

NMR SPECTRA

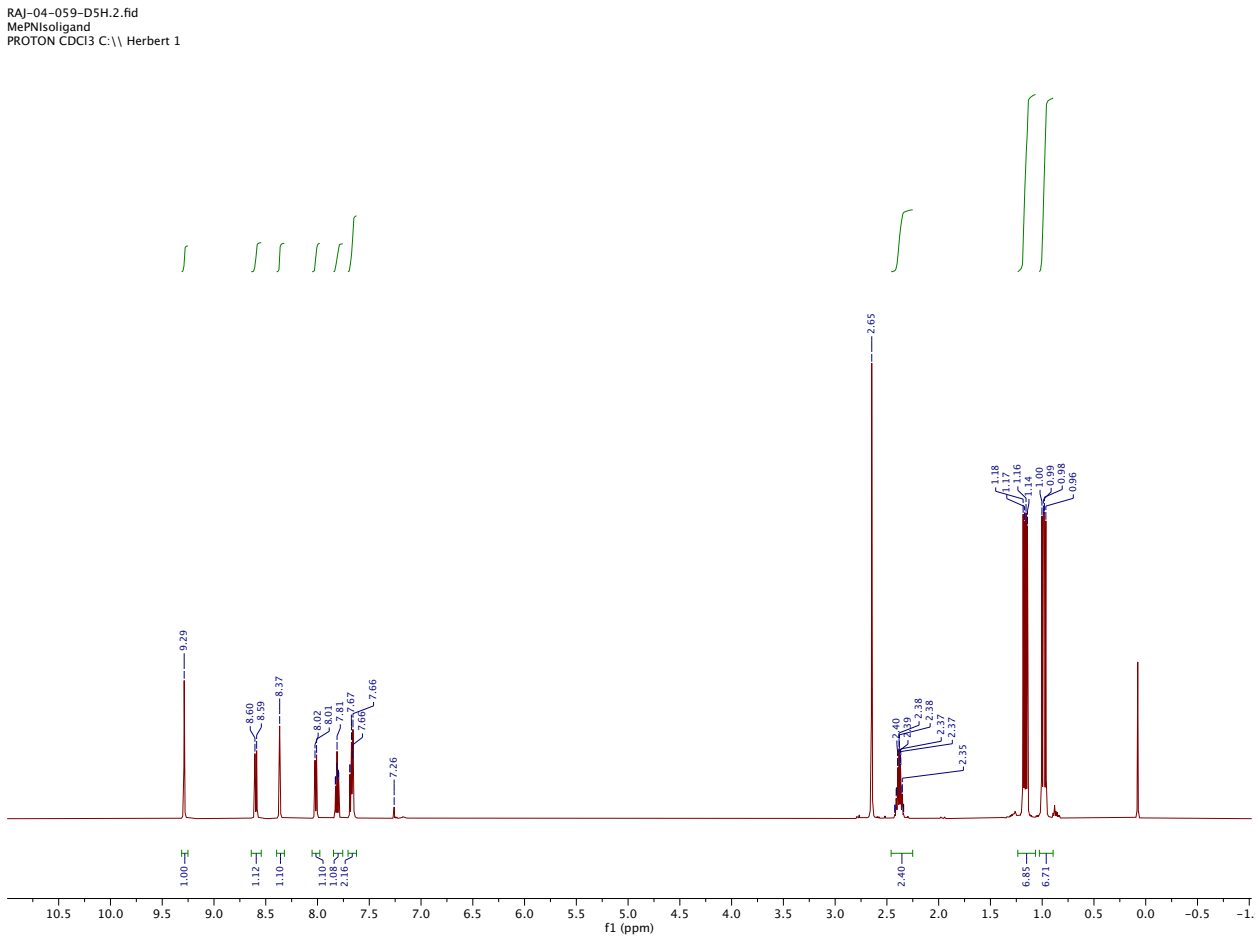

Figure S6. ^{1}H NMR (500 MHz, 22°C, $CDCl_3$) of $^{\mathbf{Phen}}\mathbf{L}^{\mathbf{Me,}\mathit{i}\mathbf{Pr}}$.

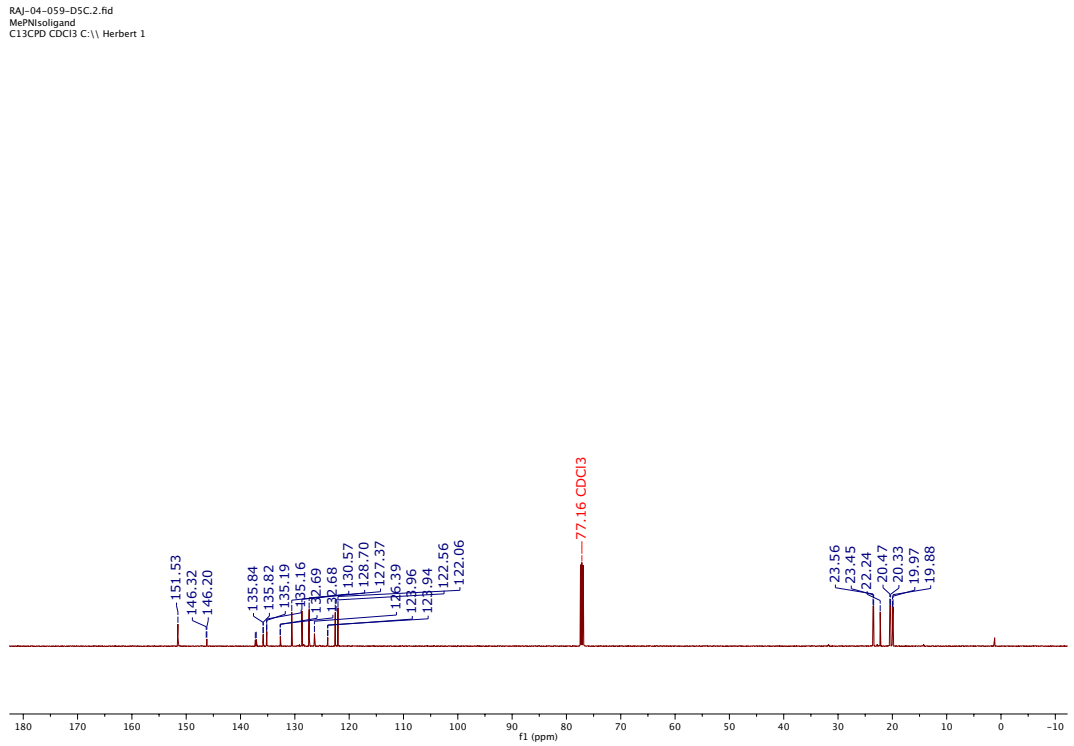

Figure S7. ^{13}C NMR (126 MHz, 22°C, $CDCl_3$) of $^{\mathbf{Phen}}\mathbf{L}^{\mathbf{Me,}\mathit{i}\mathbf{Pr}}$.

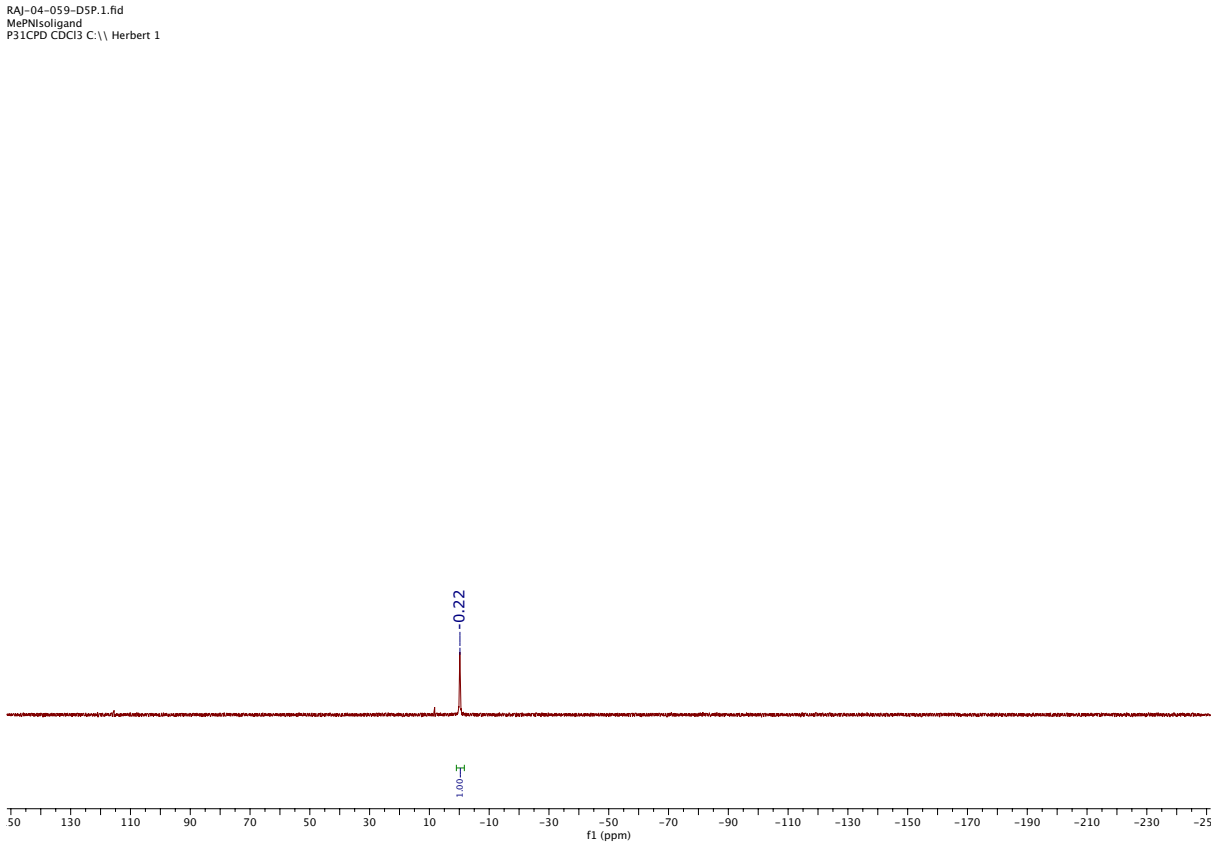

Figure S8. ^{31}P NMR (202 MHz, 22°C, $CDCl_3$) of $^{\mathbf{Phen}}\mathbf{L}^{\mathbf{Me,}\mathit{i}\mathbf{Pr}}$.

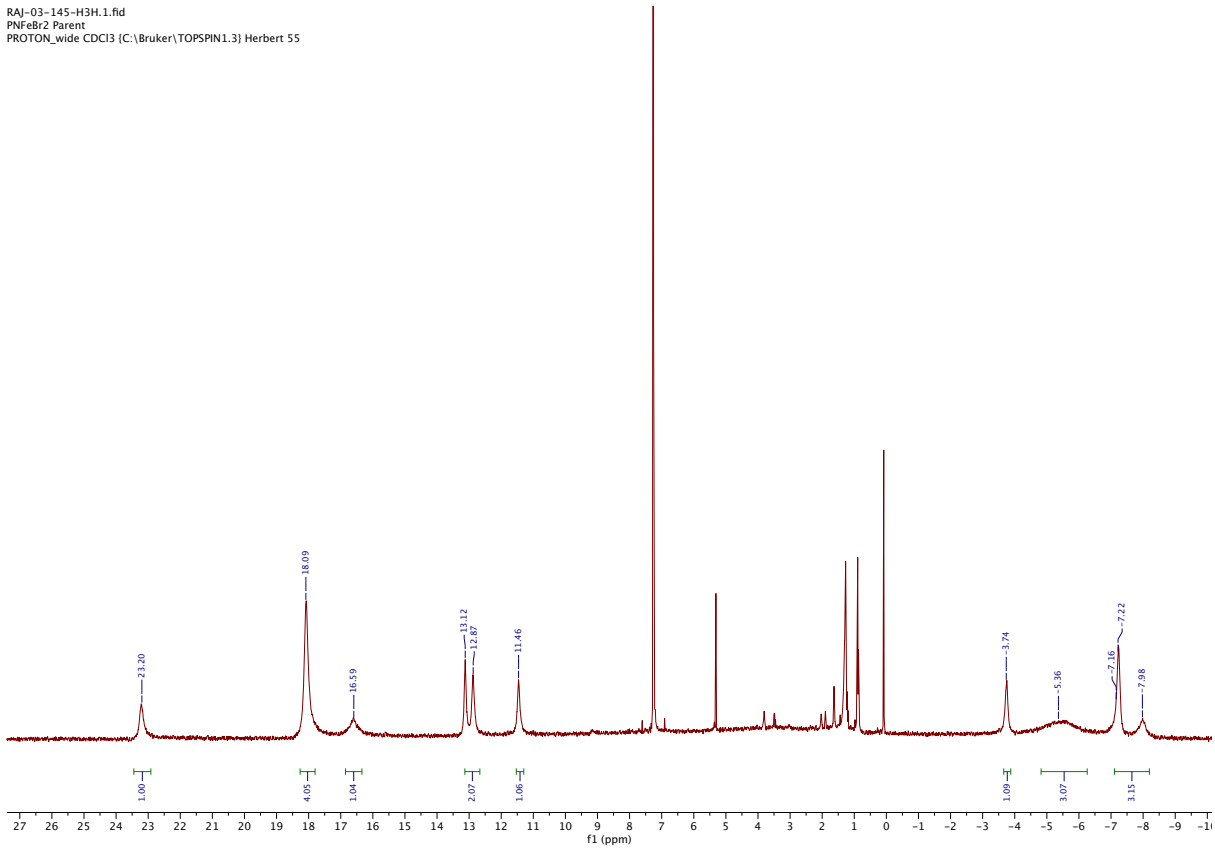

Figure S9. ^{1}H NMR (300 MHz, 22°C, $CDCl_3$) of (($^{\mathbf{Phen}}\mathbf{L}^{\mathbf{H,Ph}}$)FeBr)$_2$(μ-Br)$_2$.

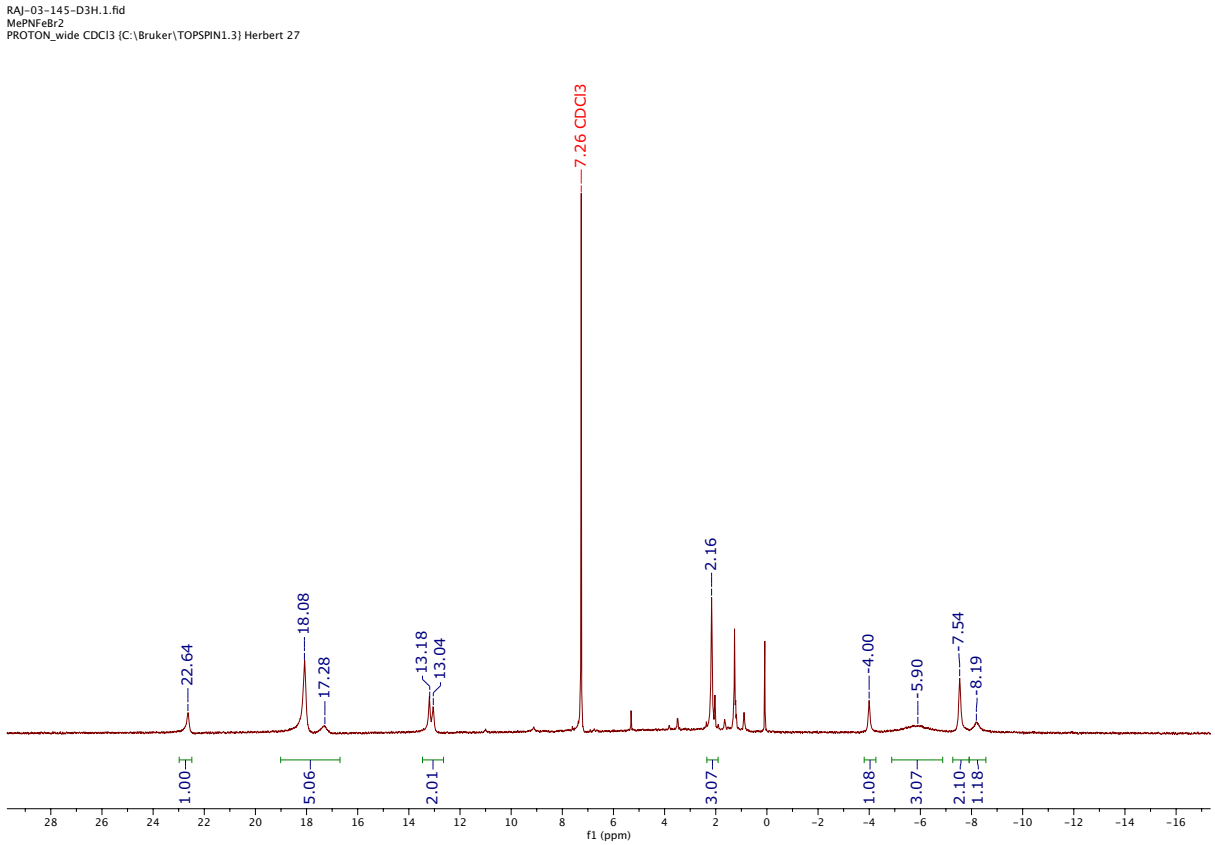

Figure S10. ^{1}H NMR (300 MHz, 22°C, $CDCl_3$) of ($^{\mathbf{Phen}}\mathbf{L}^{\mathbf{Me,Ph}}$)$FeBr_2$.

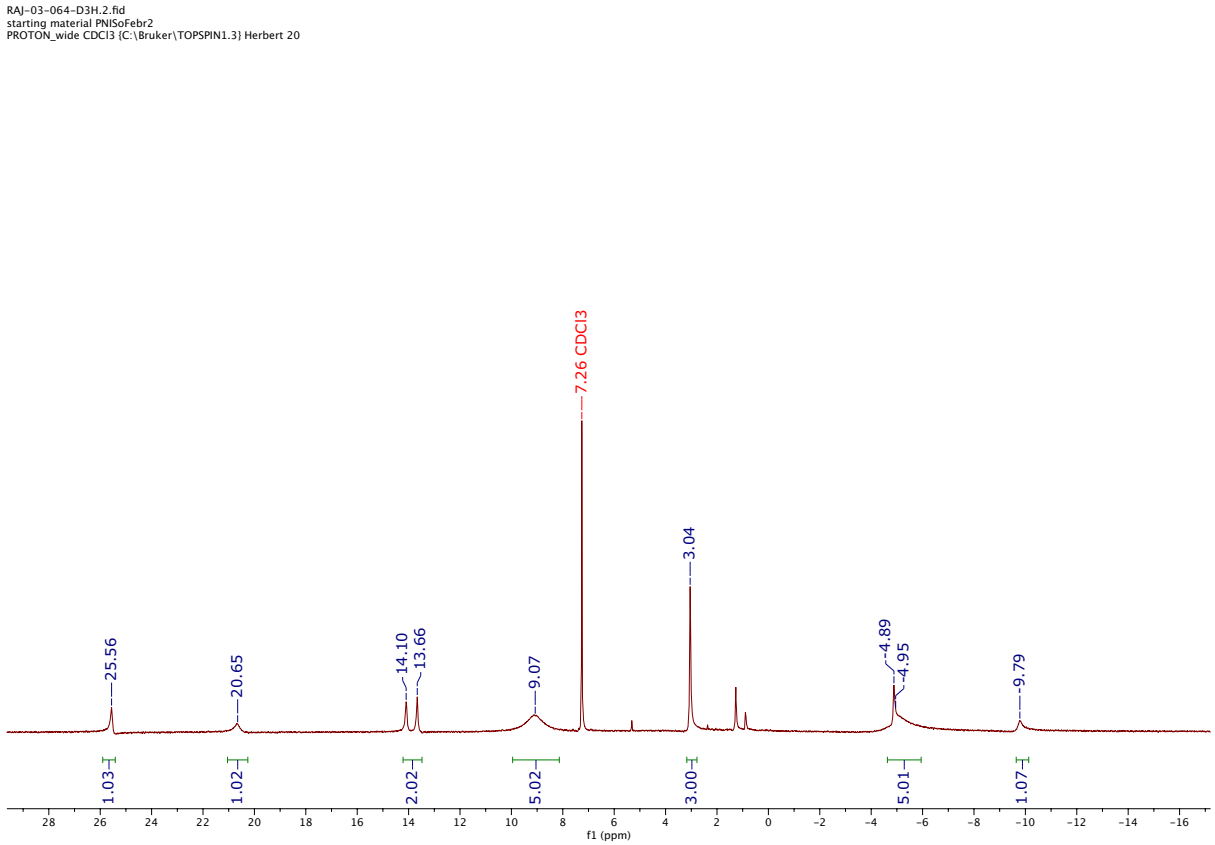

Figure S11. ^{1}H NMR (300 MHz, 22°C, $CDCl_3$) of ($^{\mathbf{Phen}}\mathbf{L}^{\mathbf{Me},\mathit{i}\mathbf{Pr}}$)$FeBr_2$.

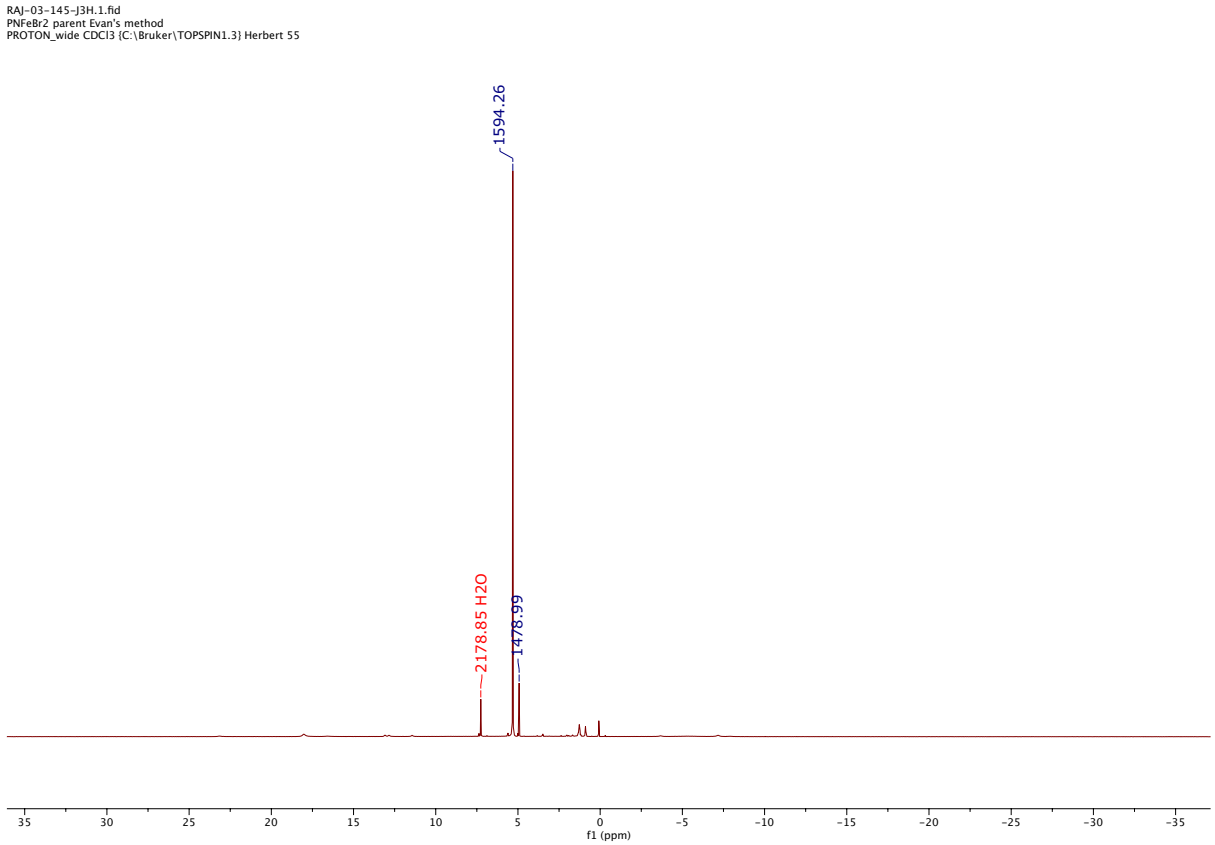

Figure S12. Evans' method ^{1}H NMR spectrum (300 MHz, 22°C, $CDCl_3$) of (($^{\mathbf{Phen}}\mathbf{L}^{\mathbf{H,Ph}}$)FeBr)$_2$(μ-Br)$_2$ using CH_2Cl_2.

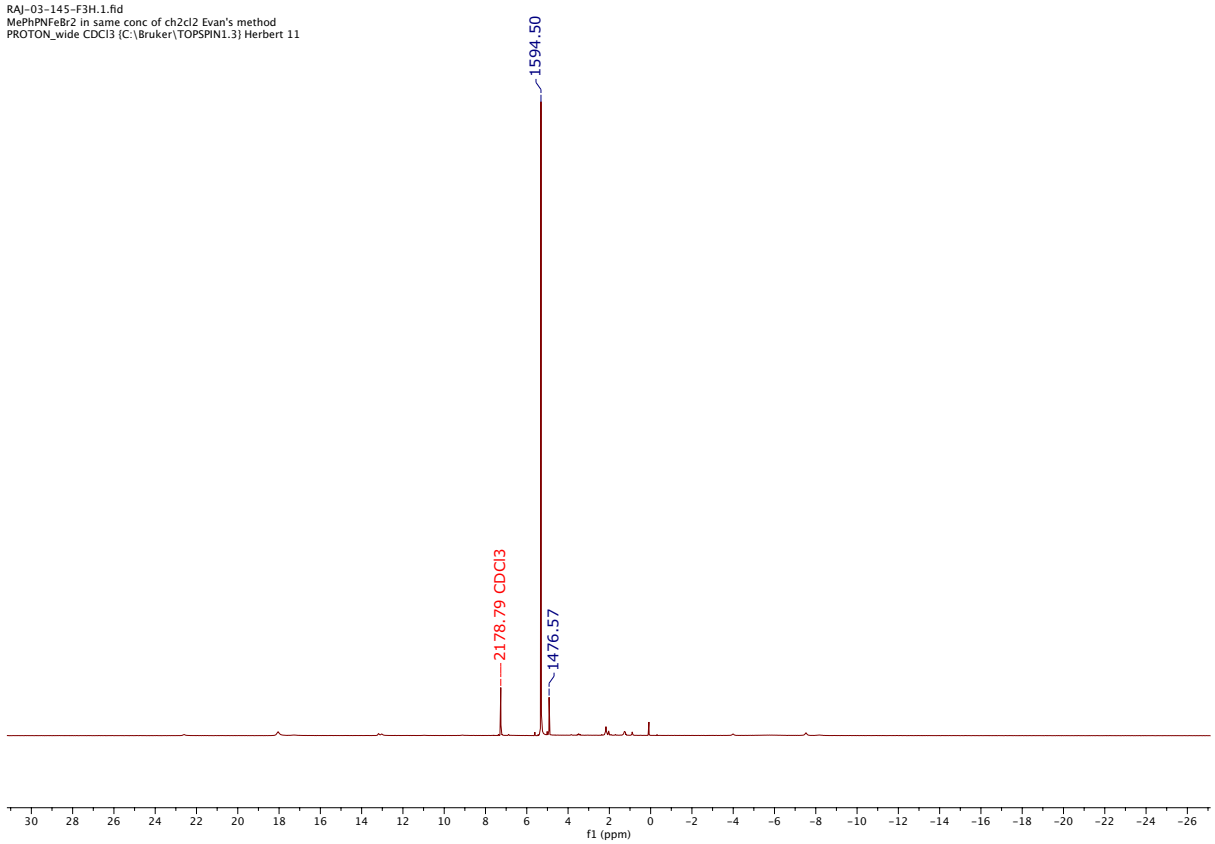

Figure S13. Evans' method ^{1}H NMR spectrum (300 MHz, 22°C, $CDCl_3$) of ($^{\mathbf{Phen}}\mathbf{L}^{\mathbf{Me,Ph}}$)$FeBr_2$ using CH_2Cl_2.

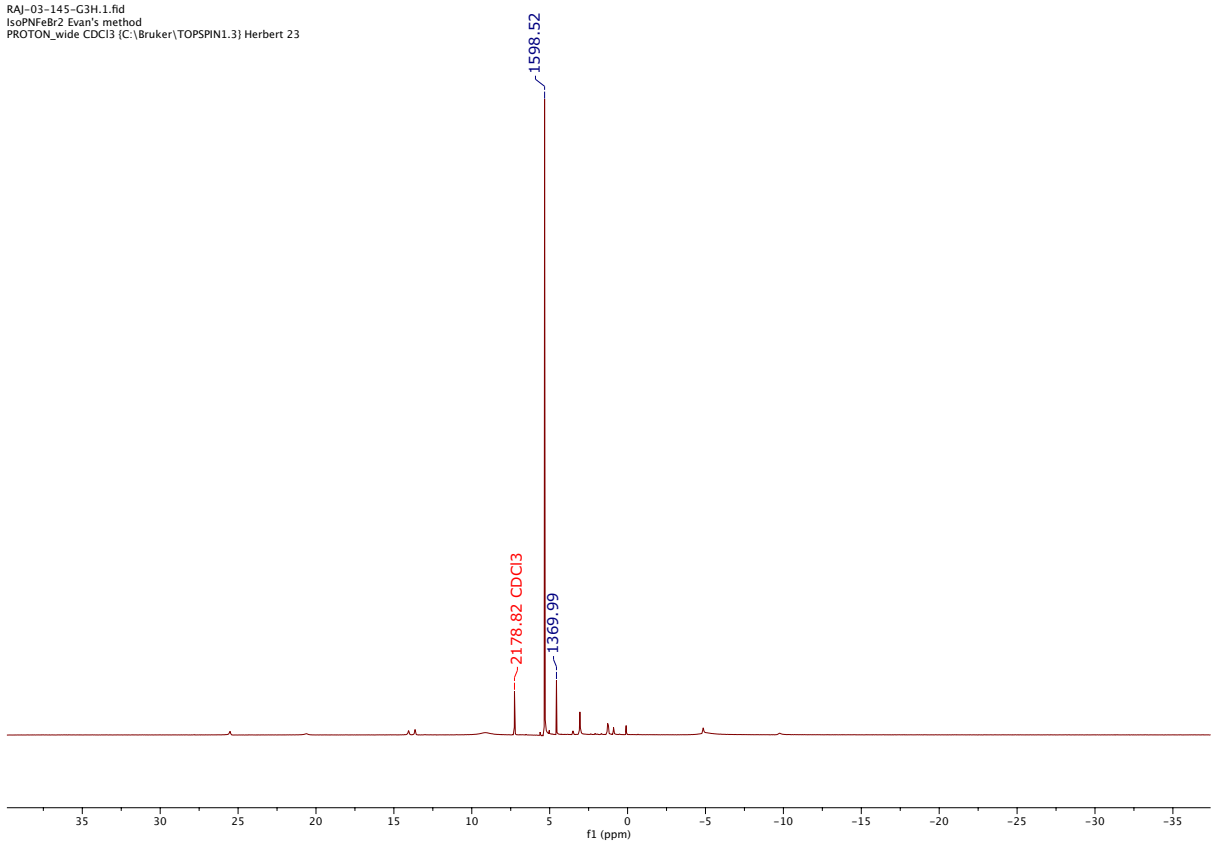

Figure S14. Evans' method ^{1}H NMR spectrum (300 MHz, 22°C, $CDCl_3$) of ($^{\mathbf{Phen}}\mathbf{L}^{\mathbf{Me,}\mathit{i}\mathbf{Pr}}$)$FeBr_2$ using CH_2Cl_2.

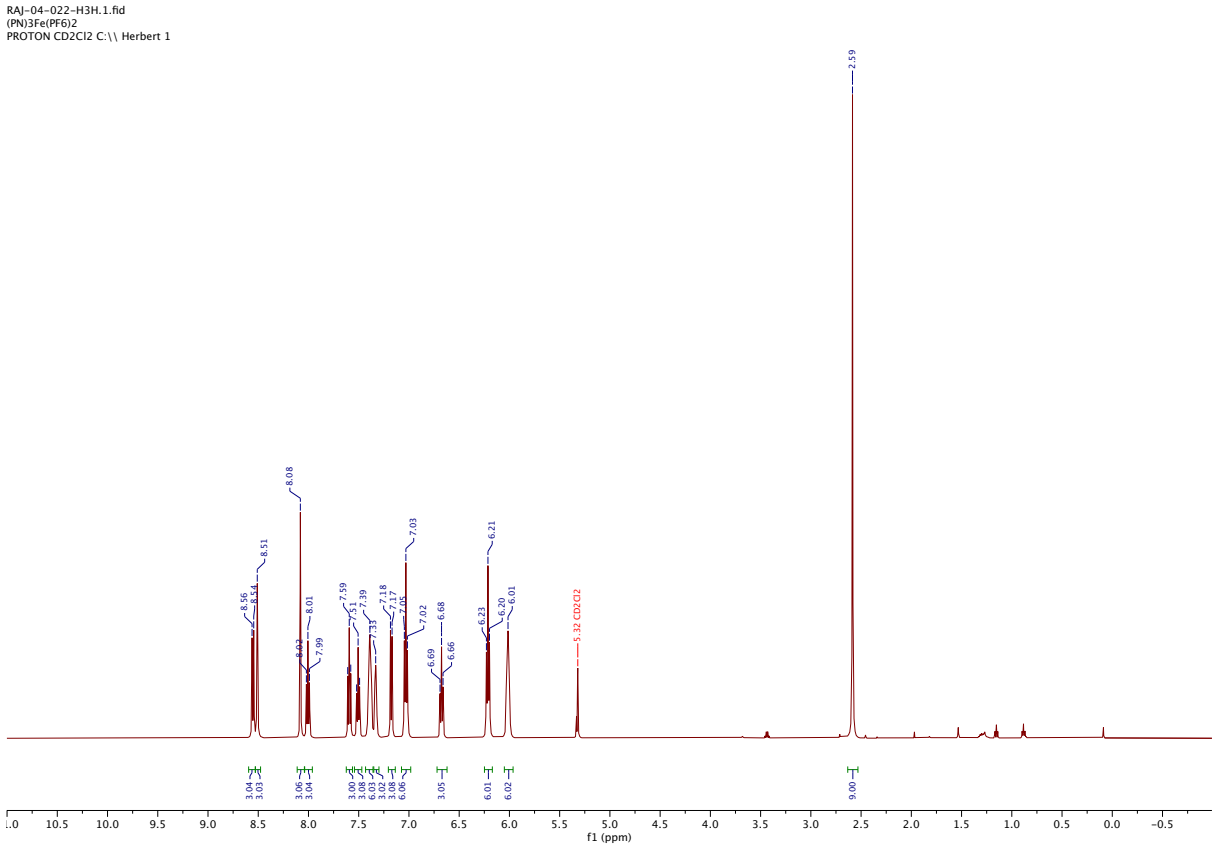

Figure S15. ^{1}H NMR (500 MHz, 22°C, CD_2Cl_2) of $[(^{\mathbf{Phen}}\mathbf{L}^{\mathbf{Me,Ph}})_3Fe][PF_6]_2$.

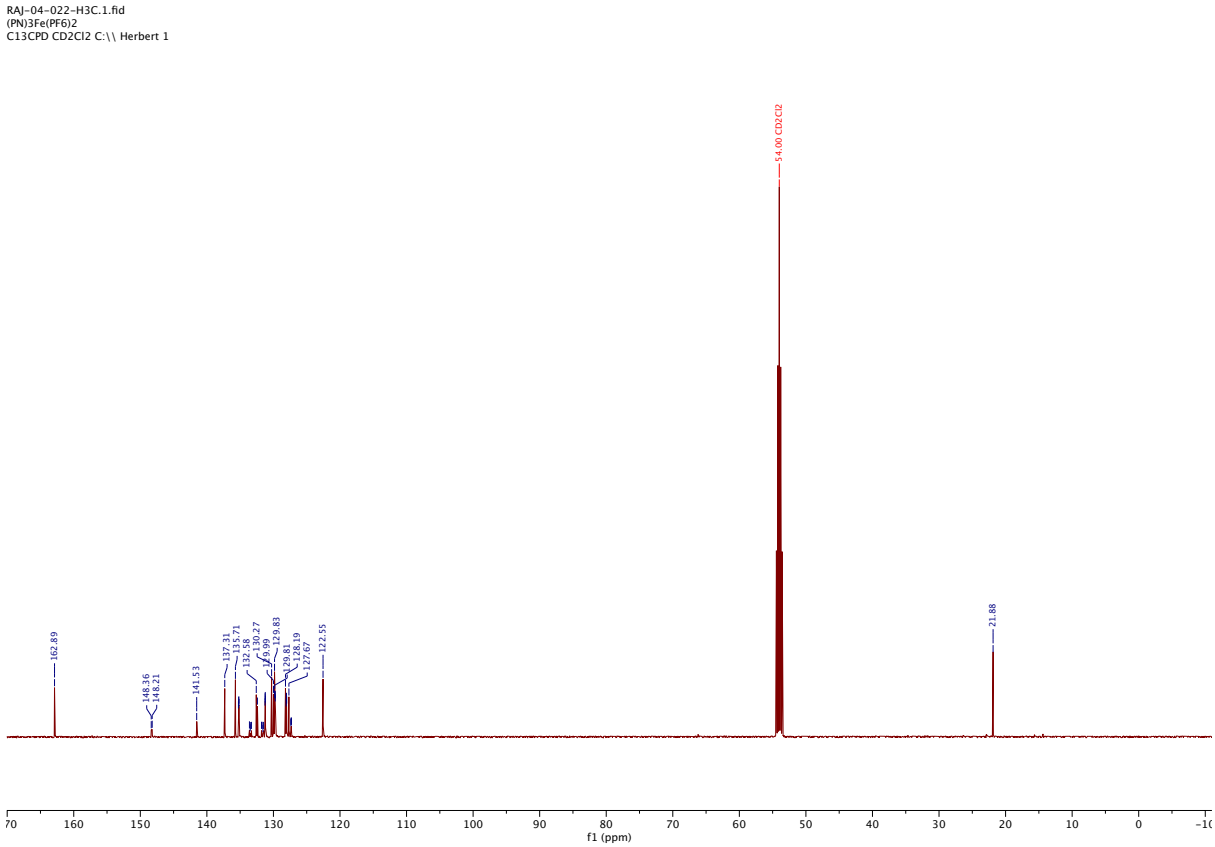

Figure S16. $^{13}C\{^{1}H\}$ NMR (126 MHz, 22°C, CD_2Cl_2) of $[(^{\mathbf{Phen}}\mathbf{L}^{\mathbf{Me,Ph}})_3Fe][PF_6]_2$.

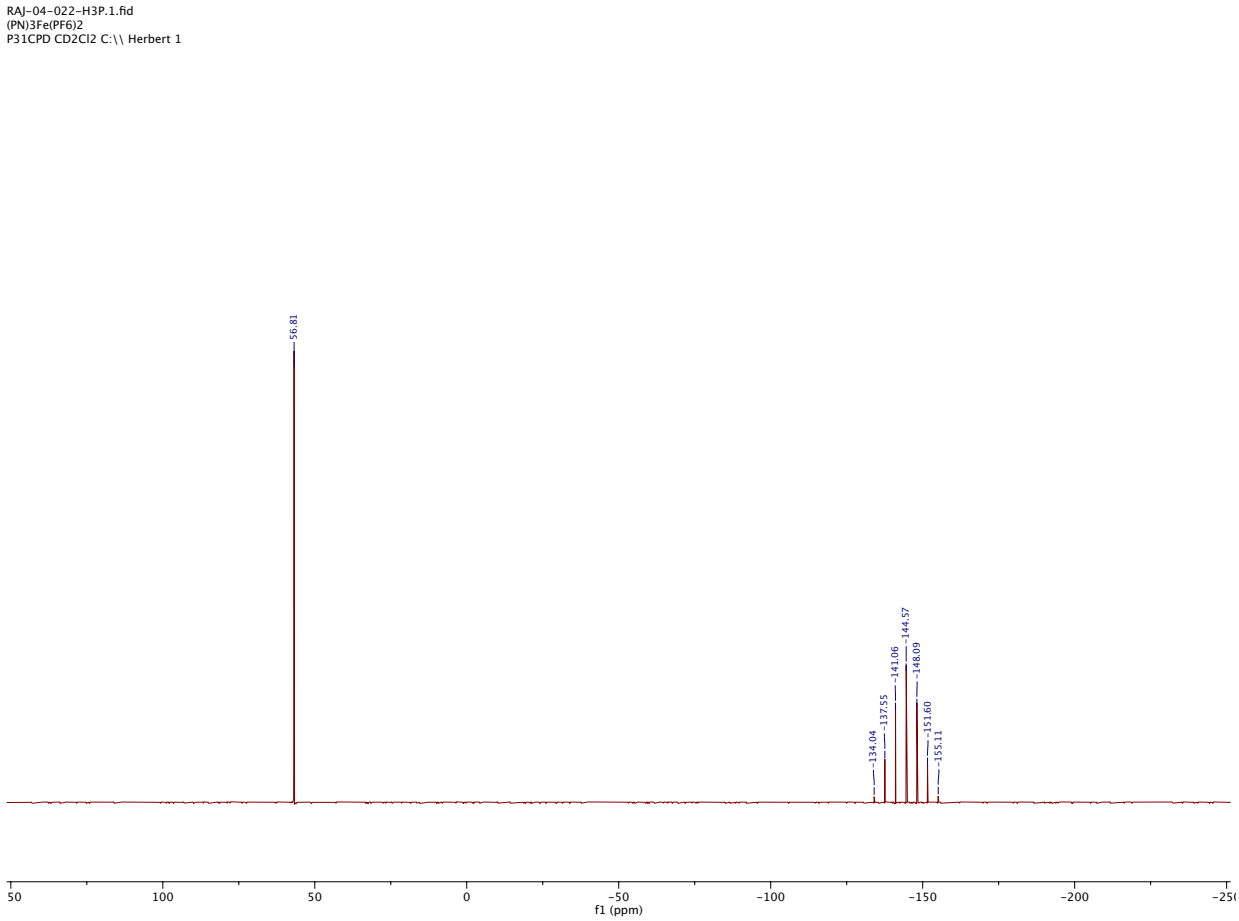

Figure S17. $^{31}P\{^{1}H\}$ NMR (202 MHz, 22°C, CD_2Cl_2) of $[(^{\mathbf{Phen}}\mathbf{L}^{\mathbf{Me,Ph}})_3Fe][PF_6]_2$.

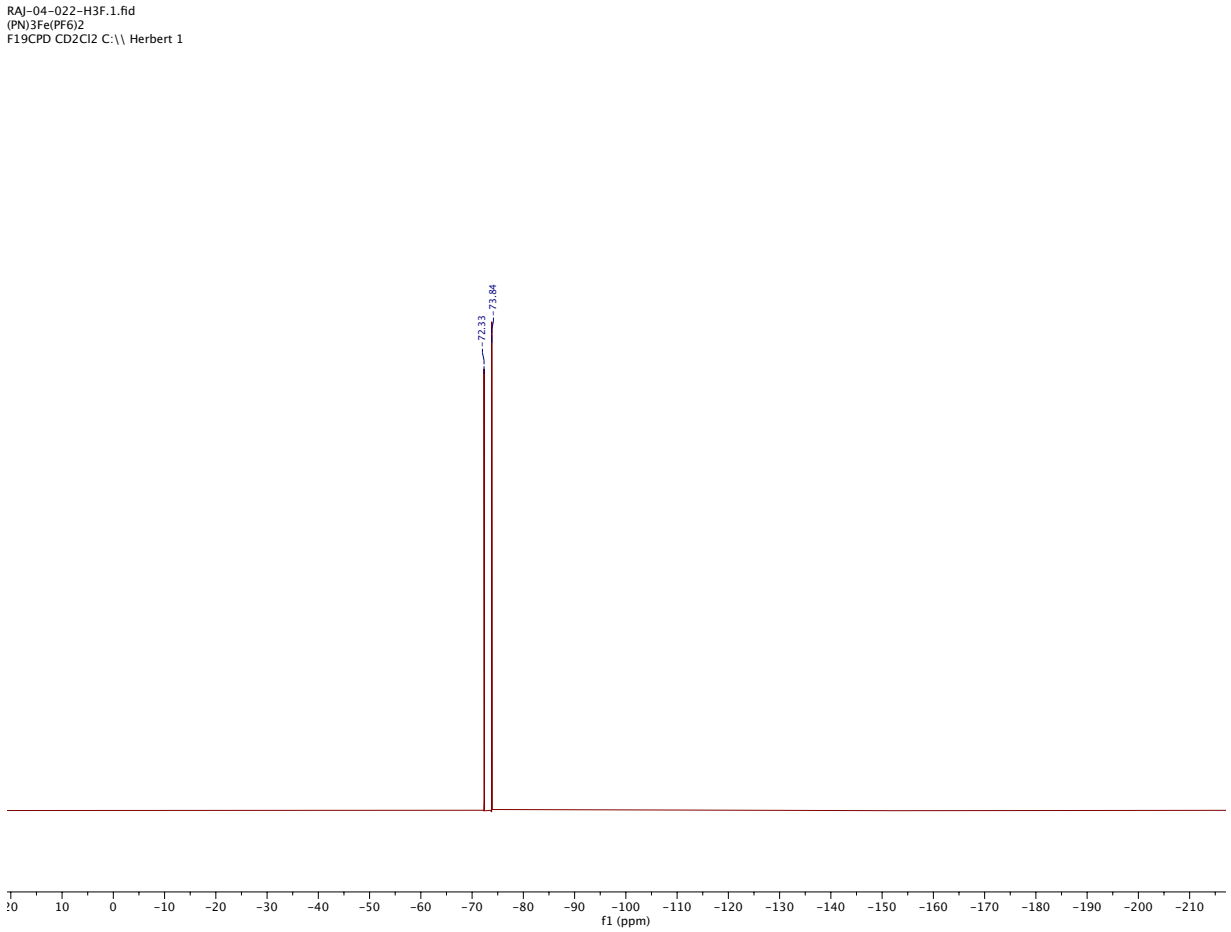

Figure S18. ^{19}F NMR (470 MHz, 22°C, CD_2Cl_2) of $[(^{\mathbf{Phen}}\mathbf{L}^{\mathbf{Me,Ph}})_3Fe][PF_6]_2$.

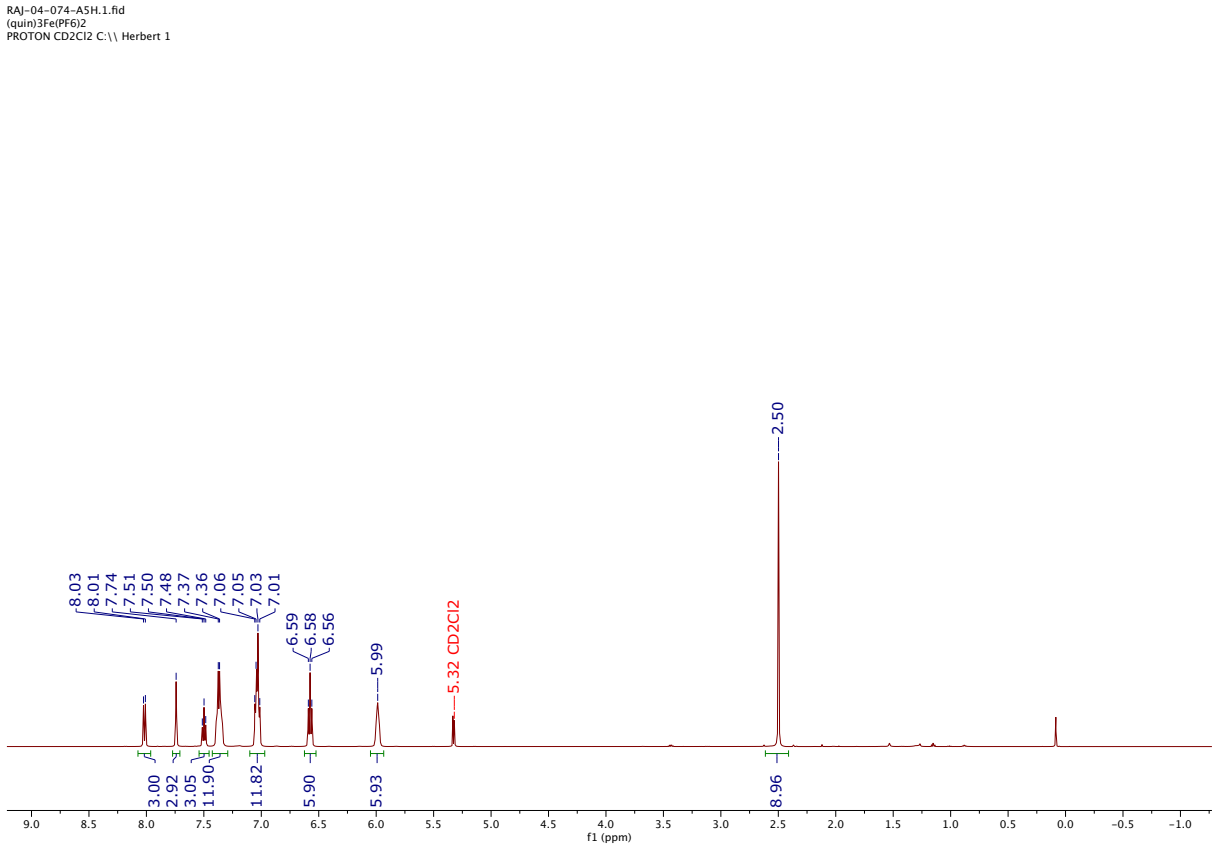

Figure S19. ^{1}H NMR (500 MHz, 22°C, CD_2Cl_2) of $[(^{\mathbf{Quin}}\mathbf{L}^{\mathbf{Me,Ph}})_3Fe][PF_6]_2$.

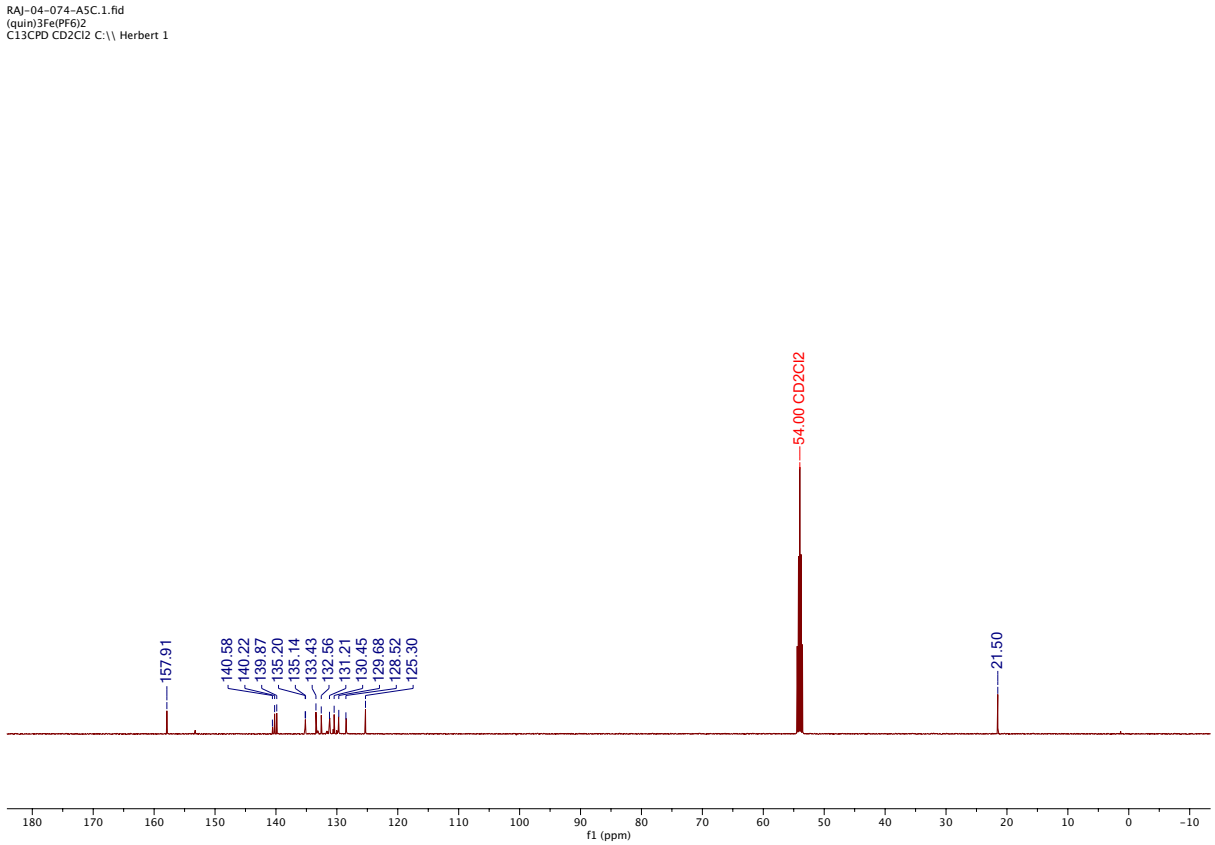

Figure S20. $^{13}C\{^{1}H\}$ NMR (126 MHz, 22°C, CD_2Cl_2) of $[(^{\mathbf{Quin}}\mathbf{L}^{\mathbf{Me,Ph}})_3Fe][PF_6]_2$.

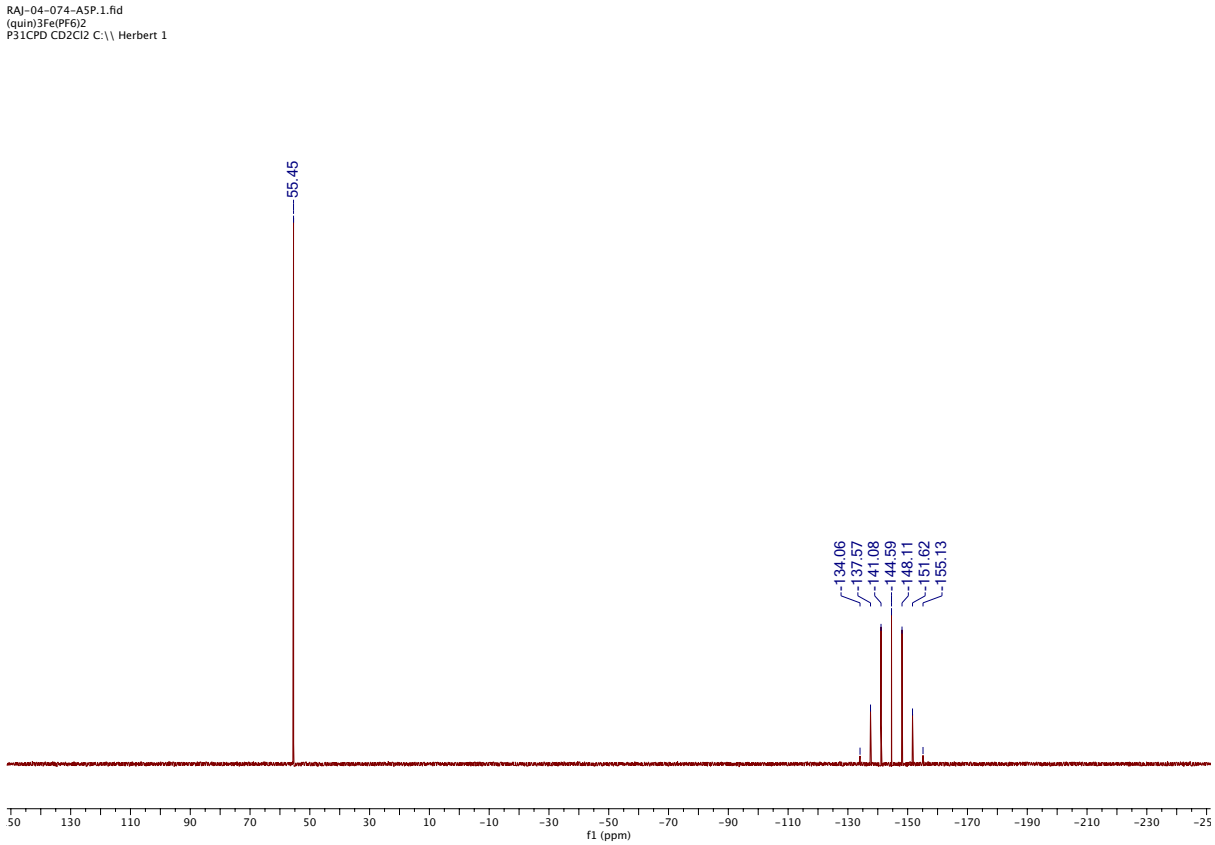

Figure S21. ^{31}P NMR (202 MHz, 22°C, CD_2Cl_2) of $[(^{\mathbf{Quin}}\mathbf{L}^{\mathbf{Me,Ph}})_3Fe][PF_6]_2$.

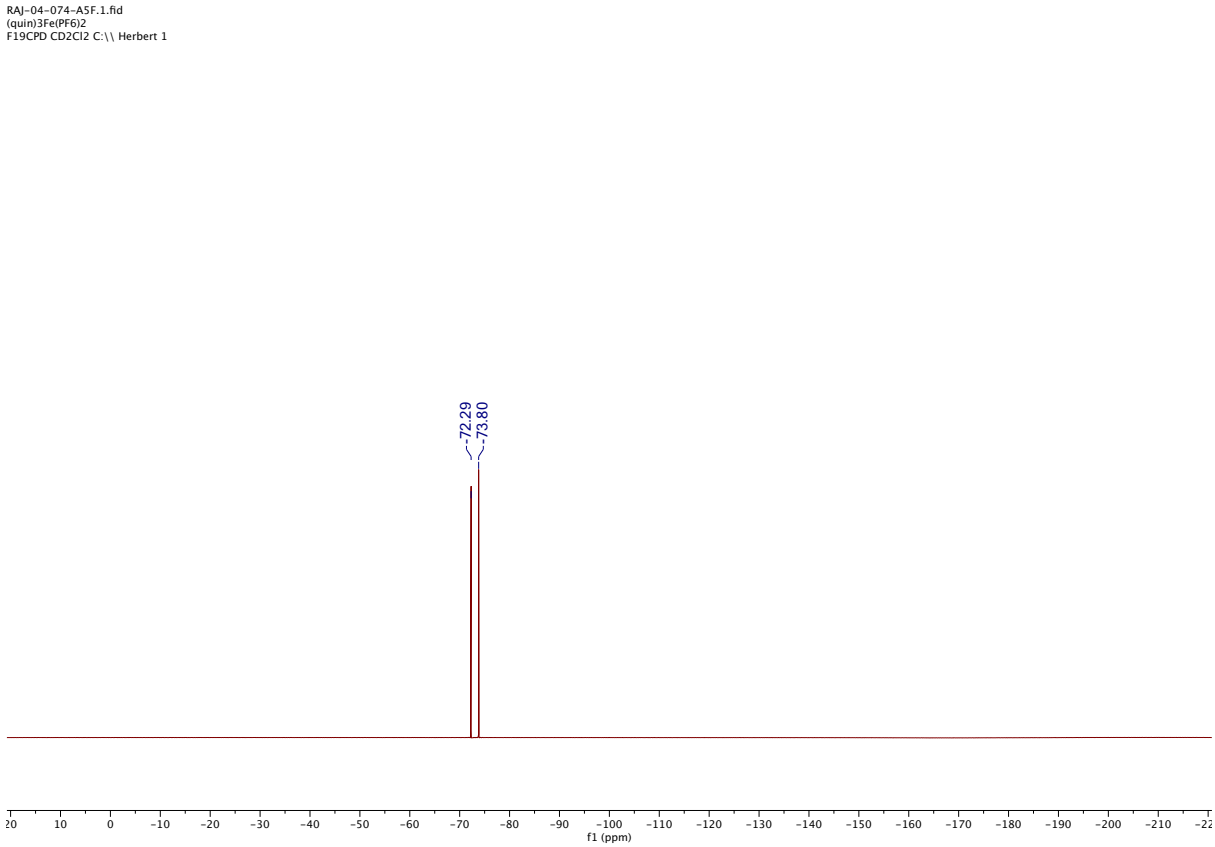

Figure S22. ^{19}F NMR (470 MHz, 22°C, CD_2Cl_2) of $[(^{\mathbf{Quin}}\mathbf{L}^{\mathbf{Me,Ph}})_3Fe][PF_6]_2$.

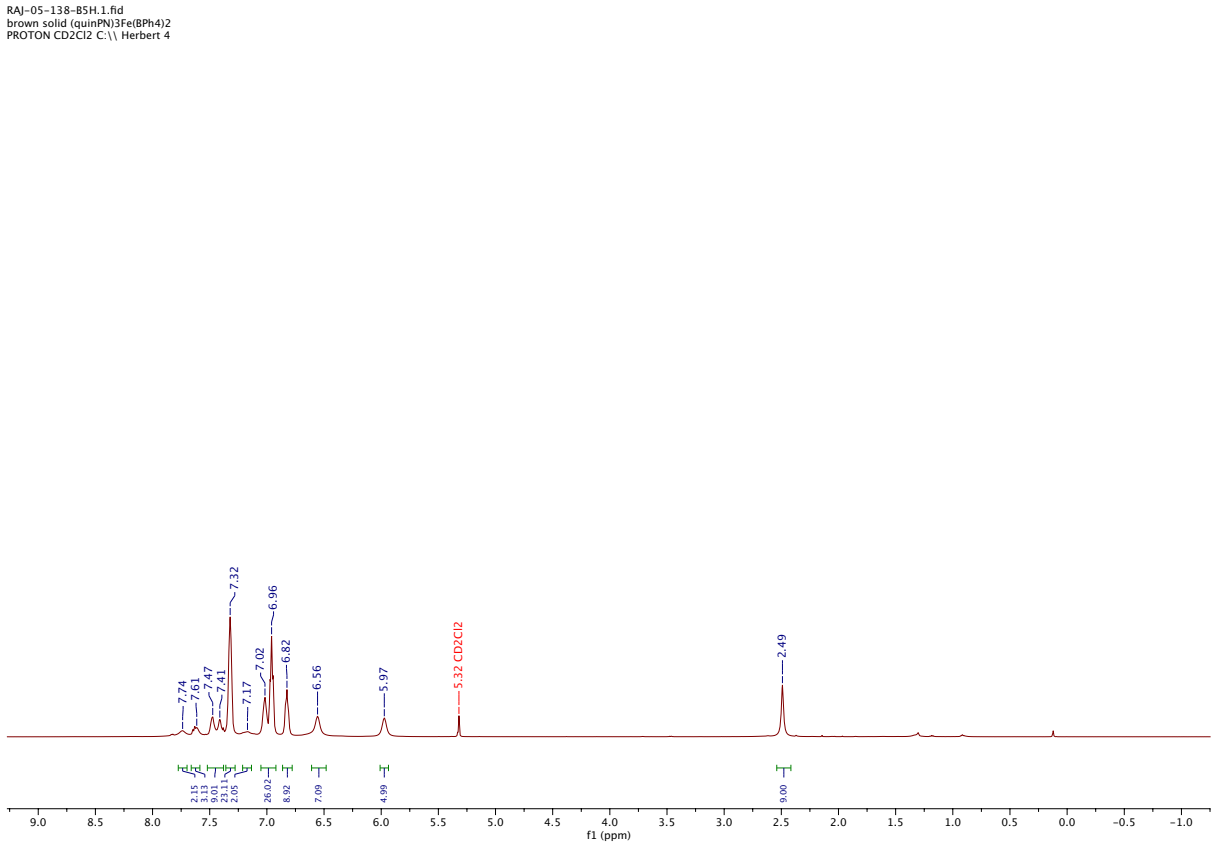

Figure S23. ^{1}H NMR (500 MHz, 22°C, CD_2Cl_2) of $[(^{\mathbf{Quin}}\mathbf{L}^{\mathbf{Me,Ph}})_3Fe][BPh_4]_2$.

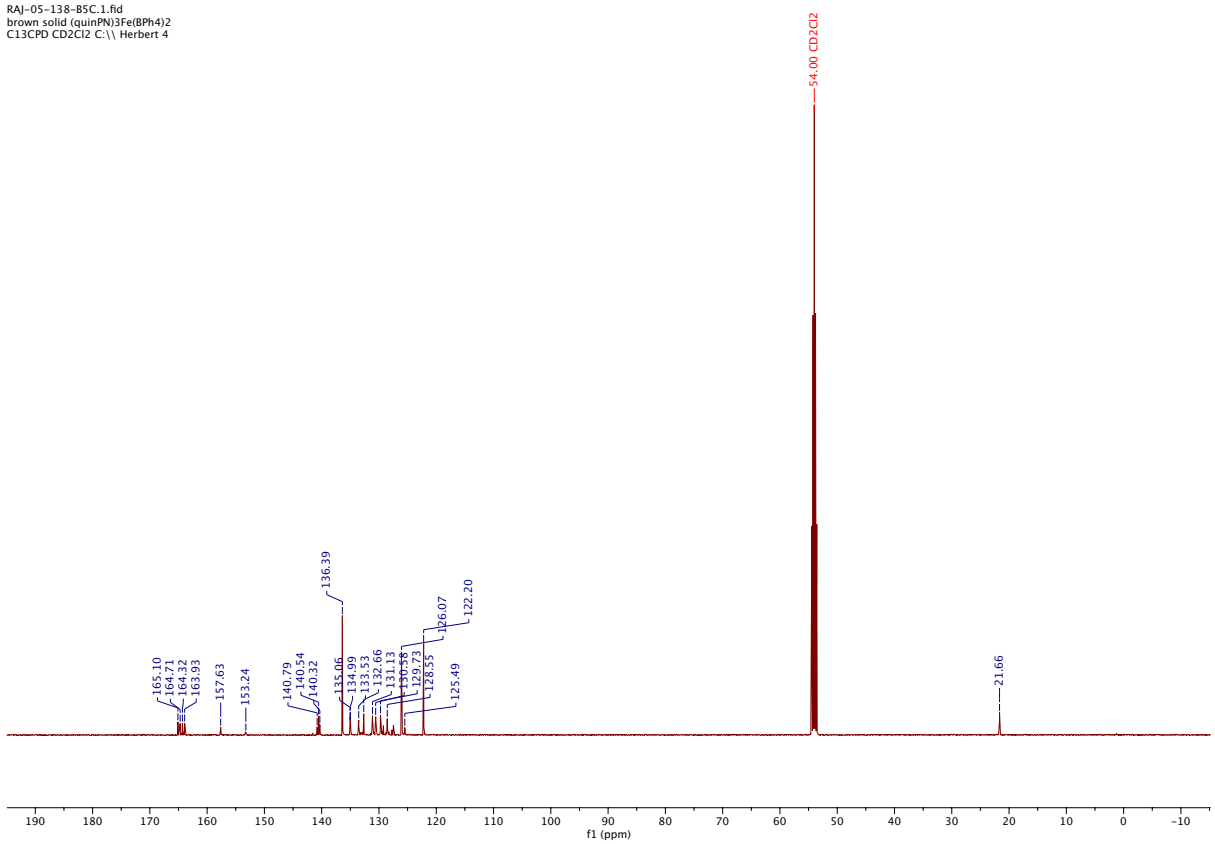

Figure S24. $^{13}C\{^{1}H\}$ NMR (126 MHz, 22°C, CD_2Cl_2) of $[(^{\mathbf{Quin}}\mathbf{L}^{\mathbf{Me,Ph}})_3Fe][BPh_4]_2$.

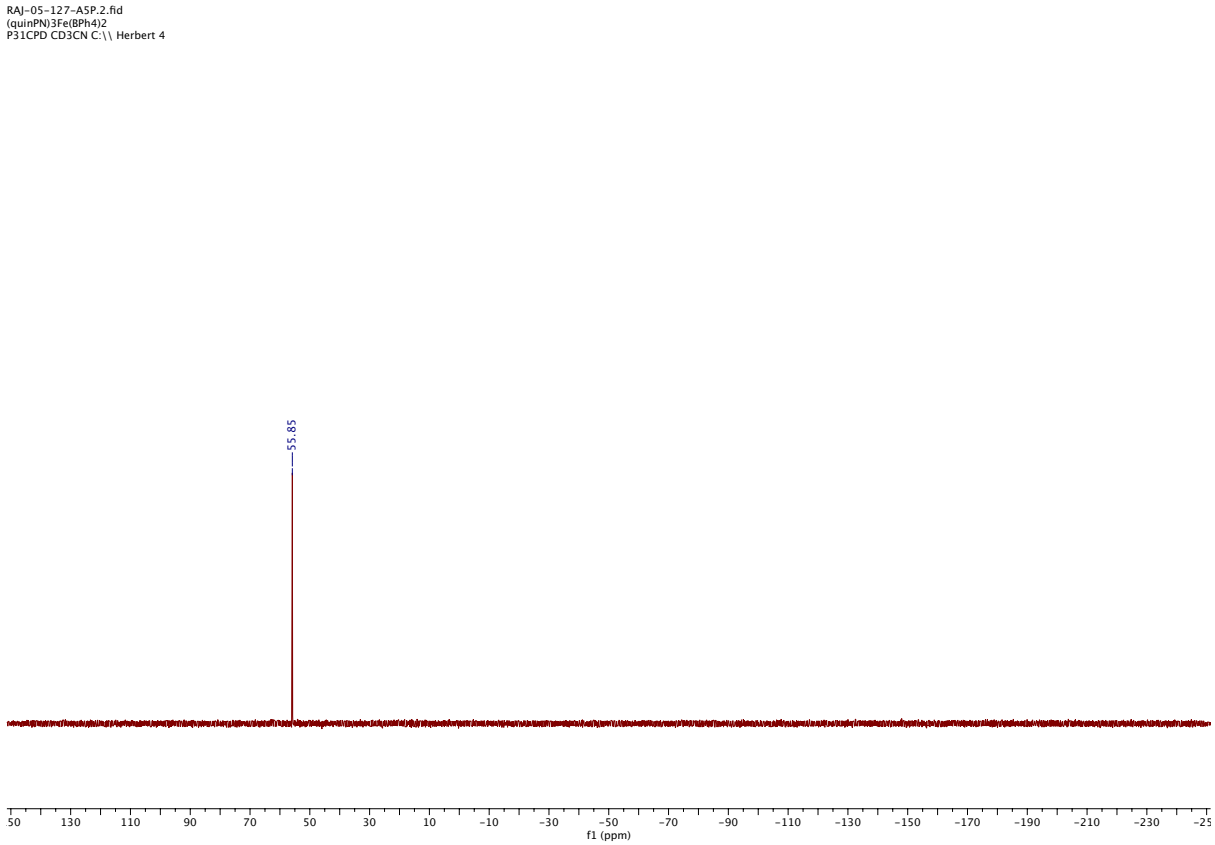

Figure S25. $^{31}P\{^{1}H\}$ NMR (202 MHz, 22°C, CD_3CN) of $[(^{\mathbf{Quin}}\mathbf{L}^{\mathbf{Me,Ph}})_3Fe][BPh_4]_2$.

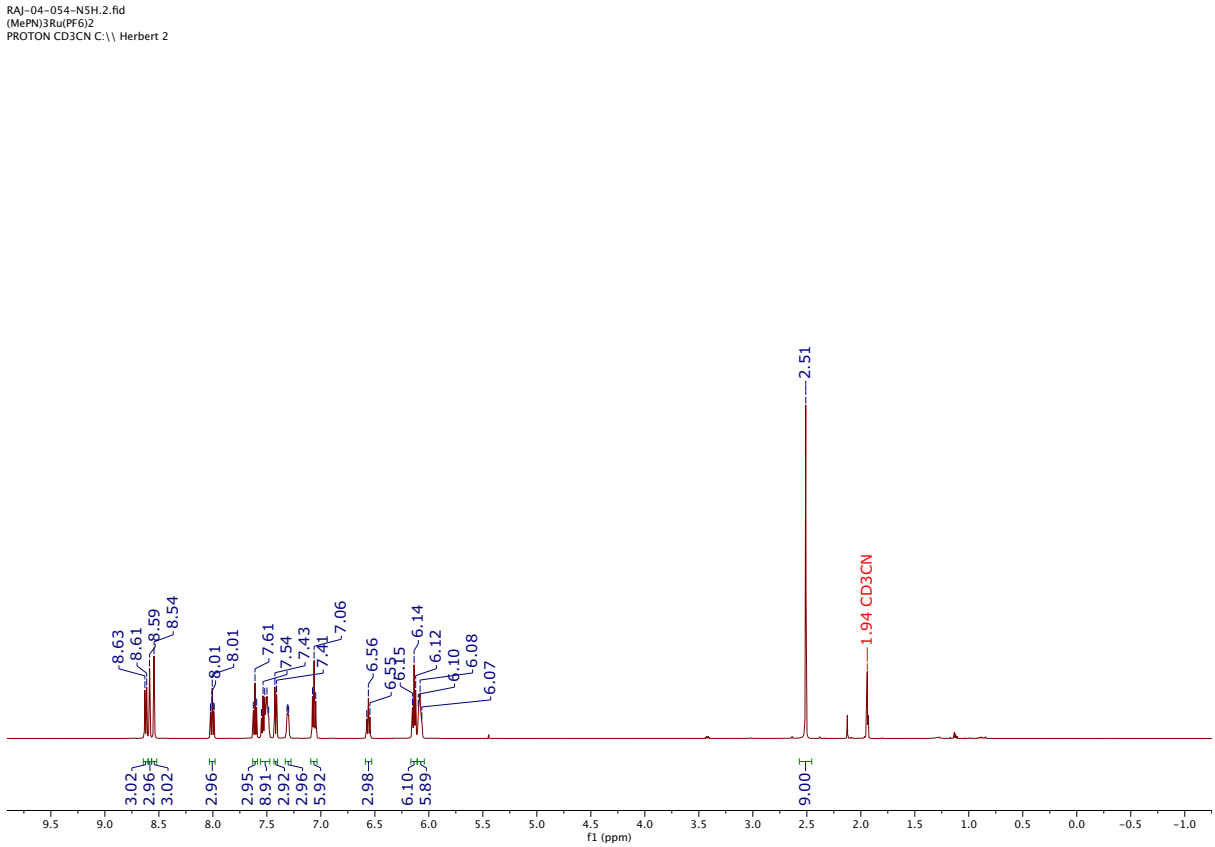

Figure S26. ^{1}H NMR (500 MHz, 22°C, CD_3CN) of $[(^{\mathbf{Phen}}\mathbf{L}^{\mathbf{Me,Ph}})_3Ru][PF_6]_2$.

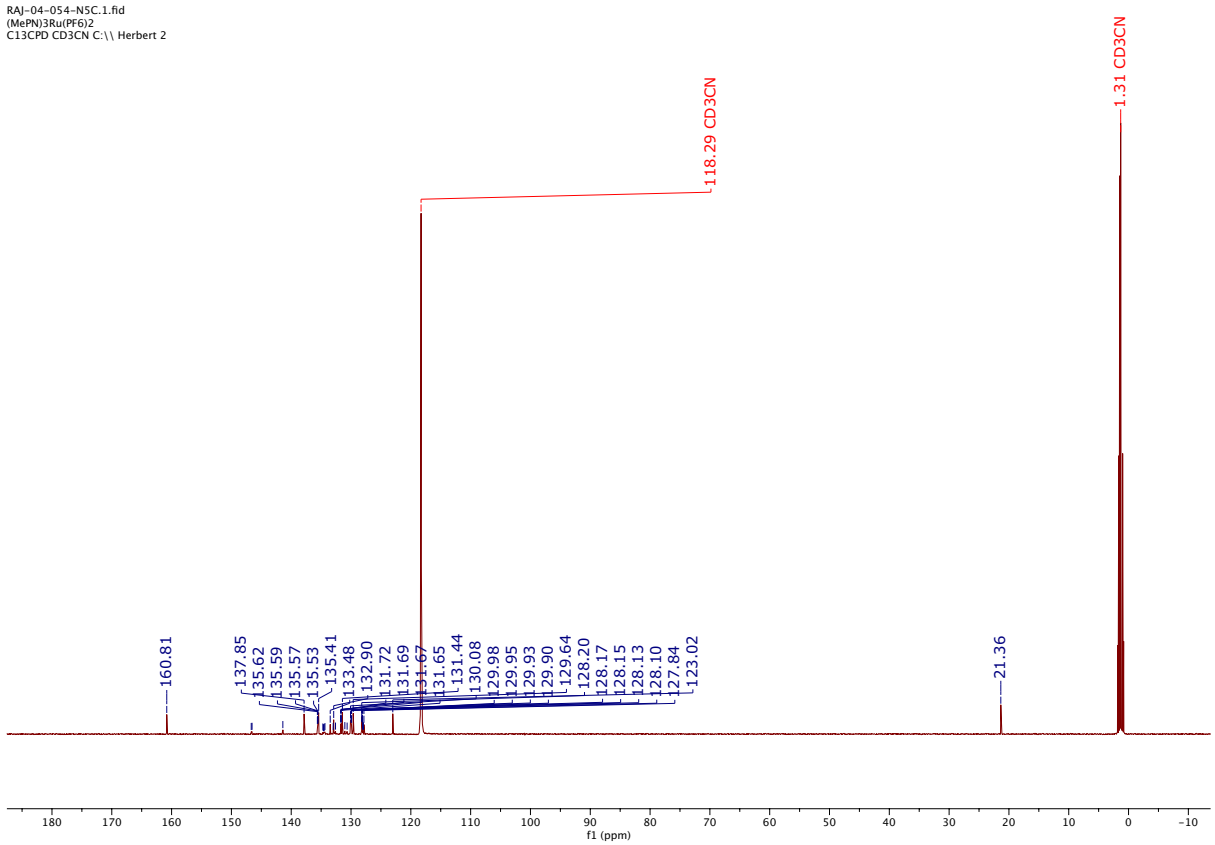

Figure S27. $^{13}C\{^{1}H\}$ NMR (126 MHz, 22°C, CD_3CN) of $[(^{\mathbf{Phen}}\mathbf{L}^{\mathbf{Me,Ph}})_3Ru][PF_6]_2$.

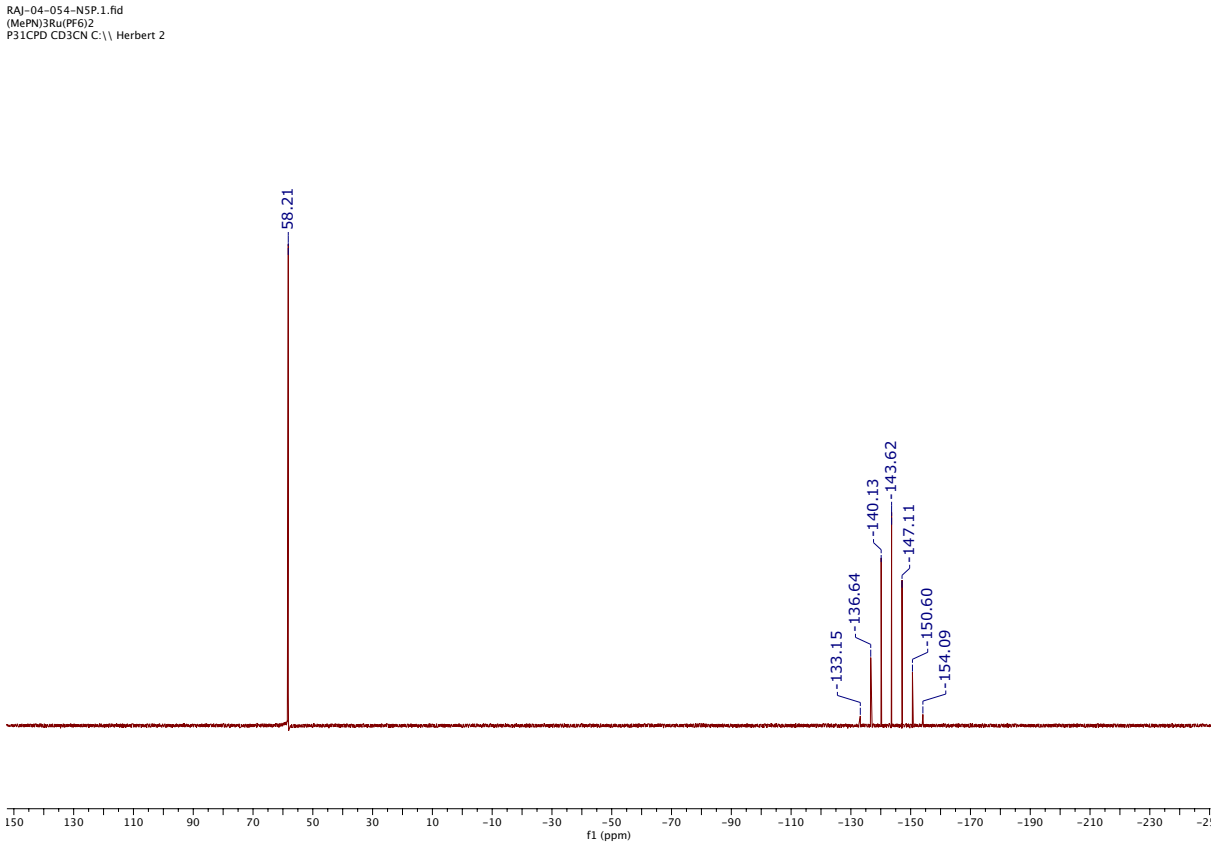

Figure S28. $^{31}P\{^{1}H\}$ NMR (202 MHz, 22°C, CD_3CN) of $[(^{\mathbf{Phen}}\mathbf{L}^{\mathbf{Me,Ph}})_3Ru][PF_6]_2$.

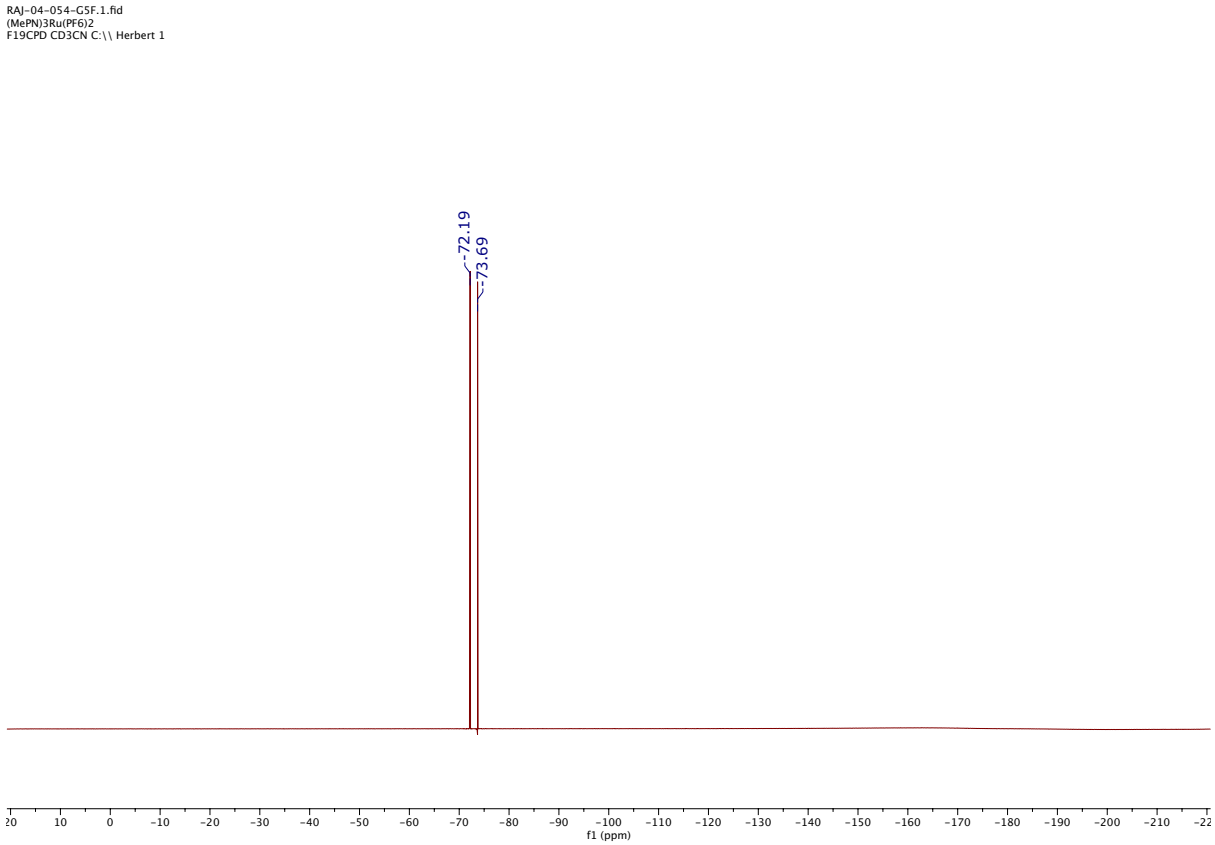

Figure S29. ^{19}F NMR (470 MHz, 22°C, CD_3CN) of $[(^{\mathbf{Phen}}\mathbf{L}^{\mathbf{Me,Ph}})_3Ru][PF_6]_2$.

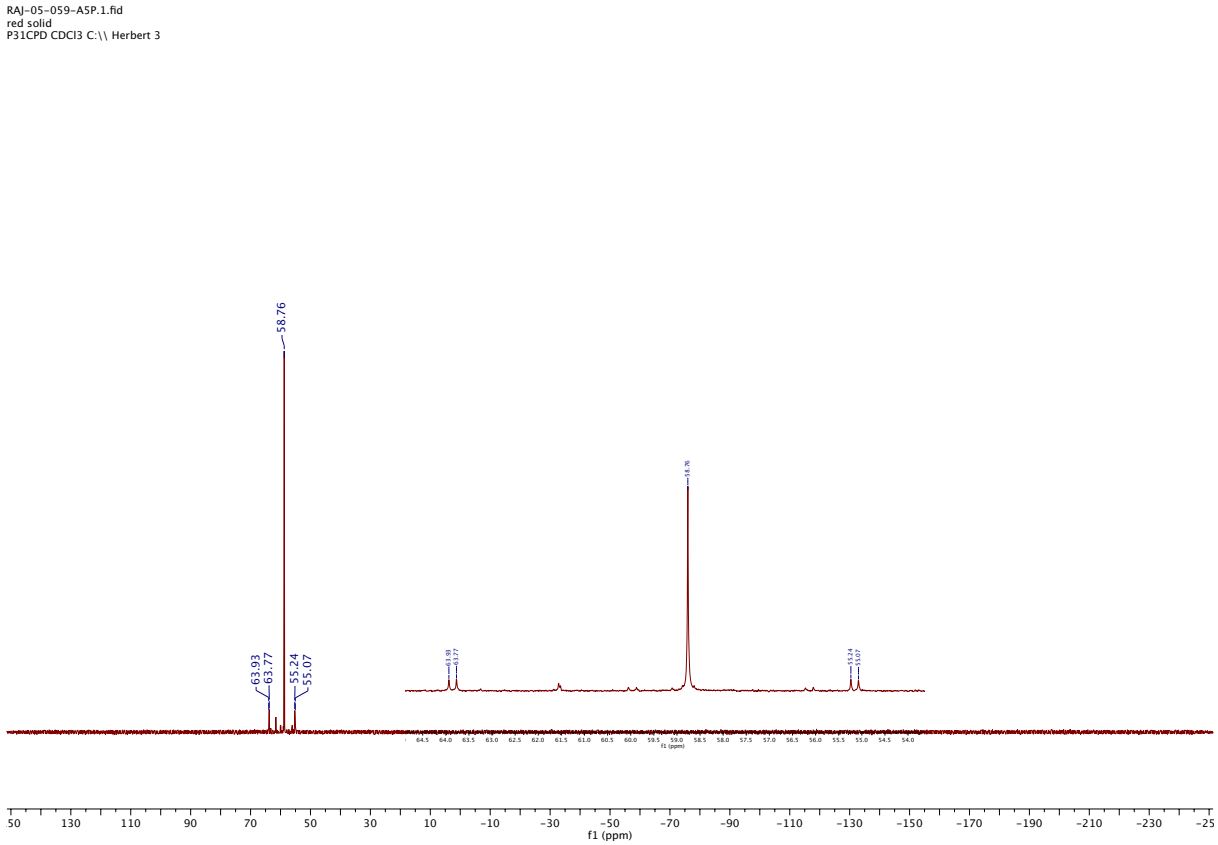

Figure S30. $^{31}P\{^{1}H\}$ NMR (202 MHz, 22°C, $CDCl_3$) of a mixture of (**$^{Phen}L^{Me,Ph}$**)Ru(DMSO)$_2$Cl$_2$ and (**$^{Phen}L^{Me,Ph}$**)$_2$RuCl$_2$.

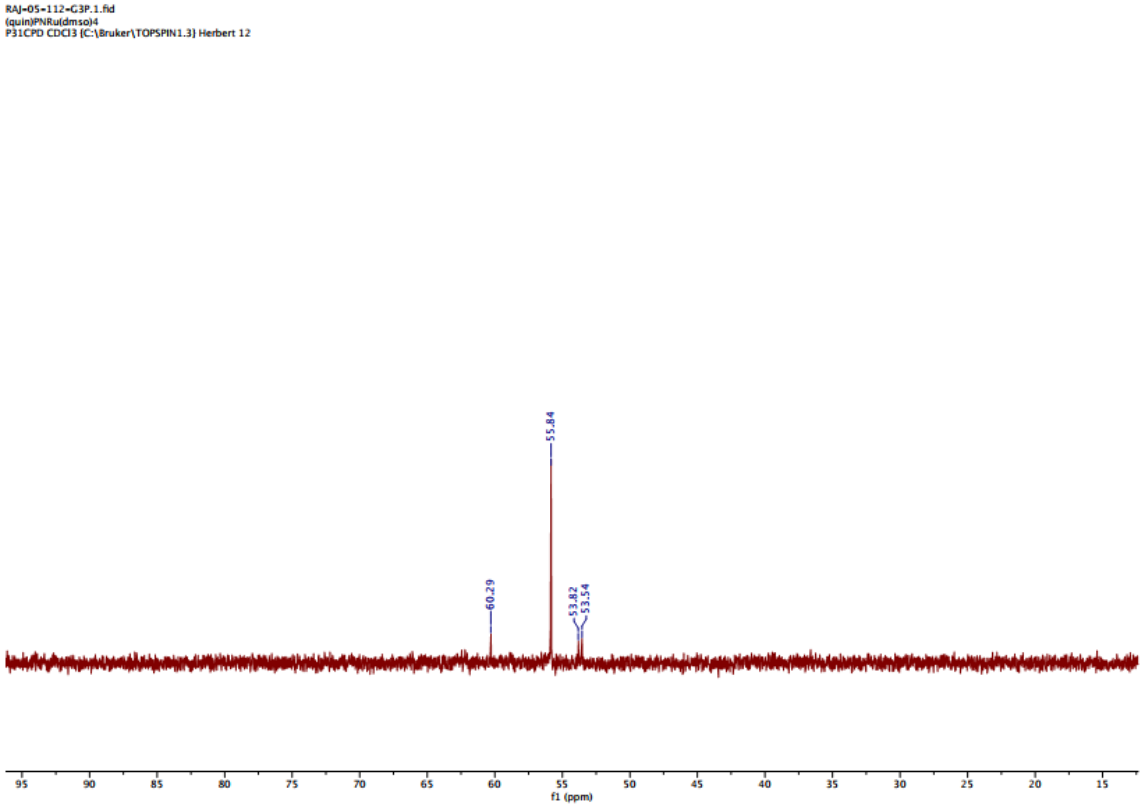

Figure S31. $^{31}P\{^{1}H\}$ NMR (121 MHz, 22°C, $CDCl_3$) of a mixture of ($^{Quin}\mathbf{L}^{Me,Ph}$)$RuCl_2(DMSO)_2$ and ($^{Quin}\mathbf{L}^{Me,Ph}$)$_2RuCl_2$.

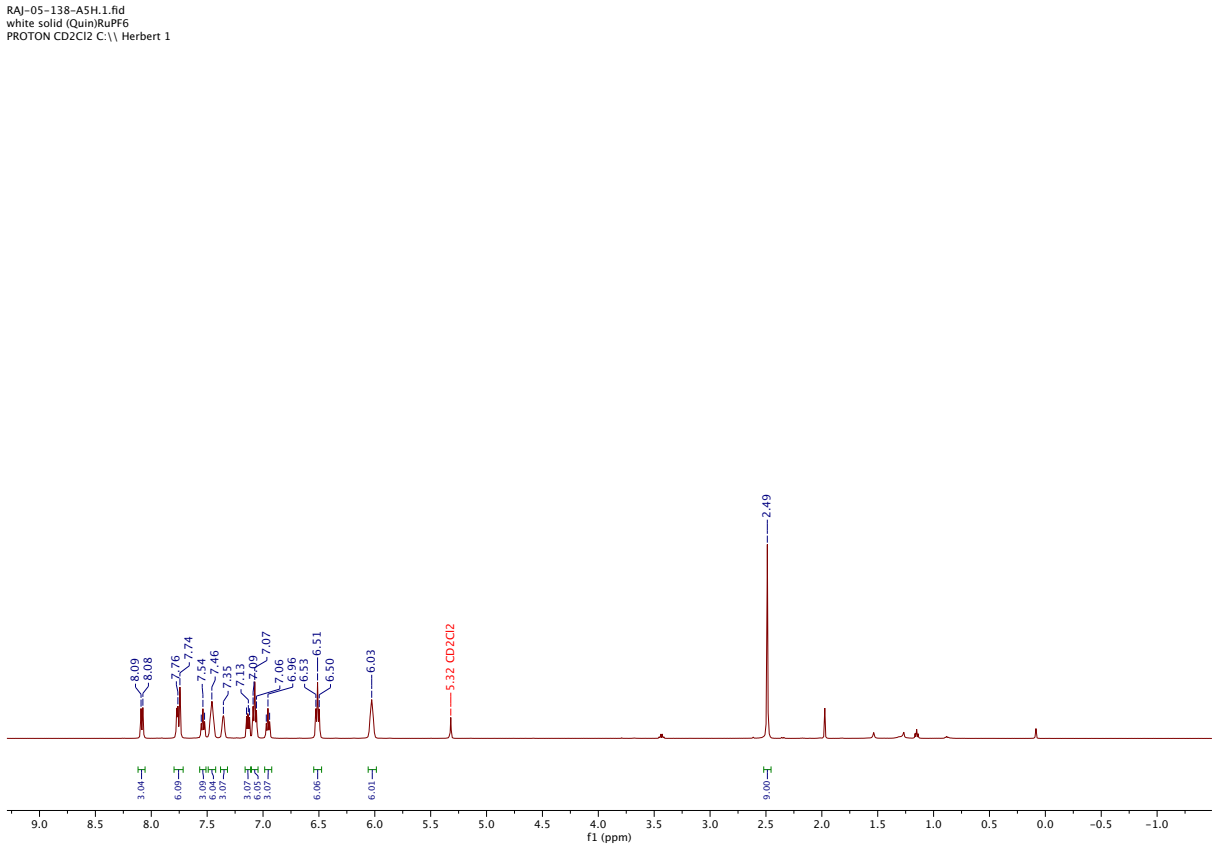

Figure S32. ^{1}H NMR (500 MHz, 22°C, CD_2Cl_2) of $[(^{\mathbf{Quin}}\mathbf{L}^{\mathbf{Me,Ph}})_3]Ru[PF_6]_2$.

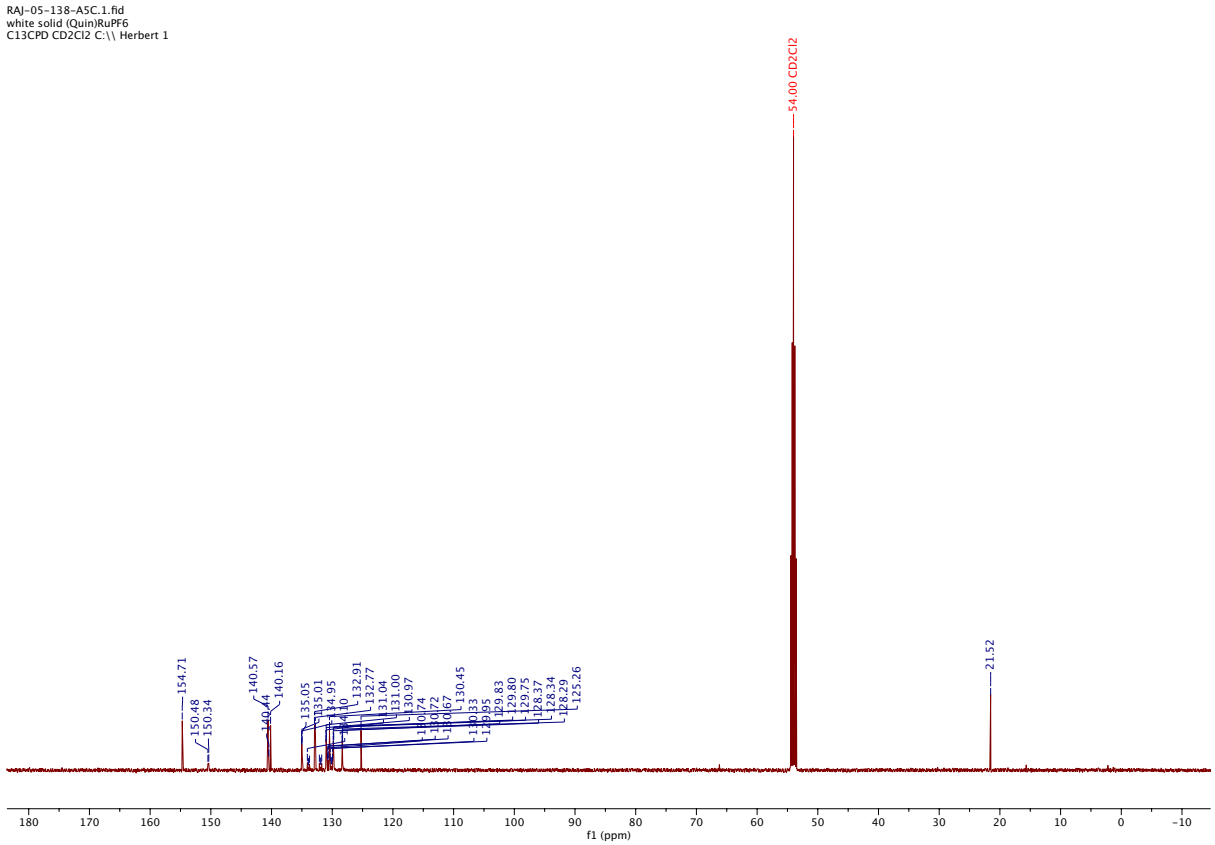

Figure S33. $^{13}C\{^{1}H\}$ NMR (126 MHz, 22°C, CD_2Cl_2) of $[(^{\mathbf{Quin}}\mathbf{L}^{\mathbf{Me,Ph}})_3]Ru[PF_6]_2$.

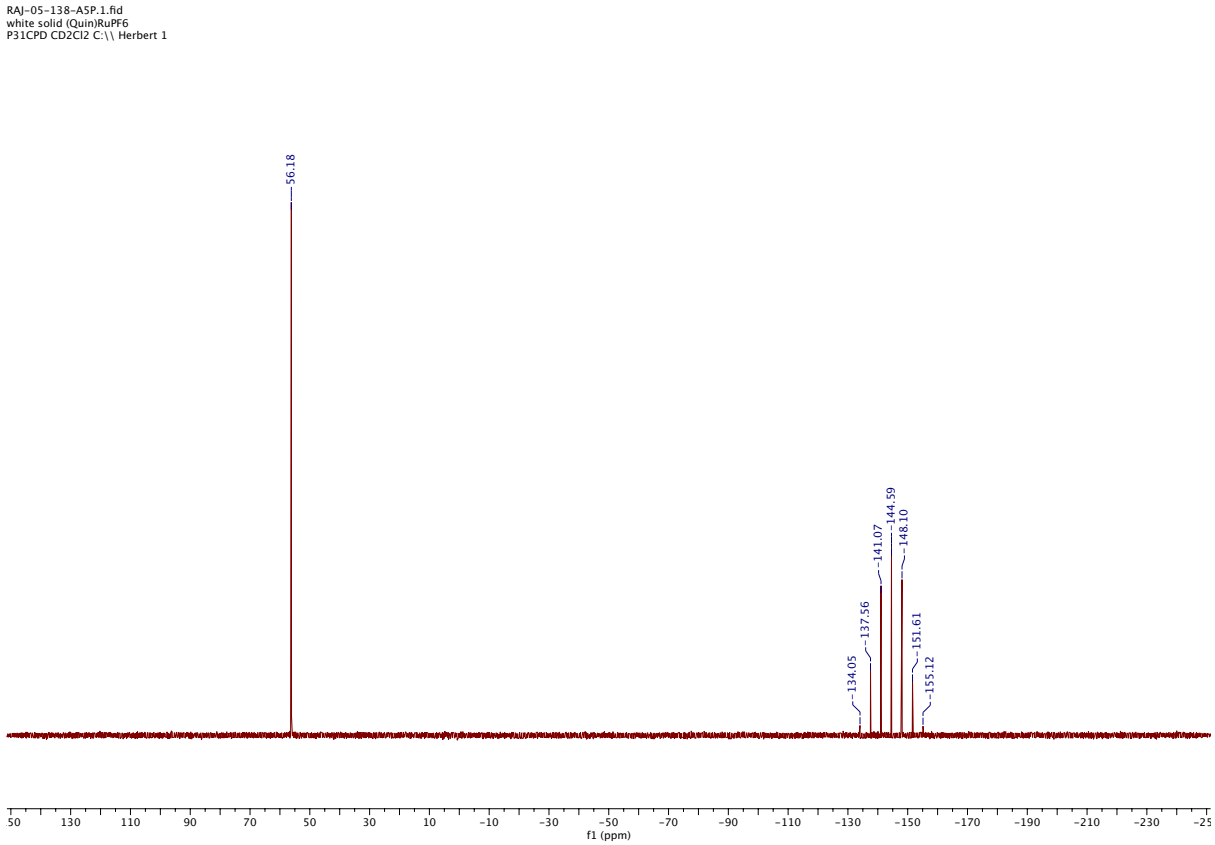

Figure S34. ^{31}P NMR (202 MHz, 22°C, CD_2Cl_2) of $[(^{\mathbf{Quin}}\mathbf{L}^{\mathbf{Me,Ph}})_3Ru][PF_6]_2$.

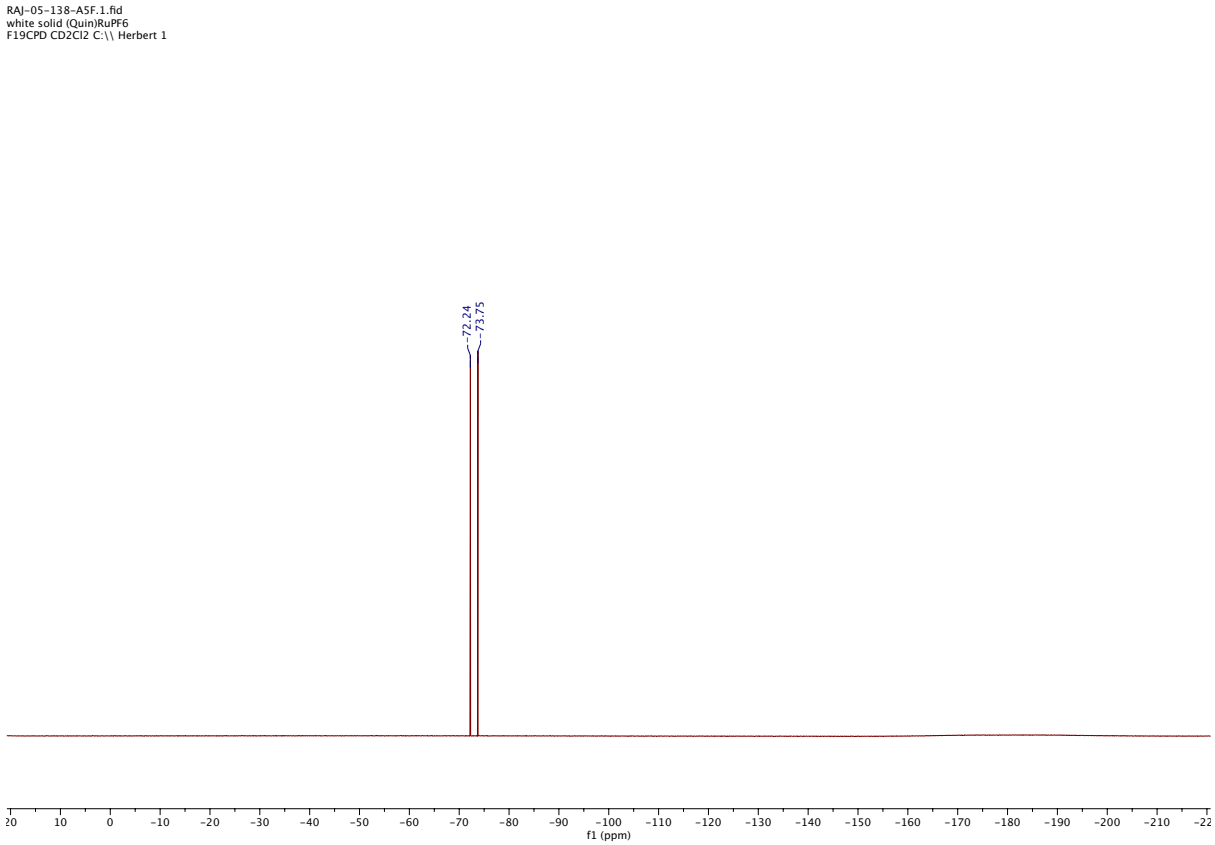

Figure S35. ^{19}F NMR (470 MHz, 22°C, CD_2Cl_2) of $[(^{\mathbf{Quin}}\mathbf{L}^{\mathbf{Me,Ph}})_3Ru][PF_6]_2$.

High-Resolution Mass Spectra

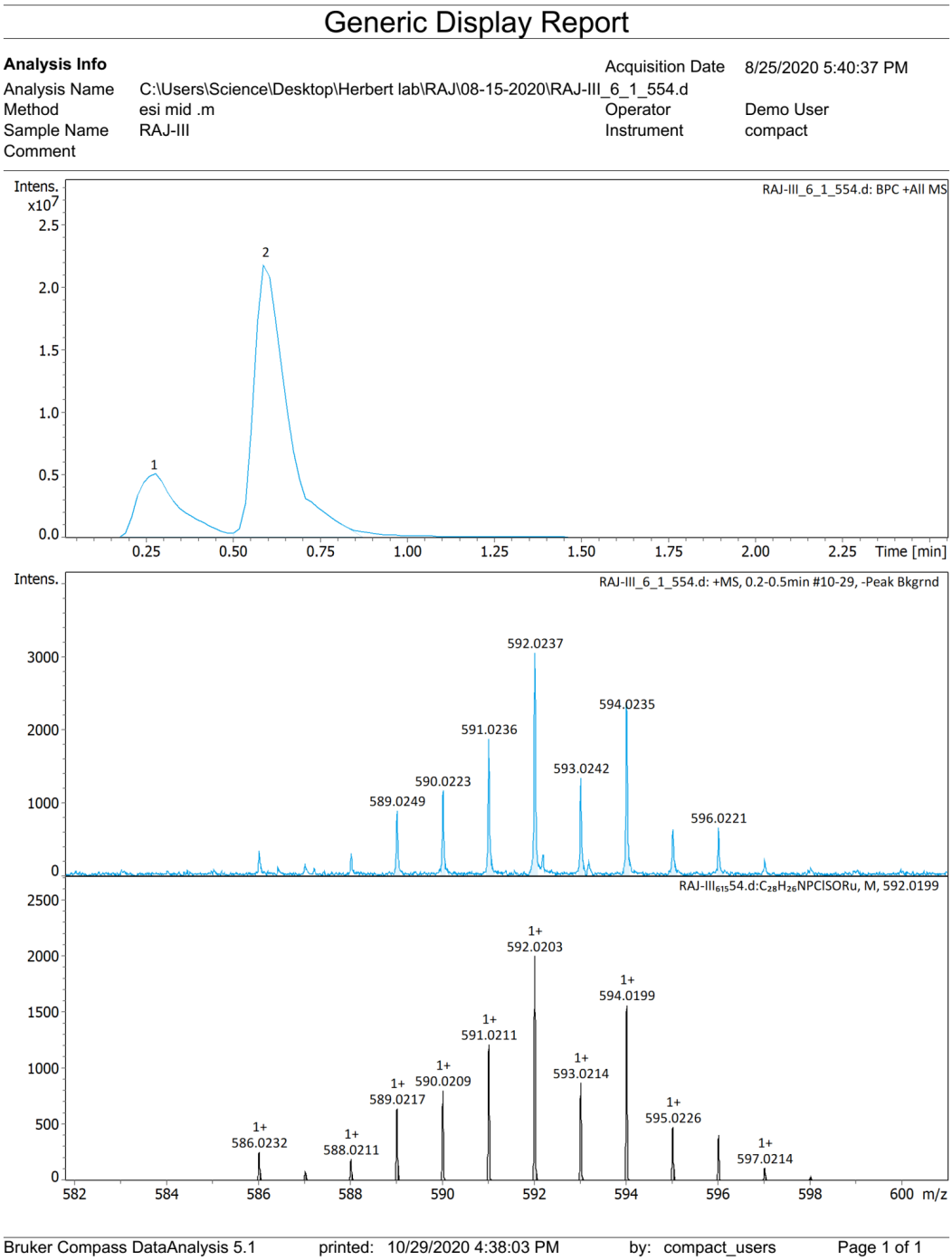

Figure S36. HRMS of $(^{\mathbf{Phen}}\mathbf{L}^{\mathbf{Me,Ph}})Ru(DMSO)_2Cl_2$.

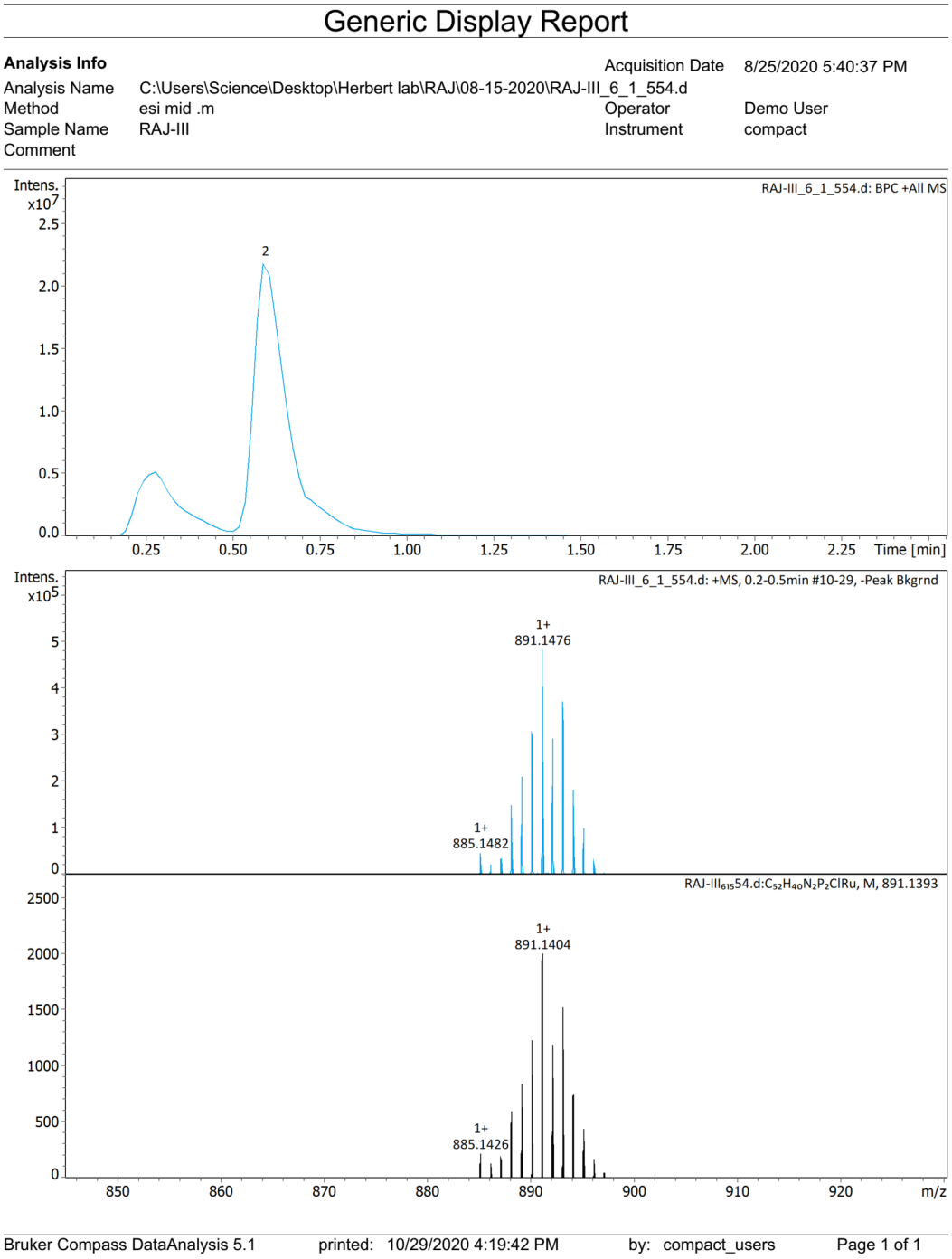

Figure S37. HRMS of $(^{\mathbf{Phen}}\mathbf{L}^{\mathbf{Me,Ph}})_2RuCl_2$.

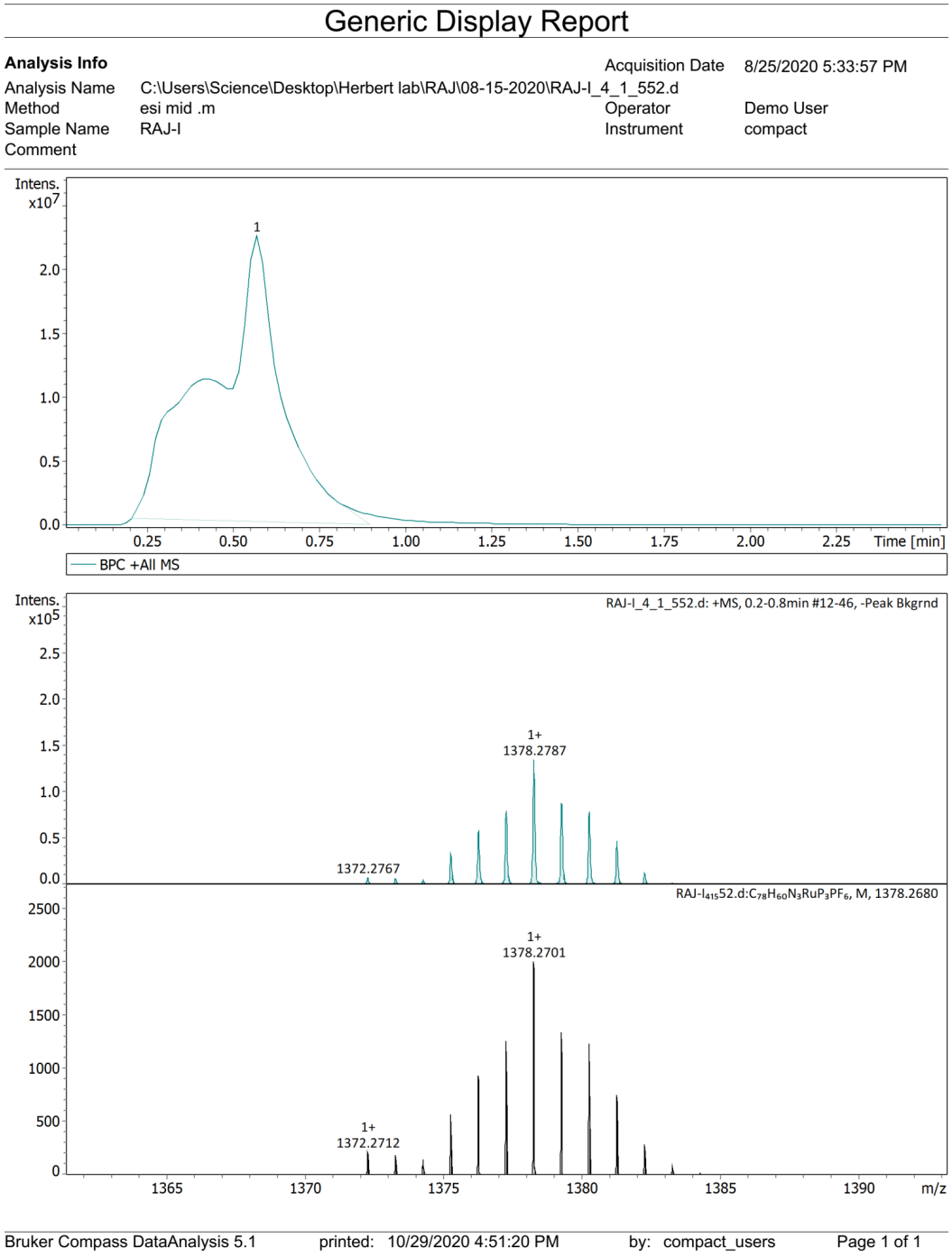

Figure S38. HRMS of $[(^{\mathbf{Phen}}\mathbf{L}^{\mathbf{Me,Ph}})_3\mathrm{Ru}][\mathrm{PF}_6]_2$.

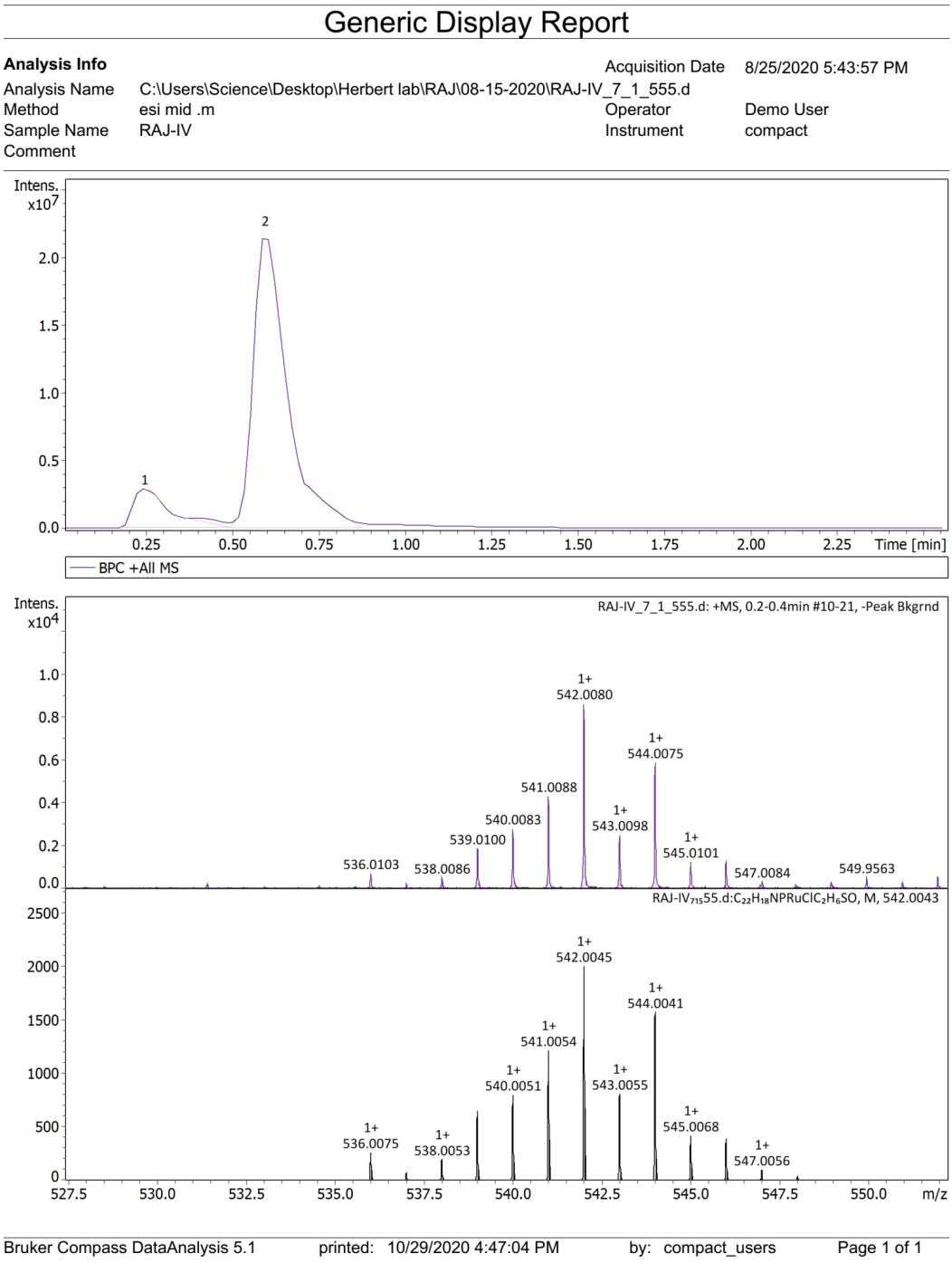

Figure S39. HRMS of (^{Quin}**L**^{Me,Ph})$RuCl_2(dmso)_2$.

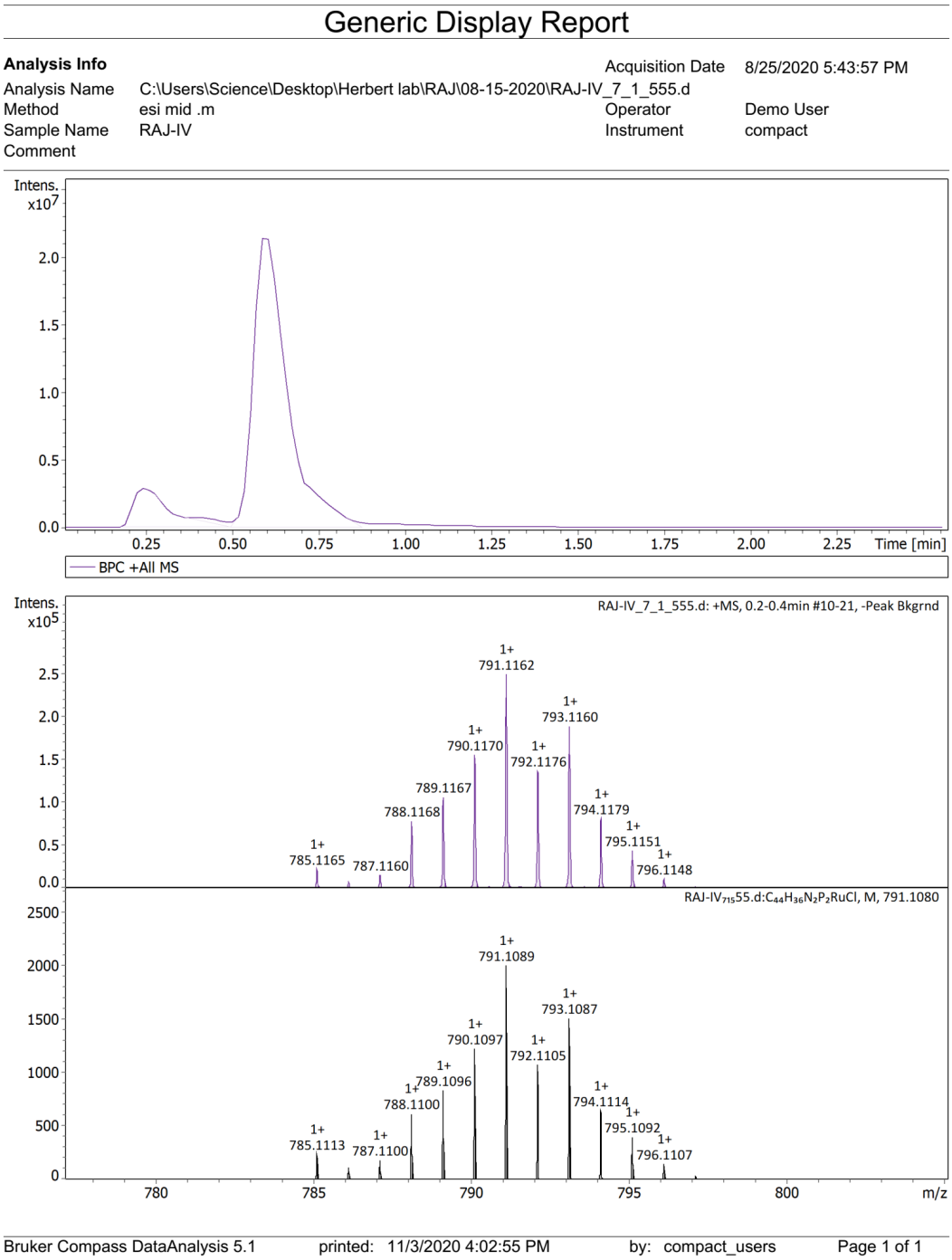

Figure S40. HRMS of $(^{\mathbf{Quin}}\mathbf{L}^{\mathbf{Me,Ph}})_2RuCl_2$.

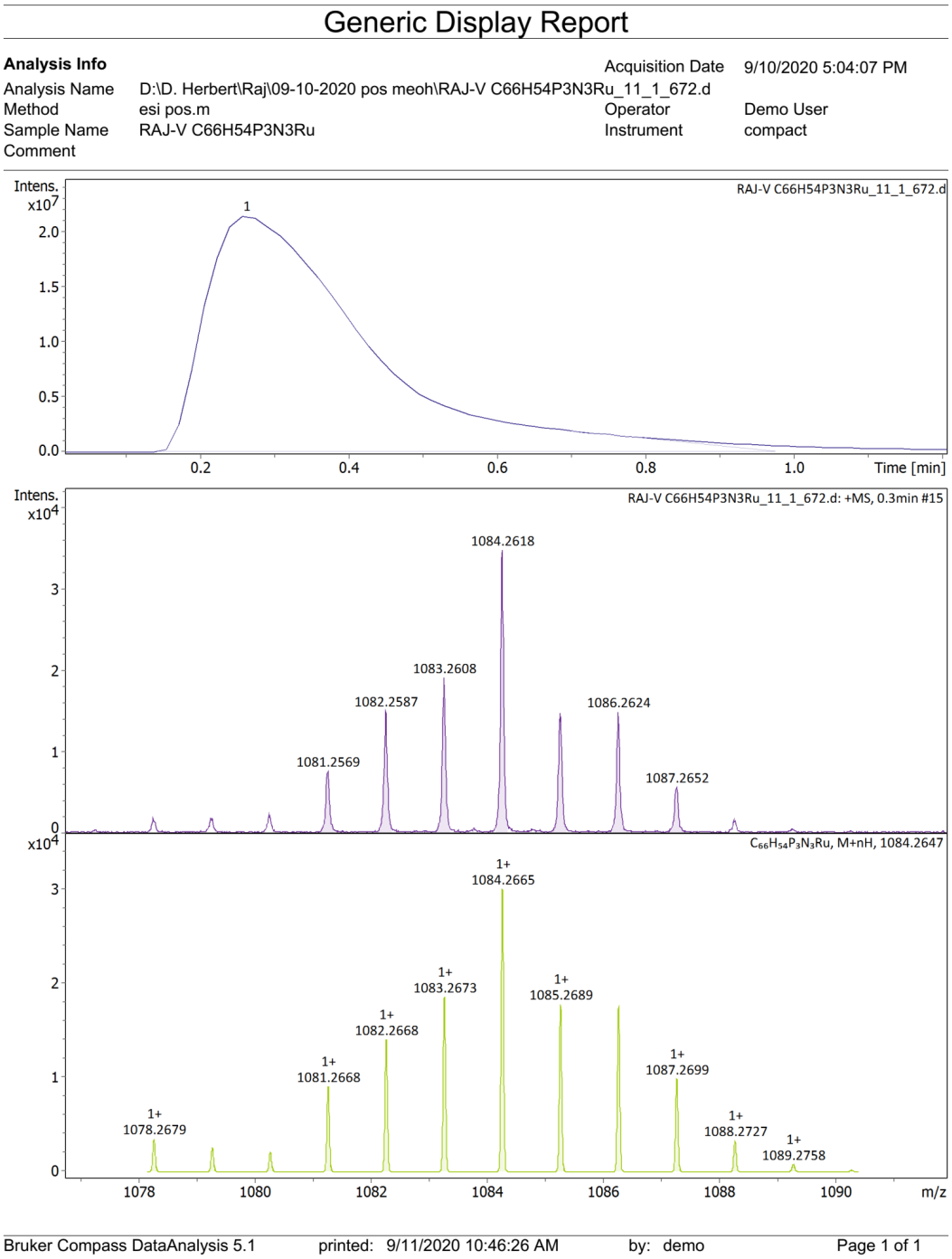

Figure S41. HRMS of $[(^{\mathbf{Quin}}\mathbf{L}^{\mathbf{Me,Ph}})_3\mathrm{Ru}][\mathrm{PF}_6]_2$.

Energies and Reaction Coordinates

$[(^{Quin}\mathbf{L}^{Me,Ph})_3Fe]^{2+}$

HF=-4997.6320435 Hartrees

Zero-point correction= 1.023812 (Hartree/Particle)

Thermal correction to Gibbs Free Energy= 0.930327

Sum of electronic and zero-point Energies= -4996.608231

Sum of electronic and thermal Free Energies= -4996.701717

Standard orientation:

Center Number	Atomic Number	Atomic Type	Coordinates (Angstroms) X	Y	Z
1	6	0	1.773117	-0.991910	-2.920667
2	1	0	1.791482	0.056877	-3.201390
3	6	0	2.526611	-1.908044	-3.677972
4	1	0	3.108668	-1.539268	-4.523255
5	6	0	2.529757	-3.234936	-3.315875
6	1	0	3.122046	-3.974850	-3.858786
7	6	0	1.747469	-3.645232	-2.209272
8	6	0	0.981537	-2.657521	-1.514720
9	6	0	0.169656	-3.070384	-0.425013
10	6	0	0.164538	-4.393910	-0.030792
11	1	0	-0.453868	-4.704338	0.812900

12	6	0	0.948488	-5.381165	-0.685707
13	6	0	1.716118	-4.992957	-1.767741
14	1	0	2.325333	-5.724821	-2.303430
15	6	0	0.926590	-6.798146	-0.185560
16	1	0	1.544550	-7.457206	-0.811566
17	1	0	-0.102148	-7.193972	-0.169221
18	1	0	1.304938	-6.848929	0.849236
19	6	0	-0.813662	-2.167965	2.142592
20	6	0	-0.032985	-1.395299	3.009863
21	1	0	0.492764	-0.525524	2.632863
22	6	0	0.053570	-1.708229	4.368049
23	1	0	0.666527	-1.087250	5.025056
24	6	0	-0.657164	-2.797247	4.878106
25	1	0	-0.597322	-3.043777	5.940982
26	6	0	-1.458707	-3.564176	4.024357
27	1	0	-2.026925	-4.410137	4.418530
28	6	0	-1.541336	-3.252503	2.665582
29	1	0	-2.182242	-3.851817	2.017831
30	6	0	-2.561931	-2.273494	-0.114728
31	6	0	-2.793845	-3.082975	-1.235440
32	1	0	-1.957974	-3.448323	-1.832467
33	6	0	-4.098906	-3.426761	-1.601576
34	1	0	-4.263147	-4.055177	-2.480106

35	6	0	-5.184571	-2.968795	-0.852542
36	1	0	-6.203663	-3.238173	-1.140120
37	6	0	-4.960647	-2.160009	0.266825
38	1	0	-5.802272	-1.793746	0.858958
39	6	0	-3.660181	-1.812752	0.631661
40	1	0	-3.506873	-1.183268	1.506491
41	26	0	0.038937	0.086188	-0.701877
42	7	0	1.027584	-1.329120	-1.871438
43	15	0	-0.853252	-1.761809	0.351370
44	6	0	-1.600456	-0.693613	-3.108496
45	1	0	-0.642511	-1.077597	-3.446685
46	6	0	-2.744670	-0.928528	-3.894345
47	1	0	-2.636576	-1.480734	-4.828542
48	6	0	-3.971607	-0.496991	-3.444424
49	1	0	-4.888052	-0.698744	-4.003375
50	6	0	-4.040843	0.221274	-2.225710
51	6	0	-2.824592	0.470366	-1.521769
52	6	0	-2.869397	1.254021	-0.338110
53	6	0	-4.081528	1.686572	0.161661
54	1	0	-4.102821	2.286300	1.074379
55	6	0	-5.310436	1.385849	-0.488546
56	6	0	-5.267005	0.681184	-1.677632
57	1	0	-6.189381	0.454318	-2.217451

58	6	0	-6.604603	1.840526	0.125277
59	1	0	-7.462890	1.603990	-0.519328
60	1	0	-6.593414	2.927022	0.310772
61	1	0	-6.760808	1.351308	1.101600
62	6	0	-1.624057	2.013577	2.127817
63	6	0	-2.113547	0.960836	2.914925
64	1	0	-2.271770	-0.020023	2.478040
65	6	0	-2.407297	1.153516	4.265447
66	1	0	-2.780326	0.315540	4.858622
67	6	0	-2.217476	2.407961	4.852175
68	1	0	-2.440787	2.559906	5.910908
69	6	0	-1.747507	3.468636	4.072737
70	1	0	-1.606083	4.456862	4.516846
71	6	0	-1.456887	3.276886	2.719071
72	1	0	-1.092104	4.118954	2.132321
73	6	0	-0.972594	3.412305	-0.296197
74	6	0	-1.945002	4.076612	-1.057837
75	1	0	-2.901765	3.599136	-1.268445
76	6	0	-1.695013	5.355992	-1.564436
77	1	0	-2.461830	5.858070	-2.159357
78	6	0	-0.473276	5.985644	-1.317115
79	1	0	-0.277286	6.982953	-1.718115
80	6	0	0.501305	5.329457	-0.557751

81	1	0	1.463948	5.808210	-0.364203
82	6	0	0.255672	4.052064	-0.053788
83	1	0	1.033937	3.551852	0.522331
84	7	0	-1.618830	-0.029952	-1.956398
85	15	0	-1.239655	1.704427	0.350828
86	6	0	0.187867	2.170639	-2.831313
87	1	0	-0.821814	1.814809	-3.014828
88	6	0	0.698689	3.211269	-3.631888
89	1	0	0.068438	3.628329	-4.417882
90	6	0	1.968197	3.682297	-3.392546
91	1	0	2.397717	4.493370	-3.984800
92	6	0	2.725204	3.111591	-2.339191
93	6	0	2.135638	2.055781	-1.577909
94	6	0	2.875254	1.503226	-0.500417
95	6	0	4.128441	1.997647	-0.190509
96	1	0	4.676147	1.576603	0.656077
97	6	0	4.731943	3.042596	-0.940780
98	6	0	4.022587	3.577012	-2.001815
99	1	0	4.450265	4.387080	-2.597475
100	6	0	6.100620	3.535275	-0.562497
101	1	0	6.435636	4.345301	-1.225594
102	1	0	6.838051	2.716962	-0.612306
103	1	0	6.108278	3.908495	0.475032

104	6	0	2.421488	0.717964	2.190244
105	6	0	1.681463	1.769639	2.749703
106	1	0	0.891332	2.241915	2.176932
107	6	0	1.929249	2.212283	4.048815
108	1	0	1.327377	3.023882	4.463675
109	6	0	2.935444	1.610296	4.811240
110	1	0	3.130120	1.948942	5.831684
111	6	0	3.691815	0.573730	4.257777
112	1	0	4.486544	0.102265	4.840973
113	6	0	3.440053	0.128395	2.956024
114	1	0	4.043905	-0.680505	2.547310
115	6	0	3.136262	-1.285162	0.264927
116	6	0	4.168889	-1.329579	-0.680984
117	1	0	4.376572	-0.464823	-1.311139
118	6	0	4.934486	-2.489938	-0.836168
119	1	0	5.731314	-2.512137	-1.583389
120	6	0	4.679474	-3.613383	-0.047383
121	1	0	5.276484	-4.519847	-0.172755
122	6	0	3.650474	-3.575715	0.899878
123	1	0	3.438619	-4.450684	1.518427
124	6	0	2.881143	-2.422769	1.052431
125	1	0	2.079807	-2.409243	1.791768
126	7	0	0.867485	1.591465	-1.847335

127	15	0	2.049278	0.186119	0.459823

$[(^{Phen}L^{Me,Ph})_3Fe]^{2+}$

HF=-5458.3193835 Hartrees

Zero-point correction= 1.165981 (Hartree/Particle)

Thermal correction to Gibbs Free Energy= 1.062581

Sum of electronic and zero-point Energies= -5457.153403

Sum of electronic and thermal Free Energies= -5457.256803

Standard orientation:

Center Number	Atomic Number	Atomic Type	Coordinates (Angstroms) X	Y	Z
1	26	0	0.029645	-0.062175	-0.069649
2	15	0	-0.947822	-1.872421	0.983635
3	15	0	-1.250833	1.617864	0.861811
4	15	0	1.963264	0.256295	1.167264
5	7	0	-1.568089	-0.311957	-1.380660
6	6	0	-2.688291	-1.034740	-0.970924
7	6	0	-1.627573	0.322012	-2.528256
8	1	0	-0.750653	0.879235	-2.848210
9	6	0	-3.900570	-1.043283	-1.711925

10	6	0	-2.608536	-1.774512	0.232985
11	6	0	-4.950846	-2.412875	0.032060
12	6	0	-2.772355	0.352138	-3.375269
13	6	0	-3.953908	-0.320492	-2.965897
14	6	0	-5.011355	-1.734166	-1.178430
15	1	0	-5.953366	-1.726474	-1.726886
16	6	0	-3.719126	-2.439080	0.725072
17	1	0	-3.642667	-3.004142	1.656460
18	6	0	-5.098556	-0.228279	-3.788260
19	1	0	-6.023172	-0.729556	-3.502053
20	6	0	-2.747378	1.097821	-4.578320
21	1	0	-1.826412	1.612685	-4.862467
22	6	0	-6.152095	-3.107841	0.610224
23	1	0	-6.464741	-2.620493	1.549321
24	1	0	-5.921748	-4.157144	0.856192
25	1	0	-7.003876	-3.090507	-0.084435
26	6	0	-3.881327	1.174985	-5.365058
27	1	0	-3.872249	1.751668	-6.292363
28	6	0	-5.058572	0.506078	-4.963422
29	1	0	-5.953181	0.570153	-5.587297
30	7	0	0.779514	1.479707	-1.252556
31	6	0	-1.378074	2.093583	2.632730
32	6	0	-3.001424	1.770404	0.303138

33	6	0	-4.025564	1.120435	1.013189
34	1	0	-3.799823	0.557574	1.918197
35	6	0	-0.475410	1.558710	3.559047
36	1	0	0.250134	0.819260	3.240054
37	6	0	-5.346433	1.188493	0.570043
38	1	0	-6.130329	0.676771	1.132810
39	6	0	-1.478524	2.850399	5.339685
40	1	0	-1.519654	3.145344	6.391036
41	6	0	-3.327559	2.485545	-0.858198
42	1	0	-2.548585	2.994043	-1.426787
43	6	0	-0.516531	1.936547	4.902634
44	1	0	0.197368	1.501099	5.605242
45	6	0	-4.651216	2.546773	-1.303702
46	1	0	-4.886287	3.097540	-2.217448
47	6	0	-2.353459	3.002100	3.082308
48	1	0	-3.086076	3.414466	2.387792
49	6	0	-5.663425	1.900144	-0.591985
50	1	0	-6.696808	1.945021	-0.943821
51	6	0	-2.399333	3.377369	4.426782
52	1	0	-3.161427	4.084536	4.762934
53	6	0	1.626905	1.246642	-2.228132
54	1	0	1.857631	0.211828	-2.466370
55	6	0	0.466617	2.806413	-0.958136

56	6	0	-0.466945	3.073988	0.070952
57	6	0	1.071311	3.896903	-1.645311
58	6	0	2.276325	2.253360	-2.996881
59	6	0	2.018898	3.617648	-2.704405
60	6	0	-0.155598	5.474782	-0.226627
61	6	0	0.743408	5.212286	-1.251647
62	1	0	1.216991	6.052168	-1.760252
63	6	0	-0.765120	4.379818	0.423267
64	1	0	-1.481242	4.577885	1.221819
65	7	0	1.183722	-1.419317	-1.116195
66	6	0	3.063643	-0.932557	0.322016
67	6	0	2.508025	-1.664610	-0.752585
68	6	0	0.667426	-2.134059	-2.087584
69	1	0	-0.370411	-1.953588	-2.355550
70	6	0	3.307483	-2.643726	-1.408224
71	6	0	2.713109	-3.430825	-2.470673
72	6	0	1.363053	-3.148554	-2.805549
73	6	0	5.181684	-2.116440	0.087105
74	6	0	4.366470	-1.163350	0.735302
75	1	0	4.772107	-0.599895	1.578894
76	6	0	4.636245	-2.836566	-0.969357
77	1	0	5.257337	-3.582422	-1.465948
78	6	0	3.371949	-4.470228	-3.164957

79	1	0	4.406335	-4.721465	-2.930833
80	6	0	2.705926	-5.188606	-4.146299
81	1	0	3.228405	-5.992434	-4.670214
82	6	0	0.698013	-3.888402	-3.811655
83	1	0	-0.343728	-3.652905	-4.040721
84	6	0	6.595286	-2.335377	0.550136
85	1	0	7.184070	-1.407328	0.460368
86	1	0	7.095722	-3.120338	-0.034284
87	1	0	6.618019	-2.625428	1.613593
88	6	0	-0.341941	-3.517169	0.393347
89	6	0	-1.127580	-4.337932	-0.430504
90	1	0	-2.135925	-4.034685	-0.710862
91	6	0	0.960045	-3.936325	0.720216
92	1	0	1.601808	-3.315136	1.343800
93	6	0	1.460535	-5.145207	0.235663
94	1	0	2.478526	-5.446169	0.492863
95	6	0	-0.621959	-5.547514	-0.917230
96	1	0	-1.245110	-6.167910	-1.565662
97	6	0	0.672394	-5.954708	-0.588152
98	1	0	1.070515	-6.894026	-0.978741
99	6	0	1.363877	-4.900671	-4.476469
100	1	0	0.856964	-5.480615	-5.250539
101	6	0	2.708239	4.604113	-3.444162

102	1	0	2.536919	5.661809	-3.244374
103	6	0	3.866188	2.876038	-4.713820
104	1	0	4.584959	2.607834	-5.490941
105	6	0	3.201768	1.892539	-4.005616
106	1	0	3.382716	0.833274	-4.203026
107	6	0	3.613715	4.235848	-4.427229
108	1	0	4.141640	5.010786	-4.987993
109	6	0	-1.313848	-2.187340	2.761649
110	6	0	-1.998082	-1.209903	3.499561
111	1	0	-2.314168	-0.286603	3.024103
112	6	0	-0.941260	-3.379667	3.403452
113	1	0	-0.421663	-4.164690	2.855638
114	6	0	-1.224919	-3.572555	4.758405
115	1	0	-0.922339	-4.504150	5.242586
116	6	0	2.329065	-0.127368	2.937393
117	6	0	1.851470	-1.333974	3.468846
118	1	0	1.282295	-2.012933	2.844123
119	6	0	2.089367	-1.678695	4.799011
120	1	0	1.693981	-2.618847	5.189527
121	6	0	3.081670	0.721831	3.764073
122	1	0	3.484710	1.657512	3.380018
123	6	0	2.822832	-0.818456	5.622371
124	1	0	3.007077	-1.080341	6.667035

125	6	0	3.322978	0.376174	5.097658
126	1	0	3.907870	1.050255	5.728138
127	6	0	2.279606	2.998415	1.645553
128	1	0	1.463128	2.872305	2.356659
129	6	0	2.827215	4.266019	1.449314
130	1	0	2.433148	5.116161	2.010544
131	6	0	3.863923	4.448372	0.527782
132	1	0	4.283369	5.443873	0.364075
133	6	0	4.351762	3.354652	-0.190156
134	1	0	5.151444	3.489232	-0.922187
135	6	0	2.773717	1.890171	0.934122
136	6	0	3.813543	2.080159	0.013851
137	1	0	4.200538	1.238991	-0.561157
138	6	0	-2.284184	-1.404262	4.851571
139	1	0	-2.811353	-0.624616	5.406050
140	6	0	-1.891017	-2.584625	5.488912
141	1	0	-2.108158	-2.736425	6.548953
142	6	0	-0.476238	6.878372	0.205957
143	1	0	0.017911	7.622151	-0.435004
144	1	0	-0.148809	7.047464	1.245662
145	1	0	-1.562929	7.060947	0.179794

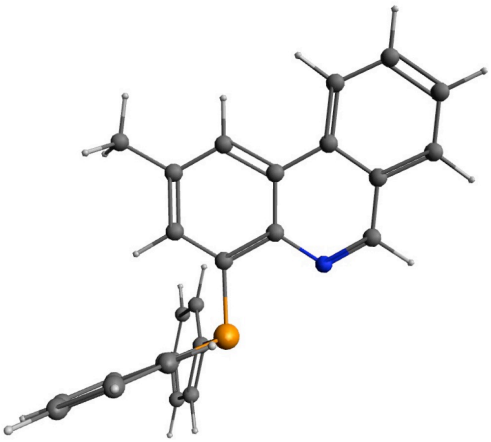

PNPhen

PNPhen (S = 0)

HF=-1398.2296205 Hartrees

C 4.6362400000 -2.8365700000 -0.9693600000

C 5.1816800000 -2.1164400000 0.0871100000

C 4.3664700000 -1.1633500000 0.7353000000

C 3.0636400000 -0.9325600000 0.3220200000

C 2.5080200000 -1.6646100000 -0.7525800000

C 3.3074800000 -2.6437300000 -1.4082200000

N 1.1837200000 -1.4193200000 -1.1162000000

C 0.6674300000 -2.1340600000 -2.0875800000

C 1.3630500000 -3.1485500000 -2.8055500000

C 2.7131100000 -3.4308300000 -2.4706700000

H 5.2573400000 -3.5824200000 -1.4659500000

H 4.7721100000 -0.5998900000 1.5788900000

H -0.3704100000 -1.9535900000 -2.3555500000

C 6.5952900000 -2.3353800000 0.5501400000

H 7.1840700000 -1.4073300000 0.4603700000

H 7.0957200000 -3.1203400000 -0.0342800000

H 6.6180200000 -2.6254300000 1.6135900000

P 1.9632600000 0.2563000000 1.1672600000

C 2.3290600000 -0.1273700000 2.9373900000

C 1.8514700000 -1.3339700000 3.4688500000

C 2.0893700000 -1.6787000000 4.7990100000

C 2.8228300000 -0.8184600000 5.6223700000

C 3.3229800000 0.3761700000 5.0976600000

C 3.0816700000 0.7218300000 3.7640700000

C 2.7737200000 1.8901700000 0.9341200000

C 2.2796100000 2.9984200000 1.6455500000

C 2.8272100000 4.2660200000 1.4493100000

C 3.8639200000 4.4483700000 0.5277800000

C 4.3517600000 3.3546500000 -0.1901600000

C 3.8135400000 2.0801600000 0.0138500000

H 1.2823000000 -2.0129300000 2.8441200000

H 1.6939800000 -2.6188500000 5.1895300000

H 3.0070800000 -1.0803400000 6.6670400000

H 3.9078700000 1.0502500000 5.7281400000

H 3.4847100000 1.6575100000 3.3800200000

H 1.4631300000 2.8723000000 2.3566600000

H 2.4331500000 5.1161600000 2.0105400000

H 4.2833700000 5.4438700000 0.3640700000

H 5.1514400000 3.4892300000 -0.9221900000

H 4.2005400000 1.2389900000 -0.5611600000

C 3.3719500000 -4.4702300000 -3.1649600000

C 2.7059300000 -5.1886100000 -4.1463000000

C 1.3638800000 -4.9006700000 -4.4764700000

C 0.6980100000 -3.8884000000 -3.8116600000

H 4.4063400000 -4.7214700000 -2.9308300000

H 3.2284100000 -5.9924300000 -4.6702100000

H 0.8569600000 -5.4806200000 -5.2505400000

H -0.3437300000 -3.6529100000 -4.0407200000

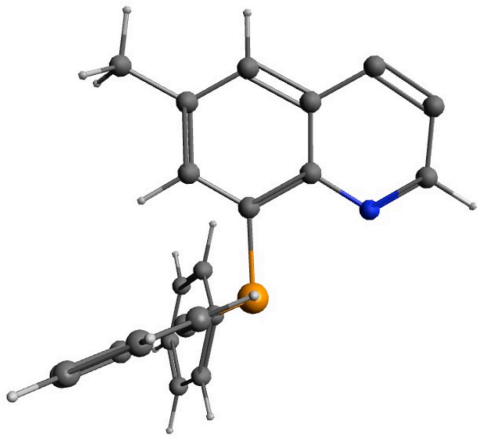

PNQuin(-2H)

PNQuin(-2H) (S = 1)

HF=-1243.2805748 Hartrees

C 4.6362400000 -2.8365700000 -0.9693600000

C 5.1816800000 -2.1164400000 0.0871100000

C 4.3664700000 -1.1633500000 0.7353000000

C 3.0636400000 -0.9325600000 0.3220200000

C 2.5080200000 -1.6646100000 -0.7525800000

C 3.3074800000 -2.6437300000 -1.4082200000

N 1.1837200000 -1.4193200000 -1.1162000000

C 0.6674300000 -2.1340600000 -2.0875800000

C 1.3630500000 -3.1485500000 -2.8055500000

C 2.7131100000 -3.4308300000 -2.4706700000

H 5.2573400000 -3.5824200000 -1.4659500000

H 4.7721100000 -0.5998900000 1.5788900000

H -0.3704100000 -1.9535900000 -2.3555500000

C 6.5952900000 -2.3353800000 0.5501400000

H 7.1840700000 -1.4073300000 0.4603700000

H 7.0957200000 -3.1203400000 -0.0342800000

H 6.6180200000 -2.6254300000 1.6135900000

P 1.9632600000 0.2563000000 1.1672600000

C 2.3290600000 -0.1273700000 2.9373900000

C 1.8514700000 -1.3339700000 3.4688500000

C 2.0893700000 -1.6787000000 4.7990100000

C 2.8228300000 -0.8184600000 5.6223700000

C 3.3229800000 0.3761700000 5.0976600000

C 3.0816700000 0.7218300000 3.7640700000

C 2.7737200000 1.8901700000 0.9341200000

C 2.2796100000 2.9984200000 1.6455500000

C 2.8272100000 4.2660200000 1.4493100000

C 3.8639200000 4.4483700000 0.5277800000

C 4.3517600000 3.3546500000 -0.1901600000

C 3.8135400000 2.0801600000 0.0138500000

H 1.2823000000 -2.0129300000 2.8441200000

H 1.6939800000 -2.6188500000 5.1895300000

H 3.0070800000 -1.0803400000 6.6670400000

H 3.9078700000 1.0502500000 5.7281400000

H 3.4847100000 1.6575100000 3.3800200000

H 1.4631300000 2.8723000000 2.3566600000

H 2.4331500000 5.1161600000 2.0105400000

H 4.2833700000 5.4438700000 0.3640700000

H 5.1514400000 3.4892300000 -0.9221900000

H 4.2005400000 1.2389900000 -0.5611600000

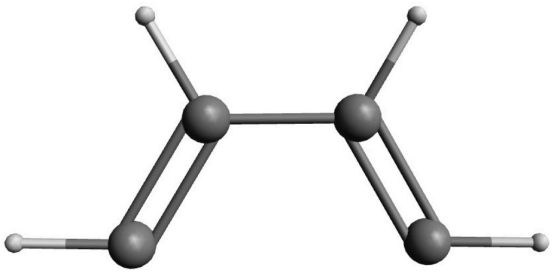

s-*cis*-Butadiene(-2H)

s-*cis*-Butadiene(-2H) (S = 1)

HF=-154.4996253 Hartrees

C 3.3719500000 -4.4702300000 -3.1649600000

C 2.7059300000 -5.1886100000 -4.1463000000

C 1.3638800000 -4.9006700000 -4.4764700000

C 0.6980100000 -3.8884000000 -3.8116600000

H 4.4063400000 -4.7214700000 -2.9308300000

H 3.2284100000 -5.9924300000 -4.6702100000

H 0.8569600000 -5.4806200000 -5.2505400000

H -0.3437300000 -3.6529100000 -4.0407200000

References

(1) Mandapati, P.; Giesbrecht, P. K.; Davis, R. L.; Herbert, D. E. Phenanthridine-Containing Pincer-like Amido Complexes of Nickel, Palladium, and Platinum. *Inorg. Chem.* **2017**, *56*, 3674–3685.

(2) Mondal, R.; Giesbrecht, P. K.; Herbert, D. E. Nickel(II), Copper(I) and Zinc(II) Complexes Supported by a (4-Diphenylphosphino)Phenanthridine Ligand. *Polyhedron* **2016**, *108*, 156–162.

(3) Mondal, R.; Lozada, I. B.; Davis, R. L.; Williams, J. A. G.; Herbert, D. E. Site-Selective Benzannulation of N-Heterocycles in Bidentate Ligands Leads to Blue-Shifted Emission from $[(P\hat{}N)Cu]_2(\mu\text{-}X)_2$ Dimers. *Inorg. Chem.* **2018**, *57*, 4966–4978.

(4) Bratsos, I.; Alessio, E.; Ringenberg, M. E.; Rauchfuss, T. B. Ruthenium (II) Chloro Complexes of Dimethyl Sulfoxide. *Inorg. Synth.* **2010**, *35*, 148–152.

(5) Suzuki, T.; Kuchiyama, T.; Kishi, S.; Kaizaki, S.; Takagi, H. D.; Kato, M. Ruthenium(II) Complexes Containing 8-(Dimethylphosphino)Quinoline (Me_2Pqn): Preparation, Crystal Structures, and Electrochemical and Spectroscopic Properties of $[Ru(bpy\ or\ phen)_{3-n}(Me_2Pqn)_n](PF_6)_2$ (Bpy = 2,2'-Bipyridine; Phen = 1,10-Phenanthroline; n = 1, 2, or 3). *Inorg. Chem.* **2003**, *42*, 785–795.

(6) Bruker-AXS. *APEX3 V2016.1-0*; Madison, Wisconsin, USA, 2016.

(7) Sheldrick, G. M. *SADABS, Program for Absorption Correction for Data from Area Detector Frames*; University of Göttingen: Göttingen, Germany, 2008.

(8) Sheldrick, G. M. A Short History of SHELX. *Acta Cryst.* **2008**, *A64*, 112–122.

(9) Spek, A. L. Structure Validation in Chemical Crystallography. *Acta Cryst.* **2009**, *D65*, 148–155.

(10) Frisch, M. J.; Trucks, G. W.; Schlegel, H. B.; Scuseria, G. E.; Robb, M. A.; Cheeseman, J. R.; Scalmani, G.; Barone, V.; Petersson, G. A.; Nakatsuji, H.; Li, X.; Caricato, M.; Marenich, A. V.; Bloino, J.; Janesko, B. G.; Gomperts, R.; Mennucci, B.; Hratchian, H. P.; Ortiz, J. V.; Izmaylov, A. F.; Sonnenberg, J. L.; Williams; Ding, F.; Lipparini, F.; Egidi, F.; Goings, J.; Peng, B.; Petrone, A.; Henderson, T.; Ranasinghe, D.; Zakrzewski, V. G.; Gao, J.; Rega, N.; Zheng, G.; Liang, W.; Hada, M.; Ehara, M.; Toyota, K.; Fukuda, R.; Hasegawa, J.; Ishida, M.; Nakajima, T.; Honda, Y.; Kitao, O.; Nakai, H.; Vreven, T.; Throssell, K.; Montgomery Jr., J. A.; Peralta, J. E.; Ogliaro, F.; Bearpark, M. J.; Heyd, J. J.; Brothers, E. N.; Kudin, K. N.; Staroverov, V. N.; Keith, T. A.; Kobayashi, R.; Normand, J.; Raghavachari, K.; Rendell, A. P.; Burant, J. C.; Iyengar, S. S.; Tomasi, J.; Cossi, M.; Millam, J. M.; Klene, M.; Adamo, C.; Cammi, R.; Ochterski, J. W.; Martin, R. L.; Morokuma, K.; Farkas, O.; Foresman, J. B.; Fox, D. J. *Gaussian 16 Rev. C.01*; Wallingford, CT, 2016.

(11) Marenich, A. V.; Cramer, C. J.; Truhlar, D. G. Universal Solvation Model Based on Solute Electron Density and on a Continuum Model of the Solvent Defined by the Bulk Dielectric Constant and Atomic Surface Tensions. *J. Phys. Chem. B* **2009**, *113*, 6378–6396.

(12) Grimme, S.; Ehrlich, S.; Goerigk, L. Effect of the Damping Function in Dispersion Corrected Density Functional Theory. *J. Comput. Chem.* **2011**, *32*, 1456–1465.

(13) Becke, A. D. Density-Functional Thermochemistry. III. The Role of Exact Exchange. *J. Chem. Phys.* **1993**, *98*, 5648–5652.

(14) Lee, C.; Yang, W.; Parr, R.G. Development of the Colle-Salvetti Correlation-Energy Formula into a Functional of the Electron Density. *Phys. Rev. B Condens. Matter.* **1988**, *37*, 785–789.

(15) Vosko, S. H.; Wilk, L.; Nusair, M. Accurate Spin-Dependent Electron Liquid Correlation Energies for Local Spin Density Calculations: A Critical Analysis. *Can. J. Phys.* **1980**, *58*, 1200–1211.
(16) Stephens, P. J.; Devlin, F. J.; Chabalowski, C. F.; Frisch, M. J. Ab Initio Calculation of Vibrational Absorption and Circular Dichroism Spectra Using Density Functional Force Fields. *J. Phys. Chem.* **1994**, *98*, 11623–11627.
(17) Weigend, F.; Ahlrichs, R. Balanced Basis Sets of Split Valence, Triple Zeta Valence and Quadruple Zeta Valence Quality for H to Rn: Design and Assessment of Accuracy. *Phys. Chem. Chem. Phys.* **2005**, *7*, 3297–3305.
(18) Tao, J.; Perdew, J. P.; Staroverov, V. N.; Scuseria, G. E. Climbing the Density Functional Ladder: Nonempirical Meta--Generalized Gradient Approximation Designed for Molecules and Solids. *Phys. Rev. Lett.* **2003**, *91*, 146401.
(19) Staroverov, V. N.; Scuseria, G. E.; Tao, J.; Perdew, J. P. Comparative Assessment of a New Nonempirical Density Functional: Molecules and Hydrogen-Bonded Complexes. *J. Chem. Phys.* **2003**, *119*, 12129–12137.
(20) O'Boyle, N. M.; Tenderholt, A. L.; Langner, K. M. Software News and Updates Cclib: A Library for Package-Independent Computational Chemistry Algorithms. *J. Comput. Chem.* **2008**, *29*, 839–845.
(21) Lu, T.; Chen, F. Multiwfn: A Multifunctional Wavefunction Analyzer. *J. Comput. Chem.* **2012**, *33*, 580–592.
(22) Xiao, M; Lu, T. Generalized Charge Decomposition Analysis (GCDA) Method. *J. Adv. Phys. Chem.* **2015**, *4*, 111–124.